LBL--33364

DE93 007720

Sol-Gel Preparation of Ion-Conducting Ceramics for Use in Thin Films

MARGARET IRENE STEINHAUSER
M.S. Thesis

DEPARTMENT OF MATERIALS SCIENCE AND MINERAL ENGINEERING
University of California, Berkeley

and

Center for Advanced Materials
MATERIALS SCIENCES DIVISION
Lawrence Berkeley Laboratory
University of California
Berkeley, CA 94720

DECEMBER, 1992

This work was supported by the Division of Materials Science, Office of Basic Energy Research, United States Department of Energy, under contract No. DE-AC0376SF00098 with the Lawrence Berkeley Laboratory.

Sol-Gel Preparation of Ion-Conducting Ceramics for Use in Thin Films

by

Margaret Irene Steinhauser

Abstract

A metal alkoxide sol-gel solution suitable for depositing a thin film of $La_{0.6}Sr_{0.4}CoO_3$ on a porous substrate has been developed; such films should be useful in fuel cell electrode and oxygen separation membrane manufacture. Crack-free films have been deposited on both dense and porous substrates by dip-coating and spin-coating techniques followed by a heat treatment in air. Fourier transform infrared spectroscopy has been used to determine the chemical structure of the metal alkoxide solution system. X-ray diffraction has been used to determine the crystalline phases formed at various temperatures, while scanning electron microscopy has been used to determine the physical characteristics of the films. Surface coatings have been successfully applied to porous substrates through the control of the substrate pore size, deposition parameters, and firing parameters. Conditions have been defined for which films can be deposited, and for which the physical and chemical characteristics of the film can be improved. A theoretical discussion of the chemical reactions taking

place before and after hydrolysis in the mixed metal alkoxide solutions is presented, and the conditions necessary for successful solution synthesis are defined. The applicability of these films as ionic and electronic conductors is discussed.

Sol-Gel Preparation of Ion-Conducting Ceramics for Use in Thin Films

Table of Contents

Acknowledgements

I would like to thank Professor Lutgard De Jonghe for guiding my research, and Dr. Steven Visco, Dr. Thomas Richardson, and Dr. Timothy Kueper for their advice and support. I also thank my other group members and coworkers for their help and everyday encouragement.

In addition, I would like to thank the other faculty members who took the time to carefully read this thesis and make valued suggestions, Professor Fiona Doyle and Professor Alan Searcy.

Chapter 1: Introduction

1A: General Introduction

Fuel cells and gas sensors produce an external current as a result of ions flowing through a layer of electrolyte material separating gases of different compositions. Electrodes on either side of the electrolyte carry this current out of the cell. The ability to produce an electrolyte thin enough to have a low ohmic drop while remaining continuous to prevent gas leakage is among the problems which currently limit fuel cell performance. Another problem is the manufacture of electrodes having the essential characteristics of resistance to degradation at elevated temperatures, correct pore structure, and good contact with the electrolyte. The thicknesses of electrolytes produced by conventional ceramic processing require the cell to be run at high (1000-1200°C) temperatures for adequate conductivity. Even for thin electrolytes, temperatures of over 600°C are necessary, and the electrodes are exposed to oxidizing and reducing atmospheres. Oxidation and reduction must occur at the gas/electrolyte/electrode triple interface for electrical current and ions to flow in their proper paths. The electrode must therefore be highly porous for gas to reach the electrode-electrolyte interface and to present as extensive an interface as possible to the gas.

A related device is the solid oxide membrane gas purifier. Like the fuel cell electrolyte, this membrane must be thin enough to have a low ohmic drop while remaining continous to prevent leakage. Mixed conductors such as those for fuel cell electrodes may be used for these membranes, with the advantage that only one continuous layer on a supporting substrate is needed to obtain a

working device. A large potential market in non-cryogenic oxygen separation from air exists for such devices.

An attractive method for producing very thin, dense ceramic films is the sol-gel process. A variety of materials has been produced as continuous films of less than one micron thickness on flat, continuous substrates[1,2,3]. A fuel cell containing a thin film electrolyte made by this process could be operated at the comparatively low temperature of 650°C or less with an acceptable ohmic drop. However, an ordinary electrode capable of conducting only electrons poses difficulties as a surface to deposit such a film on, since the electrode must be porous. This in turn places some restrictions on the process parameters of sol-gel deposition of the electrolyte. The logical choice for the supporting electrode is therefore a thin layer of mixed (electronic and ionic) conductor, so that both dense and porous areas will conduct electricity and allow access by ions or gas, incidentally increasing the current density of the fuel cell. The dense or nearly dense electrode layer can be deposited via sol-gel on a graded-porosity substrate and will probably present a much less difficult surface to deposit the unbroken electrolyte layer on.

The goal of this research is to study the formation of thin ceramic layers on porous substrates using the sol-gel technique. The solution chemistry, phase formation, and effect of substrate conditions will be discussed. The sol-gel solution chemistry, process parameters and substrate characteristics which are necessary for successful film formation are defined, and the suitability of this process for electrode and oxygen separation applications is also discussed.

1B: Factors Affecting Fuel Cell Efficiency

A fuel cell is a device used to produce electrical energy from the chemical energy supplied by two gases, a fuel gas and an oxidizer. The gases are kept separated and allowed to react only by ionic migration in one direction and electronic migration through an external circuit in the other. This operation depends on the presence of a thin separator, either a liquid or a solid, which conducts only those ions desired for the chemical reaction; it must have good ionic conductivity, negligible electronic conductivity, and be impervious to gas molecules. An electrode on either side of this electrolytic layer is used to conduct electricity out of the cell to the external circuit.

Fuel cells have a higher theoretical efficiency than more conventional methods of energy conversion, which are subject to Carnot inefficiencies. This feature of fuel cells is what has generated so much ongoing interest in them. In practice, of course, the theoretical efficiency of the cell is reduced in actual operation. The cell design, which includes the electrodes, electrolyte, supports, and seals, is vital to the determination of the true operating efficiency.

Normally, electricity is generated using the process of burning fuel to heat steam to turn electrical generators. The Carnot cycle therefore places a definite upper limit on the efficiency of electricity generation by this method, since it depends on the temperature difference which can be produced, and is limited to around 45% in most practical cases. This is because, as the high end temperature is increased, gains from the larger temperature difference begin to be offset by increased frictional losses and heat wastage. A more direct conversion of energy is achieved in fuel cell operation, where chemical energy is converted directly into electrical energy and the Carnot cycle is avoided. In a hydrogen-oxygen fuel cell, the following reaction occurs:

$$H_2 + 1/2\,O_2 \rightarrow H_2O \qquad (1.1)$$

The theoretical efficiency of this reaction depends on its thermodynamics, and is defined as the ratio of the work obtained to the energy consumed. The Nernst equation can be used to calculate the work obtained. This equation also sets the voltage produced by the reaction, so

$$E = -\frac{\Delta G}{nF} = -\frac{\Delta G^\circ}{nF} - \frac{RT}{nF}\ln\left[\frac{P'}{P''}\right] \qquad (1.2)$$

where n is the number of moles of electrons transferred, F is the Faraday constant, R is the gas constant, T is the temperature, and P' and P" are the partial pressures of oxygen at the air and fuel (hydrogen or hydrocarbon) electrodes, respectively. ΔG is the molar change in Gibbs free energy for the cell reaction and ΔG° is the molar change in Gibbs free energy for the cell reaction measured at a defined set of thermodynamic standard conditions. The optimum efficiency[4] can be described by the equation:

$$\eta = \frac{-\Delta G}{-\Delta H} = 1 - \frac{T\Delta S}{\Delta H} \qquad (1.3)$$

for exothermic reactions. Inefficiency, in the form of wasted heat, is quantified by the entropy term in this equation. Since this term will increase as the temperature increases, low temperatures provide more thermodynamically efficient energy conversion in fuel cells.

The use of a thin electrolyte layer allows a cell to operate at a lower temperature, which in turn increases the thermodynamic efficiency of the cell. In

addition, less insulation is necessary and the time for thermal cycling is shorter. Other advantages are that thermal stresses and electrode sintering are reduced, and degradation reactions are slowed. More options are available for construction materials, as well.

A lower operating temperature has some disadvantages, as well as the advantages listed above. Decreasing the temperature also decreases the rates of electrode reactions and gas diffusion. These in turn reduce the current density at which the device is capable of operating without dramatic voltage drops due to polarization. A primary concern as the temperature is lowered is the electrode reaction rates[5,6]. More expensive catalytic electrodes are generally necessary to improve reaction rates. However, the available options may be increased by new materials under investigation[5,6,7]. Another disadvantage is that restrictions are placed on the fuel that may be used. Free hydrogen is required at the fuel electrode to react efficiently with the ionic oxygen diffusing through the electrolyte to form water, and at high temperatures (above 1000°C) this is obtained as an in-situ reaction product from such convenient fuels as methanol, ammonia, or hydrocarbons. At lower temperatures these hydrogen-producing reactions are unfavorable, and it may therefore be necessary to build conversion facilities to supply hydrogen to the fuel cell.

The structure of the porosity in the support and electrode (or supporting electrode) is very important for successful fuel cell operation. Normally, electrode reactions must take place at the triple interface joining the electrode, electrolyte, and gas phases. The total length of this triple interface per unit area of electrolyte surface therefore determines how high a current density can be obtained from the fuel cell, and so the support and electrode must contain many

extremely fine pores at the electrolyte interface. At the same time, however, the pores should have large diameters to provide an adequate supply of gas to the interface. The cross section must be large in comparison to the mean free path of the gas molecules to avoid Knudsen diffusion[8]. An ideal support material will therefore have a graded porosity, large at the intersection with the gas flow, and small at the intersection with the electrolyte phase.

1C: Other Devices

Electrolyte/electrode systems with qualities similar to those desired for fuel cells are necessary for a number of other devices, including gas sensing and gas separation devices. Gas sensors operate in a fashion very similar to fuel cells, in that a difference in gas composition leads to a potential difference between the two surfaces of the electrolyte, which is then used to determine the composition of the gas on one side of the membrane. Electrolyzers operate somewhat like fuel cells in reverse, with an applied voltage driving a reaction between the two separated gases. Oxygen separation membranes do not require electrodes and operate like shorted fuel cells, where the difference in oxygen partial pressures between the two compartments drives the ionic and electronic fluxes across the membrane[9]. Equation 1.2 governs the behaviors of these applications as it does that of the fuel cell. Oxygen ion conductors, such as yttria-stabilized zirconia, are used for most applications, but proton conductors, such as doped strontium cerium oxide are used for some applications involving hydrogen reactions, and mixed conductors like lanthanum strontium cobalt oxide are used as electrodes and oxygen separators.

1D: Fuel Cell Electrodes

Electrodes in fuel cells have two basic functions. The first of these is to conduct electrical current through an external circuit. The second is to break apart catalytically the gas molecules that impinge on their surfaces, producing the ions that are conducted through the electrolyte. Without this catalytic effect, ionization would take place too slowly for the fuel cell to be an effective energy source.

Overpotential and Polarization

The electromotive force, or emf, of a fuel cell is measured as the potential across the two electrodes of the cell when no current is being extracted and it is working reversibly. It is found theoretically by using the Nernst equation (1.2). This equation, however, gives no information on the rate at which the cell's electrochemical reactions occur.

The concept of the overpotential of the cell is needed to quantify the amount of useful electrical work the cell can perform. It is defined as the difference between the measured potential of the cell under working conditions and the reversible (thermodynamic) potential. Each electrode is considered separately, so that the cell overpotential becomes the sum of the individual electrode overpotentials.

Overpotential may also be subdivided and classified according to the phenomena that produce it. These physical and chemical processes are referred to as polarization. They can be thought of as tending to set up potential differences in opposition to those either produced by the overall chemical reaction (fuel cell) or imposed by the external circuit (gas separator). There are three main types of overpotential: activation, concentration, and ohmic.

Activation overpotential in cells is analogous to activation energy in chemical reactions, and comes from the chemical reactions and physicochemical adsorption of molecules or atoms on the electrode surfaces. Concentration overpotential is produced when the concentration of reactant ions at the electrode surface is lower than in the bulk electrolyte, lowering the available concentration of reactants. The electrical resistance of an electrolyte or a nonporous electrode produces ohmic overpotentials.

Concentration and activation polarization are not usually significant factors at operating temperatures over 600°C. The only significant source of overpotential in a solid oxide fuel cell is therefore the ohmic polarization. This ohmic overpotential, V, can be found from the equation

$$V = iAR \tag{1.4}$$

where R is the resistance (Ω) of the oxide layer, i is the current density (A cm^{-2}), and A is the cross-sectional area (cm^2) of the adjoining layer's contact points (for example, the cross-sectional area of the electrodes touching the electrolyte). The conductivity, k ($\Omega^{-1}cm^{-1}$), of the oxide layer is

$$k = \frac{x}{RA} \tag{1.5}$$

where x is the layer thickness (cm). Substituting equation 1.5 into equation 1.4, the overpotential relationship is now

$$V = \frac{ix}{k} \tag{1.6}$$

From equation 1.6 it is now obvious that for a constant current density and conductivity, the thinner the nonporous oxide layers are, the smaller the ohmic overpotential will be.

Oxygen Electrodes

For a solid oxide fuel cell using a stabilized zirconia electrolyte (the most common kind) the following overall reaction takes place at the oxygen electrode:

$$4\,e^- + O_2(g) \rightarrow 2\,O^{2-} \qquad (1.7)$$

The ideal electrode material must also be resistant to oxidation by an oxygen or oxygen-enriched atmosphere at fairly high temperatures. In addition, it must be capable of catalytically ionizing oxygen gas at the cell operating temperature by the sequence:

Adsorption: $1/2\,O_2 \rightarrow O_{(ads)}$ (1.8a)

Charge Transfer: $O_{(ads)} + 2e^- \rightarrow O^{2-}{}_{(ads)}$ (1.8b)

Absorption into Vacancy: $O^{2-}{}_{(ads)} + V_o^{\cdot\cdot} \rightarrow O_o$ (1.8c)

where $V_o^{\cdot\cdot}$ is an oxide vacancy and O_o is a mobile lattice oxygen ion. Continuity requires that in the steady state

$$J = k(Ce - Cs) = -D\frac{\partial c}{\partial x} \qquad (1.9)$$

where J is the flux (atom cm^{-2} sec^{-1}) of atomic oxygen through the boundary layer, k is the surface exchange coefficient (cm sec^{-1}), C_e is the equilibrium concentration of atomic oxygen (atom cm^{-3}) where C_s is the actual surface concentration of atomic oxygen (atom cm^{-3}), D is the diffusion coefficient (cm^2 sec^{-1}), and $\partial c/\partial x$ is the concentration gradient of oxygen across the thickness of the boundary layer (atom cm^{-3})[9]. This boundary layer may be defined as half the average thickness of the pore walls of the oxygen electrode for simplicity.

In addition, the electrode must have a thermal expansion coefficient matching that of the electrolyte, and it must not react unfavorably with the electrolyte. Finally, it must have good electronic conductivity and (when nonporous) oxide ion conductivity at least as good as that of the electrolyte. Some electron-conducting metal oxides have the best mixture of characteristics of any class of materials.

1E: $La_{1-x}Sr_xCoO_3$ and $La_{1-x}Sr_xMnO_3$ Electrodes

Substituted perovskite-type metal oxides have a number of advantages as fuel cell electrodes and oxygen separation membranes. Specifically, the $La_{1-x}Sr_xCoO_3$ (LSC) and $La_{1-x}Sr_xMnO_3$ (LSM) perovskites have excellent prospects as electrodes. Both are stable in oxidizing atmospheres at fairly low pressures and neither reacts with the yttria-stabilized zirconia (YSZ) electrolyte at 600°C. $La_2Zr_2O_7$ and $SrZrO_3$ are formed by reactions between LSC and zirconia at 800°C, while similar reactions between LSM and YSZ begin to occur between 1000°C and 1300°C[10,11,12]. Manganese begins to diffuse into YSZ via grain boundaries at 1200°C. The formation of $La_2Zr_2O_7$ and $SrZrO_3$ produces high impedance layers and degrades the quality of the electrical

contact between the electrode and the electrolyte. Manganese diffusion into the electrolyte decreases its ionic conductivity, as well[11]. Cobalt diffusion probably has a similar effect, and since cobalt is generally more active than manganese, interdiffusion probably begins occurring at a significant rate at some temperature below 1200°C.

The thermal expansion coefficients of the electrode and electrolyte materials must also be well-matched to prevent crack formation during processing or operation. The thermal expansion coefficient of YSZ has been reported as being between 9.7 and 11.6 x 10^{-6} deg^{-1} [10,13,14]. $La_{0.6}Sr_{0.4}CoO_3$ has a reported thermal expansion coefficient of 18.8 x 10^{-6} deg^{-1} [10], while that of $La_{0.6}Sr_{0.4}MnO_3$ has been reported as both 10.8 x 10^{-6} deg^{-1} and 13.0 x 10^{-6} deg^{-1} [10,13,14]. Either way, $La_{0.6}Sr_{0.4}MnO_3$ is better matched with YSZ than $La_{0.6}Sr_{0.4}CoO_3$.

There are a number of different sources that report conductivity values for these materials[9,12,13,15,16,17]. Most give total (electronic + ionic) conductivities, but two provide separate ionic values, as well. The total conductivities are likely to be electronic conductivities, since the ionic conductivity is usually three or four orders of magnitude lower than the electronic conductivity. Direct comparisons are difficult because of the different compositions, processing methods, and test conditions used by different groups, but some general conclusions can be drawn. Both materials have electrical conductivities on the order of 10^2 S cm^{-1}, but $La_{1-x}Sr_xCoO_3$ is much more conductive than $La_{1-x}Sr_xMnO_3$ at elevated (800°C and up) temperatures, and at around 600°C their conductivities are approximately the same. LSC retains significant conductivity at slightly lower temperatures (ca. 300°C) than LSM[18]. Oxide ion conductivities on the order of 10^{-1} S cm^{-1} have been measured for

LSC between 700°C and 860°C[15]. For LSM, oxide ion conductivity probably ranges between 10^{-2} S cm^{-1} at 700°C and 10^{-1} S cm^{-1} at 860°C[9,16]. In general, therefore, LSC has better conductivity in both categories than LSM and is more highly conductive over a wider temperature range. Table 1.1 gives a summary of some conductivity values reported in the literature.

The magnitude of the polarization that an electrode is subject to is another important factor in determining a suitable material. Higher overpotentials mean a less efficient electrode, and therefore a less efficient fuel or oxygen concentration cell. Again, factors such as contact area, grain size, and material composition have an important effect on cathodic overpotentials, but some general conclusions can be drawn. Two studies involving LSC and LSM obtained, for a 0.10 A cm^{-2} current density and a temperature of 800°C, somewhat different overpotentials for the two materials. The overpotential for $La_{0.6}Sr_{0.4}MnO_3$ was given as 100 mV[10], while that of $La_{0.7}Sr_{0.3}MnO_3$ was reported as 120 mV and that of $La_{0.7}Sr_{0.3}CoO_3$ as 80 mV [12]. It would therefore seem that LSC would be the better choice of cathode material for use at high current densities.

A particularly important criterion for choosing low temperature cathodes is the rate at which they can reduce oxygen molecules to oxide (O^{2-}) ions. This rate is highly affected by surface conditions and material composition, but in general the LSC materials seem to have better catalytic properties than the LSM materials, consistent with their generally better ionic conductivities at similar compositions.

An additional observation should be made as to the rate of oxygen diffusion into these electrodes. At low temperatures (around 500 to 600°C), the oxygen coverage of the cathode is fairly high, and so the rate determining step

in the reaction is the charge transfer step (page 9). At high temperatures (above 600°C), the oxygen coverage of the surface is fairly low, and the dissociative adsorption (page 9) becomes the rate determining step[10,18].

In conclusion, $La_{1-x}Sr_xCoO_3$ with x between 0.3 and 0.5 has generally better electrical properties than $La_{1-x}Sr_xMnO_3$ of similar composition. However, the manganites have better mechanical properties and better sintering characteristics. It would therefore seem to be the best conclusion that lanthanum strontium manganese oxide, perhaps cobalt-substituted to try and improve the electrical properties without losing the good thermal expansion match, would make the best fuel cell or gas sensor cathode. On the other hand, in an oxygen separation cell the compatibility of the LSC with an electrolyte is not a problem at all, since no other material needs to attach to it except for a support structure that might be made from the same material. Its superior electrical properties make LSC the better material choice in this case.

1F:Proton-Conducting Electrolytes: $SrCe_{0.95}Y_{0.05}O_3$

Some early work in this investigation was performed on yttria-substituted strontium cerium oxide (SCY), and for this reason a brief introduction to this material and its properties is made here.

Strontium cerium oxide is a proton, or H^+ ion, conductor. Its electrical properties have been extensively investigated by a group headed by Iwahara. They have used it to construct experimental hydrogen concentration cells, hydrogen-oxygen fuel cells, and "steam concentration cells," possibly useful as humidity sensors[19]. They report doped strontium cerium oxide as having two types of conductivity: protonic and hole. Proton conductance is dependent on the mean vapor pressure of water in the cell, and on the temperature at which it

operates, increasing when either of these factors is increased. The conductivity as a whole goes down as the mean humidity increases, however, because the less mobile protons are being conducted at the expense of the holes. The hole conductivity rises with temperature and the partial pressure of oxygen in the cell. These investigators' hydrogen concentration cells operated stably between 800° C and 1000°C using wet ($P_{H2O} \cong 20$ Torr) hydrogen and produced proton conductivities on the order of 10^{-2} S cm^{-1} and electric conductivities of about 10^{-4} S cm^{-1} [20].

The ohmic overpotential of this electrolyte is fairly significant (at 800°C and 0.10 A cm^{-1}, the overpotential for a 0.5 mm thick electrolyte is about 0.7 V added to a 0.2 V potential difference) and these investigators emphasize that if this material could be synthesized in the form of a thin film that these devices might actually be made efficient enough for practical applications[20].

1G: Current Methods of LSC Electrode and SCY Electrolyte Production

$La_{1-x}Sr_xCoO_3$ Electrode Production

Currently, LSC electrodes are manufactured for testing by fairly conventional methods. Some investigators use ordinary oxide/carbonate powders as precursors and manufacuture pellets in the conventional way[13,16]. Other methods include: making pyrolyzed acetate powders and painting them onto the electrolyte prior to firing[10,18,21], manufacturing pellets from powders made by dissolving acetates[15], and sputtering coatings[12]. The painted slurry and sputtered coatings produce the thinnest layers, but neither method produces a surface suitable for coating with a sol-gel derived electrolyte layer, being designed to coat onto an electrolyte, not vice-versa. Both produce coatings with large (1 micron) pores that would induce cracking in a zirconia sol-gel film.

$SrCe_{1-x}Y_xO_3$ Electrolyte Production

Doped strontium cerium oxide electrolytes have not been produced by any method other than conventional oxide/carbonate mixing and sintering [22] in the available literature. Pieces of about 0.5 millimeters in thickness have been manufactured.

1H: Basic Sol-Gel Chemistry

The starting materials in the sol-gel process are generally alkoxides of the desired metals, although other materials such as metal 2,4-pentanedionates can be used as well. The metal alkoxides are dissolved in a dry organic solvent. This solution is then converted to a gel via hydrolysis; for example,

$$La[OCH(CH_3)_2]_3 + H_2O \rightarrow LaOH[OCH(CH_3)_2]_2 + HOCH(CH_3)_2 \qquad (1.10)$$

The hydrolyzed molecules may then react together, forming a condensation product wherein the two metals are joined by an oxygen link. Larger polymers form as the hydrolysis and condensation reaction continue, eventually linking the polymers into a continuous gel network. Precipitation may occur instead of gelation, unless the reaction process is carefully managed.

For processes using multiple metal alkoxides the chemistry of the sol-gel solution becomes considerably more complex than for single metal alkoxide syntheses. Ideally, the condensation rates of all the alkoxides should be closely matched, so that they will all bond into a single, stoichiometric, intimately mixed polymer network. For example:

$$RO\text{–}M_1\text{–}OH + RO\text{–}M_2\text{–}OH + RO\text{–}M_3\text{–}OH \rightarrow RO\text{–}M_2\text{–}O\text{–}M_1\text{–}O\text{–}M_3\text{–}OH + 2ROH \quad (1.11)$$

In practice, of course, matching condensation rates without deliberate modification is probably a fortuitous accident. It therefore becomes necessary to modify chemically one or more of the alkoxides to obtain matching rates of condensation.

A problem frequently encountered in hydrolyzing metal alkoxide solutions is that one or more of the alkoxides will condense with itself to form an insoluble precipitate. These precipitates destroy the homogeneity of the alkoxide sol-gel, and in thin films they may act as sites for crack nucleation. Again, modification of the ligands bonding to the offending metal alkoxide is possible in order to prevent precipitation.

Finally, solvating all of the necessary metal alkoxides in the same solvent or mixture of solvents may be difficult. Care must be taken not to use chemicals as solvents that react with the metal alkoxides to form bonds too strong for the hydrolysis reaction to break. Changing one or more of the ligands on the insoluble alkoxides can be done while still allowing the hydrolysis and condensation reactions to take place.

Chelating Ligands

Some chemicals, such as diethanolamine (DEA) and acetylacetone (acac), react with metal alkoxides to produce very strongly bonded ligands that hydrolyze very slowly. For example[23],

$$RO\text{–}M\text{–}OR + (HOCH_2CH_2)_2NH \rightarrow \begin{matrix} O\text{-}CH_2\text{-}CH_2 \\ M \\ O\text{-}CH_2\text{-}CH_2 \end{matrix}\!\!>\!NH + 2ROH \quad (1.12)$$

This reaction may have a combination of three effects on the metal alkoxide molecule. It may increase the solubility of the alkoxide in the chosen solvent; it may retard, sometimes severely, the rates of hydrolysis and condensation of the alkoxide; and it often prevents or reduces the formation of precipitates as the alkoxide undergoes hydrolysis[24].

Acid Catalysts

Acids, for example acetic acid, may be used for a slightly different kind of metal alkoxide modification. A reaction between a metal alkoxide and an organic acid may look something like:

$$RO\text{–}M\text{–}OR + HOCOCH_3 \rightarrow RO\text{–}M\text{–}OCOCH_3 + ROH \qquad (1.13)$$

Such reactions can be used to produce more stable solutions, dissolve precipitates, and sometimes speed up or slow down hydrolysis and condensation reactions[25]. The effect of the acid depends on the type of metal in the alkoxide. Acids act as catalysts, changing the hydrolysis and condensation rates and even the structure of the condensed gel. They act to protonate negatively charged alkoxide groups and enhance the reaction kinetics by producing good leaving groups,

$$RO\text{–}M\text{–}OR + H_3O^+ \rightarrow M^+\leftarrow:O\begin{matrix}H\\ \diagup\\ R\end{matrix} + H_2O \qquad (1.14)$$

This removes the need for proton transfer within the transition state. Acid-catalyzed condensation occurs preferentially at the ends of polymer chains and

thus creates more linear polymers. High acid concentrations severely retard condensation kinetics[26].

Solvent Exchange Reactions

Exchange reactions with the solvent may also change the behavior of the metal alkoxide. Alcohols are commonly used as solvents and may react in the following manner with the metal alkoxide:

$$RO\text{–}M\text{–}OR + R'\text{–}OH \rightarrow RO\text{–}M\text{–}OR' + ROH \qquad (1.15)$$

Such reactions generally occur to replace longer or bulkier alkoxide side group with shorter or less bulky alcohol chains. These changes may or may not have a positive effect on the solubility of the metal alkoxide, but in general the hydrolysis and condensation rates of the alkoxide are increased because of the removal of steric barriers imposed by large or bulky side groups[27].

1I: An Introduction to Sol-Gel Processing

Sol-gel processing, unlike most conventional techniques, is suitable for producing thin (<1 μm), dense, and continuous solid electrolyte or electrode films. As the solution gels, it will at some point reach a viscosity suitable for film deposition. Films can be formed by two techniques, known as dip-coating and spin-coating. In dip-coating, the substrate is submerged in a bath and then drawn out at a controlled velocity and angle. This technique is suitable for coating large surface areas. The thickness of the film can be controlled by three factors: the viscosity of the solution, and the speed and angle of withdrawal. In the spin-coating process, a pool of liquid is dropped onto the substrate, which is

then rotated at high speed, distributing the liquid uniformly on the substrate and throwing off the excess. This technique is useful only for coating small surface areas. The thickness of the coating is controlled by the viscosity of the solution and the speed at which the substrate rotates[28].

A thin layer of condensing gel is left on the substrate by either method. At this stage the gel contains polymer networks and some amount of solvent. Depending on the solvent vapor pressure, it may readily evaporate before heat treatment begins, or be driven off during the initial stages of the heat treatment. Residual organic groups trapped by or bonded to the polymer network are burned out by continued heating after the solvent is removed. This burnout can be performed either by a low (400°C) temperature hold or by slowly heating the coated substrate to the necessary crystallization temperature. Some residual carbon may remain trapped in the film and possibly reduce the efficiency of the device being manufactured. The ceramic film begins to crystallize at a fairly low temperature (400-600°C) and so a dense, crystalline structure may form without any high temperature sintering being necessary[29].

Advantages of the Sol-Gel Process

Sol-gel processing tends to produce better purity and homogeneity, significantly lower sintering temperatures, and finer control of the morphology of the thin film, when compared with techniques that rely on the consolidation of powders, such as tape casting. The higher purity comes from the fact that the starting materials for sol-gel syntheses are usually chemicals in solution. These can be purified by such methods as vacuum distillation or recrystallization, unlike bulk powders. Powder processing methods themselves can introduce impurities, via such routes as grinding operations or sintering additives.

Grinding processes are absent in sol-gel processing, and sintering additives are not necessary because the low firing temperatures used strongly suppress grain growth. Films synthesized from sol-gels therefore retain their purity much more easily during processing. The components in a sol-gel solution are mixed on a molecular level, so homogeneity is also much easier to achieve by this method than by powder mixing. Dense films may be obtained at much lower firing temperatures because the film is formed directly from a homogeneous liquid. This means that there is no minimum thickness based on particle size or inherent packing porosity in the coating.

The most significant disadvantages of the sol-gel process are the expense of the chemicals used and the high degree of shrinkage that occurs during firing. This last problem is due to solvent evaporation and the high percentage of organic material that burns out of the gel. These characteristics make the manufacture of bulk objects impractical. The small volumes of chemicals used in film manufacture mitigate their expense, however. Although shrinkage cracking of films is a problem, certain guidelines can be followed to produce crack-free films[30].

1J: Device Substrates Under Consideration

Lanthanum Strontium Manganese Cobalt Oxide

Substrates under consideration for use in solid electrolyte devices must have a number of properties. They must provide mechanical support for the device, while being porous enough to allow a free flow of gas. If a part of an electrode, as LSMC would be, they must include a means of electronic current collection from the interface with the electrolyte and also serve as a site for catalysis of surface reactions.

One possible design is a graded-porosity substrate of LSMC. This material matches well with YSZ under thermal expansion, and has good electrical conductivity, fair mechanical strength and controllable porosity. The catalytic behavior of closely related materials is also good[10]. A graded-porosity LSMC substrate will have three or four layers of material, going from a very coarse grain size (≅ 10 microns) at the bottom to a fine grain size (≅ 0.1 μm) at the top. This stack would be sintered to produce an abundant fine porosity at the surface which would then be coated with the electrode sol-gel and fired to produce a thin (< 1 μm) smooth continuous layer which could be coated with the zirconia electrolyte sol-gel. This type of substrate would also be suitable for use in oxygen concentration cells.

The main disadvantage of this LSMC substrate is that it is still experimental, and some flaw may be discovered that will make its manufacture impractical. Similar effects have been achieved commercially using alumina, however.

Controlled Porosity Alumina Substrates

Another method of substrate fabrication is to use a material that will provide a stable mechanical support with a highly aligned porosity and then coat it with another material that will provide the necessary electronic conduction and catalytic activity.

There are commercially available alumina membranes with highly controlled porosities that are applicable to high gas flow rate uses. One such membrane is the Anotec filter manufactured by Whatman. The backs of these membranes have a linear, parallel arrangement of large pores, rather like a honeycomb, which extent inward until, by controlling the fabrication process,

they branch into smaller pores. These fine scale pores can have diameters of 0.02 microns or less. This layer is less than 1 micron thick, and is synthesized on top of a 52 micron thick region of 0.2 micron diameter pores. The total porosity of these membranes is approximately 50%. The large pores extending nearly to the electrode interface allow for high gas flow rates and eliminate the possibility of diffusive polarization as a problem with these filters. The relative pore sizes and thicknesses of the two regions are controllable, as is the size, and so can be modified to suit the application.

Alumina has good thermal and chemical stability under most conditions, so application of these membranes to intermediate-temperature fuel cells or oxygen concentration cells is attractive. Alumina has a thermal expansion coefficient similar to that of zirconia, and it retains its rigidity and stability at high temperatures. The pore walls of these membranes seem to have a dense micro-crystalline structure. Therefore, they should not be subject to sintering or grain growth at intermediate (650°C) temperatures and should be dimensionally stable. Exposure to solvents and acidic environments during the sol-gel deposition steps should not affect them because of their chemical stability. These membranes have been used fairly extensively in this research project; however, they are subject to a number of problems and limitations which will be discussed in later chapters.

Another type of controlled porosity filter is the Membralox γ-alumina filter, manufactured by U. S. Filter. These filters are manufactured from size-graded layers of alumina powder with a layer of sol-gel alumina coated on top. It has a maximum pore diameter of 0.05 microns and is manufactured in the form of small cylindrical tubes with an inner diameter of 6.80 millimeters and a thickness of 2.0

millimeters. The porosity of these filters is the result of microcracks in the sol-gel layer formed during the sintering step.

The major disadvantages in using alumina membranes as substrates to coat lanthanum strontium cobalt oxide electrodes on is their lack of electrical conductivity and high degree of reactivity with cobalt. Multiple layers of sol-gel coating would be necessary to obtain good conductance through the electrode, and a low-level ongoing reaction between the electrode and the substrate could quickly destroy the cell. A more detailed description of these problems can be found in later chapters. Therefore, for a variety of reasons, a graded porosity LSMC-type substrate would be the best choice of these three possibilities, if it can be successfully developed.

References--Chapter 1

[1] A. Makishima, H. Kubo, K. Wada, Y. Kitami, and T. Shimohira,"Yellow Coatings Produced on Glasses and Aluminum by the Sol-Gel Process," *J. Am. Ceram. Soc.*, **69** [6], C-127-C-129 (1986).

[2] R. Xu, Y. Xu, C. J. Chen, and J. D. Mackenzie, "Sol-gel Processing of Strontium-Barium Niobate Ferroelectric Thin Film," *J. Mat. Res.*, **5** [5], 916-918 (1990).

[3] W. W. Davison and R. C. Buchanan, "ZrO_2 Thin Films for Packaging and Microelectronics Applications," pp. 513-521 in *Advances in Ceramics* Vol. 26, ed. M. F. Yan, K. Niwa, H. M. O'Bryan, Jr., and W. S. Young, The American Ceramic Soc., Inc., 1989.

[4] A. McDougall, *Fuel Cells*, John Wiley and Sons, New York, 1976.

[5] H. S. Isaacs, "Zirconia Fuel Cells and Electrolyzers," pp. 406-418 in *Advances in Ceramics* Vol. 3, ed. A. H. Heuer and L. W. Hobbs, The American Ceramic Soc., Inc., 1981.

[6] B. C. Steele, J. Drennan, R. K. Slotwinski, N. Bonanos, and E. P. Butler, "Factors Influencing the Performance of Zirconia-Based Oxygen Monitors," pp. 286-309 in *Advances in Ceramics* Vol. 3, ed. A. H. Heuer and L. W. Hobbs, The American Ceramic Soc., Inc., 1981.

[7] S. P. Badwal, M. J. Bannister, and W. G. Garrett, "Low-Temperature Behavior of ZrO_2 Oxygen Sensors," pp. 598-606 in *Advances in Ceramics* Vol. 12, ed. N. Claussen and A. H. Heuer, The American Ceramic Soc., Inc., 1984.

[8] G. H. Geiger and D. R. Poirier, *Transport Phenomena in Metallurgy*, pp. 463-472, Addison Wesley, Reading, MA (1973).

[9] B. C. H. Steele, "Oxygen Ion Conductors and Their Technological Applications," *Materials Science and Engineering*, **B13**, 79-87 (1992).

[10] T. Inoue, K. Eguchi, T. Setoguchi, and H. Arai, "Cathode and Anode Materials and the Reaction Kinetics for the Solid Oxide Fuel Cell," *Solid State Ionics*, **40/41**, 407-410 (1990).

[11] T. Kawada, N. Sakai, H. Yokokawa, M. Dokiya, and I. Anzai, "Reaction Between Solid Oxide Fuel Cell Materials," *Solid State Ionics*, **50**, 189-196 (1992).

[12] O. Yamamoto, Y. Takeda, R. Kanno, and M. Noda, "Perovskite-Type Oxides as Oxygen Electrodes for High Temperature Oxide Fuel Cells," *Solid State Ionics*, **22**, 241-246 (1987).

[13] E. Ivers-Tiffée, W. Wersing, M. Schieβl, and H. Greiner, "Ceramic and Metallic Components for a Planar SOFC," *Ber. Bunsenges. Phys. Chem.*, **94**, 978-981 (1990).

[14] S. Srilomsak, D. P. Schilling, and H. U. Anderson, "Thermal Expansion Studies on Cathode and Interconnect Oxides," pp. 129-140 in *Proceedings of the First International Symp. on Solid Oxide Fuel Cells* Vol. 89-11, ed. S. C. Singhal, The Electrochemical Society, Inc., 1989.

[15] Y. Teraoka, H. M. Zhang, K. Okamoto, and N. Yamazoe, "Mixed Ionic-Electronic Conductivity of $La_{1-x}Sr_xCo_{1-y}Fe_yO_{3-\delta}$ Perovskite-Type Oxides," *Mat. Res. Bull.*, **23**, 51-58 (1988).

[16] A. Belzner, T. M. Gür, and R. A. Huggins, "Measurement of the Chemical Diffusion Coefficient of Oxygen in Mixed Conductors by a Solid State Electrochemical Method," *Solid State Ionics*, **40/41**, 535-538 (1990).

[17] L. G. J. de Haart, R. A. Kuipers, K. J. de Vries, and A. J. Burggraaf, "Deposition and Electrical Properties of Thin Porous Ceramic Electrode Layers for Solid Oxide Fuel Cell Application," *J. Electrochem. Soc.*, **138**, 1970-1975 (1991).

[18] T. Inoue, N. Seki, K. Eguchi, and H. Arai, "Low-Temperature Operation of Solid Electrolyte Oxygen Sensors Using Perovskite-Type Oxide Electrodes and Cathodic Reaction Kinetics," *J. Electrochem. Soc.*, **137**, 2523-2527 (1990).

[19] H. Iwahara, H. Uchida, and N. Maeda, "Studies on Solid Electrolyte Gas Cells with High-Temperature-Type Proton Conductor and Oxide Ion Conductor," *Solid-State Ionics*, **11**, 109-115 (1983).

[20] H. Iwahara, T. Esaka, H. Uchida, T. Yamauchi, and K. Ogaki, "High Temperature Type Protonic Conductor Based on $SrCeO_3$ and Its Application to the Extraction of Hydrogen Gas," *Solid State Ionics*, **18 & 19**, 1003-1007 (1986).

[21] T. Inoue, K. Eguchi, and H. Arai, "Low Temperature Operation of Ceria-based Oxygen Sensors Using Perovskite-type Oxide Electrodes," *Chem Lett.*, 1939-1942 (1988).

[22] H. Iwahara, T. Esaka, H. Uchida, and N. Maeda, "Proton Conduction in Sintered Oxides and Its Application to Steam Electrolysis for Hydrogen Production," *Solid State Ionics*, **3/4**, 359-363 (1981).

[23] D. C. Bradley, R. C. Mehrotra, and D. P. Gaur, *Metal Alkoxides*, p. 218 (Academic Press, London 1978).

[24] Y. Takahashi and Y. Matsuoka, "Dip-Coating of TiO_2 Films Using a Sol Derived from Ti(O-*i*-Pr)$_4$-diethanolamine-H_2O-*i*-PrOH System," *J. Mat. Sci.*, **23**, 2259-2266 (1988).

[25] B. E. Yoldas, "Hydrolysis of Titanium Alkoxide and Effects of Hydrolytic Polycondensation Parameters," *J. Mat. Sci.*, **21**, 1087-1-92 (1986).

[26] C. J. Brinker and G. W. Scherer, *Sol-Gel Science: The Physics and Chemistry of Sol-Gel Processing*, 1st ed., Academic Press, Inc., San Diego Calif., pp. 47-49 (1990).

[27] C. J. Brinker and G. W. Scherer, *Sol-Gel Science: The Physics and Chemistry of Sol-Gel Processing*, 1st ed., Academic Press, Inc., San Diego Calif., pp. 52-55 (1990).

[28] L. E. Scriven, "Physics and Applications of Dip Coating and Spin Coating," pp. 717-729 in *Materials Res. Symp. Proc.* Vol. 121, ed. C. J. Brinker, D. E. Clark, and D. R. Ulrich, Mat. Res. Soc., 1988.

[29] G. C. Frye, A. J. Ricco, S. J. Martin, and C. J. Brinker, "Characterization of the Surface Area and Porosity of Sol-Gel Films Using SAW Devices," pp. 349-354 in *Materials Res. Symp. Proc.* Vol. 121, ed. C. J. Brinker, D. E. Clark, and D. R. Ulrich, Mat. Res. Soc., 1988

[30] T. W. Kueper, " Sol-Gel Derived Ceramic Electrolyte Films on Porous Substrates," Ph.D. Thesis, University of California, Berkeley (1992).

Chapter 2: Experimental Procedure

2A: General Experimental Approach

This section presents an outline of the approach used in this set of experiments, in which thin films of doped perovskite-type ceramics are prepared by the sol-gel method. A more detailed explanation of these techniques is made in the following sections.

Sol-Gel Solution Synthesis

The primary goal that must be achieved in making these sol-gels is to obtain a reasonable stable, fairly concentrated, and completely solvated mixture of two or three metal alkoxides. The solutions need to be stable under an inert atmosphere during storage, and fairly stable after brief exposures to the moisture in air so that the same solution can be used for at least a few days in coating samples. The solutions should have a concentration of at least 0.1 molar[1] to encourage condensation to take place and to ensure an adequate thickness in the ceramic layer. The metal alkoxides need to be completely solvated so that the components will be mixed together on a molecular scale, thus improving the chances of obtaining a highly homogeneous ceramic. The metal alkoxide solutions developed in these experiments contained the proportions 50 mol% strontium-50 mol% cerium, and 30 mol% lanthanum-20 mol% strontium-50 mol% cobalt. A variety of different solvents and modifying agents were used in developing the final recipes for these two solutions.

Gelation

It is possible to minimize film shrinkage and stress cracking by controlling the solution gelation conditions. Chelating ligands and water addition can be used to control the extent of the hydrolysis and condensation reactions. The amount of water added to the sol-gel controls the rate and extent of hydrolysis and the chelating ligands block hydrolysis sites. It is desirable to avoid forming a three- dimensional polymer network because it is much more rigid and cracks more easily than a two-dimensional gel. Two-dimensional gels are formed by using chelating ligands to block all but two of the hydrolysis sites on each metal atom. Condensation therefore produces long polymer chains, which collapse easily as the solvent evaporates, reducing shrinkage stress on the gel film. This collapse also improves the degree of densification of the ceramic as the gel film is fired. Bulky side groups and ligands on the metal alkoxides should be avoided because they increase the amount of organic material that must be burned out of the gel and thereby increase both the shrinkage during burnout and the amount of densification that must take place in the final ceramic film.

Solution Deposition on Porous Substrates

The metal alkoxide coating solutions tend to wet the porous ceramic substrates that they are deposited on. Flow of the solution into pores is favored by capillary pressure. There are several methods that might be used to prevent the pores from filling with liquid. These include: manipulation of the ceramic's surface energy, filling the pores with a volatile material prior to coating, or using particulate sols.

In this project, however, the coating solution was not prevented from flowing into the pores. It has been shown[2] that initially capillary pressure acts to

rapidly saturate even the smallest pores, but, for pores under 10 microns in size, leakage of the coating solution through the substrate is extremely slow after initial saturation has been achieved. Film formation is therefore unaffected by this phenomenon for substrates with small pores, since an insignificant volume of coating solution is drawn into them. The coating solutions are relatively dilute, effectively containing less than 0.2 M of perovskite; the final LSC or SCY ceramic formed is less than 1% of the solution volume. Small pores are therefore relatively free of solid perovskite, even though they were initially filled with solution.

Film Continuity: Cracking and Porosity

The gel film undergoes considerable shrinkage as the solvent evaporates and the remaining organic material burns out as the specimen is fired to produce the crystalline perovskite ceramic. This shrinkage is partially constrained by the adhesion of the film to the substrate material. Most of the shrinkage occurs during the solvent evaporation process. During this time, the film is capable of flowing plastically to relieve the building stresses. Organic burnout and crystallization also generate significant strains within the film layer, and its increasing rigidity leads to the formation of residual stresses. These stresses may then be relieved by the growth of cracks through the film. Alternatively, the film may not densify completely so that residual stresses may not build up to the point that crack growth is favorable.

The most important parameter for determining the favorability of crack growth is the thickness of the film, however. Changing the viscosity of the sol-gel or the deposition parameters can be used to control the thickness of the film. The substrate characteristics also play an important role in determining the

probability of unstable cracking by dictating the degree of adhesion of the film to its surface.

Obtaining a continuous film is always an important goal. On flat, dense substrates, very thin films may break up during firing by diffusion[3]. On porous substrates, a continuous film across the tops of the pore openings may not be present. The critical relationship which determines film continuity here is the one that exists between the film thickness and the diameter of the substrate pores.

Film Characterization

X-ray diffraction (XRD) testing has been used to determine the crystallization behavior of these film materials as a function of firing temperature and of solution composition. Scanning Electron Microscopy (SEM) has been used to characterize film morphologies and thicknesses. Electron diffraction spectroscopy (EDAX) testing was used to determine the elemental composition and homogeneity of the ceramics. The chemical characteristics of the metal alkoxide solutions were investigated using Fourier transform infrared spectroscopy (FTIR).

2B: Preparation of Sol-Gels

A number of different methods were used to prepare the sol-gel mixtures used in these experiments. The basic technique remained the same throughout but details changed as ways to improve the solubility and clarity of the solutions were discovered. The best methods are presented here, and their evolution is discussed later.

La-Sr-Co Alkoxide Sol-Gels

The lanthanum-strontium-cobalt alkoxide solutions were made by weighing out quantities of lanthanum isopropoxide, strontium isopropoxide, and cobalt methoxide (all manufactured by Johnson-Matthey) into separate bottles in the drybox. Enough dry ethylene glycol was then added to each bottle to make 0.3 M lanthanum isopropoxide solutions, and 0.4 M strontium isopropoxide and cobalt methoxide solutions. The bottles were then tightly closed, removed from the drybox and shaken for fifteen minutes in an ultrasonic cleaner. They were then returned to the drybox and a 1:1 molar ratio of glacial acetic acid to alkoxide was added to each cloudy mixture. The bottles were then closed again, removed from the drybox, and replaced in the ultrasonic cleaner, where they were shaken in warm ($\cong$ 60°C) water until the metal alkoxides dissolved. The cobalt methoxide and strontium isopropoxide both dissolved in less than half an hour under this treatment, while the lanthanum isopropoxide took at least 1½ hours to dissolve completely. The cobalt methoxide solution was a clear, very dark purple; the strontium isopropoxide was a clear, light yellow; and the lanthanum isopropoxide was clear and colorless, with a slight white cloud to it. This clouding occurred at any concentration and may be lanthanum hydroxide or oxide decomposed from the alkoxide.

Ethylene glycol was finally chosen as the solvent for three reasons. First, all three metal alkoxides were at least weakly soluble in it; and second, the low vapor pressure coupled with a high boiling point are excellent characteristics for a solvent in a thin, high surface area gel that must be dried slowly to prevent stress cracking. Third, the relatively high viscosity of ethylene glycol is convenient because by diluting with less-viscous solvents it might be possible to

control the thickness of the deposited films and, again, decrease their tendency to cracking as they dry.

These three stock solutions were then mixed together to make a solution containing the correct proportion of each metal alkoxide (30 mol% La, 20 mol% Sr, and 50 mol% Co). This mixing was sometimes done into an equal volume of dry 2-methoxyethanol and created a solution having a concentration of about 0.18 M metal alkoxide. When fresh, this final solution is a clear reddish purple in color, which darkens as it ages to a dark brownish purple. A small amount of greenish or purplish precipitate (probably a Co species, from the color) may form from the solution, as well. This indicates that the solution is somewhat unstable when exposed to air, but that is expected from any metal alkoxide solution, particularly one containing a transition metal. The solution appears to be stable for at least two weeks when not allowed to contact air. No large-scale precipitation or gelation occurs within three weeks if the exposures to air are kept brief.

Sr-Ce Alkoxide Sol-Gels

The strontium-cerium alkoxide solutions were made by weighing out stoichiometric quantities of strontium isopropoxide and cerium isopropoxide (both manufactured by Johnson-Matthey) and adding enough dry 2-methoxyethanol to produce a 0.2 to 0.4 M metal alkoxide solution. The bottle was then tightly capped, removed from the drybox, and shaken in the ultrasonic cleaner until the metal alkoxides dissolved (approximately 30 minutes), creating a clear dark brown solution.

At this point, because it was believed that some variety of preferential precipitation was occurring, an attempt was made to use small amounts of water

as a catalyst to link the two alkoxides together and so prevent one from precipitating out of solution exclusive of the other[4] during film deposition. This was done by refluxing the metal alkoxide solution for several hours under an inert atmosphere in dried glassware. A diagram of this apparatus is shown in Figure 2.1. These solutions were reasonably stable and no visual signs of aging were detected until several brief exposures to air had been made.

2C: Powder Preparations

To determine the temperatures at which various crystalline phases began to appear and then to disappear from the LSC-precursor sol-gel, a series of pellets was prepared using powder cbtained from the hydrolyzed and condensed metal alkoxides. The procedure used to mix the metal alkoxides was less sophisticated than the one detailed in the first part of this section, and so is briefly described here. The three metal alkoxides were mixed together in dry hot ethylene glycol, producing a partially solvated mixture. A small amount of DEA was added, to no visible effect. This mixture was then slowly hydrolyzed over several days, producing some color changes but no visible gelation or heavy precipitation, and then stirred and heated simultaneously to evaporate the solvent. The final product was a heavily agglomerated dark purple mottled powder.

This powder was then pressed into pellets that were fired at various temperatures to determine the progression of crystalline phase formation, as detailed in Chapter 3. At the same time, powders were prepared from a standard mixture of $La(OH)_3$, $SrCO_3$, and Co_3O_4, and from a La-Sr-Co nitrate solution in water. This solution was then mixed with either polyacrylamide (PAC) or polyacrylic acid (PAA) to form a gel. The polymer was added to the nitrate

and water solution to keep all the nitrates in an intimate mixture as the water evaporated. Crystalline phases formed in the different types of powder was compared to determine precursor homogeneity. A similar process was used to obtain some SCY-precursor powder although gelation occurred quickly in this material upon hydrolysis and so no mixing was required during the solvent evaporation step.

2D: Sol-Gel Film Deposition

The sol-gel LSC films were deposited on a variety of substrates using the two basic methods of dip and spin-coating. Initially, pieces of single crystal silicon wafer and fused quartz were used as substrates, but these were soon abandoned for various types of alumina substrates because they suited the experimental parameters better. Smooth, nonporous disks of α-alumina, porous γ-alumina U. S. Filter pieces, and disks of porous θ/δ-alumina Anotec filters were used in most experiments. The two types of alumina disk could be either spin- or dip-coated. The U. S. Filter pieces could only be dip-coated because of their shape.

The hydrolysis and condensation reactions taking place in the films were not regulated by any systematic addition of water. It was assumed, from the evidence of other experiments[2], that enough water reaches the sol-gel film from the air during deposition to encourage these reactions to take place. The extreme thinness of the film and the high surface area it presents to the air make this a reasonable assumption. Although the spin-coating rotation speed could be controlled, the pull-up rate for dip-coating could not. In dip-coating, excess solution was allowed to gather at the lowermost edge of the substrate and then carefully blotted off, but no other method of controlling the film thickness was

available. However, the results obtained were good enough to conclude, as seen later, that the films were quite forgiving of the dip-coating parameters.

The viscosity of these solutions was relatively high, since ethylene glycol is noticeably more viscous than alcohol solvents. This implies that the films deposited will be somewhat thicker than films made from solutions using the more usual alcohols. Single and multiple coating specimens were made and examined to determine the differences in film morphology and microstructure as the film thickness increased.

2E: Firing Parameters

There are two basic problems that must be solved in firing these sol-gel films. The first of these is to remove all the solvent and burn out the residual organic groups at a rate slow enough to allow the film to collapse and plastically flow to relieve stress. The solution to this problem is to use a very slow (less than 1 °C/min) temperature ramp rate. The second problem is to obtain a dense film from the initial, dilute solution layer. Unfortunately, the solution to this problem is exactly the opposite of the solution to the first problem, since good densification usually results from a high temperature ramp rate. This somewhat counter-intuitive behavior may be the result of greater hydroxyl group retention at elevated temperatures by the rapidly heated sample. These hydroxyl groups decrease the viscosity of the sample, allowing plastic flow of the film material to continue for a longer time under the stimulus of a relatively high temperature[5]. However, this high ramp rate is likely to cause bloating and shrinkage cracking at the beginning of the firing cycle, as the film rapidly loses all its solvent and organics without time to readjust.

The compromise solution, then, is to use a very slow ramp rate until organic burnout is complete, at around 400°C and then increase the ramp rate to reach the final firing temperature as rapidly as possible. The firing temperature is usually around 700 to 800°C, for reasons that will be explained later. The results of this treatment are presented in Chapter 3.

The LSC-precursor powders, once pressed into pellets, were fired using a ramp rate of 1 °C/min to temperatures between 400°C and 1100°C. Severe cracking and bloating of the sol-gel and polymer-gel pellets began occurring at around 250°C. The pellets did not densify completely because of their thickness and the large quantities of organic material that had to be burned out. The final masses of these pellets were approximately 50% of their original masses, and extremely fragile.

The film and powder specimens were then examined using XRD and SEM to determine their characteristics, as reported in Chapter 3.

References--Chapter 2

1 Y. Takahashi and Y. Matsuoka, "Dip-Coating of TiO_2 Films Using a Sol Derived from Ti(O-*i*-Pr)$_4$-diethanolamine-H_2O-*i*-PrOH System," *J. Mat. Sci.*, **23**, 2259-2266 (1988).

2 T. W. Kueper, "Sol-Gel Derived Ceramic Electrolyte Films on Porous Substrates," Ph.D. Thesis, University of California, Berkeley, 1992.

3 K. Miller, F. Lange, and D. Marshall, "The Instability of Polycrystalline Thin Films: Experiment and Theory," *J. Mat. Res.*, **5** [1], 151-160 (1990).

4 C.-H. Lu, K. Shinozaki, and N. Mizutani, "Sol-Gel Preparation of Ferroelectric Perovskite $Pb(Fe_{2/3}W_{1/3})O_3$ Powders," personal communication.

[5] C. J. Brinker and G. W. Sherer, *Sol-Gel Science: The Physics and Chemistry of Sol-Gel Processing*, 1st ed., Academic Press, Inc., San Diego Calif., pp. 712-716 (1990).

Chapter 3: Experimental Results

3A: $La_{0.6}Sr_{0.4}CoO_3$ Results

Solution Chemistry

The major problem encountered in obtaining a good quality LSC sol-gel is finding a combination of solvents and modifying chemicals that will completely solvate all three metal alkoxides, while leaving them free to hydrolyze and condense. Table 3.1 contains a chart of available solvents and the degree of solvation the three unmodified metal alkoxides experience in each one. From these results, ethylene glycol would appear to be the best solvent available for a mixture of these metal alkoxides, but at a reasonable (0.1-0.2 M metal ion or more) concentration, the quality of the overall solution is extremely poor.

Pre-Hydrolysis Chemistry and Behavior

It was determined in some experiments that adding very large quantities of diethanolamine (DEA) to the metal alkoxide solution would solvate lanthanum isopropoxide and cobalt methoxide in isopropanol or methanol, and strontium isopropoxide in isopropanol. However, such large quantities of DEA are necessary that it seem very likely that all of the alcohol ligands are replaced with diethanolamine ligands, so that a complex of the following type is formed:

$$M(OR)_x + xNH(CH_2CH_2OH)_2 \rightarrow M[(OCH_2CH_2)_2NH]_{x/2} + xROH \qquad (3.1)$$

This reaction produces an unhydrolyzable product and prevents condensation polymerization of the sol-gel. This in turn tends to have the undesirable effect of retarding crystallization in the film. If a linked condensation product is to be

obtained, no DEA should be added to strontium or cobalt (II) alkoxides, and nothing higher than a 1:1 molar ratio should be used with lanthanum (III) alkoxides.

It was discovered that adding a 1:1 molar ratio of glacial acetic acid to metal alkoxide significantly increased the solubility of all three of these metal alkoxides in ethylene glycol, from a maximum concentration of less than 0.05 M to 0.3 M for lanthanum isopropoxide and 0.4 M or more for strontium isopropoxide and cobalt (II) methoxide. Additional experiments using other solvents revealed this behavior for some of the alkoxides in some of the other solvents examined, as shown in Table 3.2. Cobalt methoxide had the most consistently increased solubility, and so if a less viscous, higher vapor pressure solvent becomes desirable, it might be possible to obtain a good solution by adding acetic acid only to this metal alkoxide and then blending the product with the other, more widely soluble, alkoxides.

The acetic acid reacts with the metal alkoxide to form a metal alkoxide-acetate, as shown below.

$$M(OR)_x + CH_3COOH \rightarrow M(OR)_{x-1}(OOCCH_3) + ROH \qquad (3.2)$$

The acetate ligand is more polar than an alkoxide group and is less bulky than most alkoxides, giving a less sterically hindered product. This metal alkoxide-acetate may then dissolve more readily in polar solvents such as methanol (CH_3OH), ethylene glycol ($HOCH_2CH_2OH$), or 2-methoxyethanol ($CH_3OCH_2CH_2OH$). The substitution of a carboxylate (any carboxylic acid ligand) for an alkoxide generally has two additional effects. First, if it is a small group, its presence may speed the rate of hydrolysis of the unsubstituted

alkoxides by removing steric barriers. Second, the carboxylate group is generally resistant to hydrolysis, and acts to block its reaction site to M-O-M bond formation.

An interesting result of this experimentation with chemical modification was seen when the three 1:1 acetic acid-substituted metal alkoxides were mixed in ethylene glycol. At first the slightly cloudy pink solution seemed to be a stable combination, but some undesirable developments occurred within twelve to twenty-four hours. Large pinkish-white irregularly shaped precipitates began to form and within two to three days the whole, unhydrolyzed mixture would gradually thicken to produce an opaque, pink, coarsely granular gel. The rapidity of this change depends in part on the amount of acetic acid added to the solution. As the solution pH goes down from 8 to 4, precipitation and gelation occur more and more rapidly. Above a pH of 8, the solution is more a light violet than pink, and no granular precipitation takes place. The solution will gradually thicken and grow opaque over a period of two or three weeks, however. A mixture of these metal alkoxides in ethylene glycol without any acid or water added had a pH between 11 and 12. A solution with a one mole metal alkoxide to one mole acetic acid ratio had a pH between 7 and 9. The pH of these solutions changes rapidly with small additions of acid from 12 down to 6, and very slowly thereafter.

The most active gel-forming component of these metal compounds is the lanthanum diisopropoxide monoacetate ($La[OCH(CH_3)_2]_2[OOCCH_3]$). Two or more moles of acetic acid cause the formation of a gel without hydrolysis, so a polymer is being formed by the reaction series:

i. $La(OOCCH_3)(OCH(CH_3)_2)_2 + CH_3COOH \rightarrow La(OOCCH_3)_2(OCH(CH_3)_2) + HOCH(CH_3)_2$ (3.3a)

ii. $2La(OOCCH_3)_2(OCH(CH_3)_2) \rightarrow ((CH_3)_2CHO)(CH_3COO)La(OOCCH_3)_2La(OOCCH_3)(OCH(CH_3)_2)$ (3.3b)

where each repeat group in the lanthanum complex oligomer is probably structured something like:

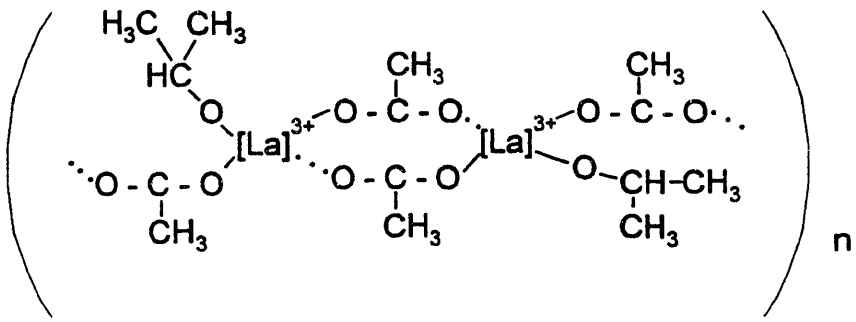

This structure is consistent with the measured FTIR absorption spectrum showing a chelated $[C^-O\cdots]^-$ group ion stretching vibration at about 1580 cm^{-1}, but not an unionized C=O stretching vibration peak at 1700 cm^{-1}. These FTIR results are consistent with an ionized

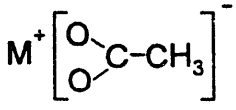

-type structure described in the book Metal Carboxylates, by Mehrotra and Bohra[1]. Since the FTIR spectra of the cobalt and strontium alkoxide acetate compounds show similar peaks, it can be concluded that they, too, contain

metal-oxygen bonds that are mostly ionic in character, and similar to the lanthanum dialkoxide monoacetate structure.

The coordination number of La(III) is usually eight or nine. The coordination sites remaining open in the oligomeric structure are filled by associations between the metal ion and the ethylene glycol or 2-methoxyethanol -OH groups.

Some other conclusions as to the pre-hydrolysis behavior of these materials can be made from the results of mixing the three acetate-substituted metal alkoxides together. A mixture of the lanthanum and strontium compounds results within minutes or hours in the formation of a hard, opaque white gel. The simplest explanation of this behavior is that the strontium isopropoxide does not convert to $Sr(OOCCH_3)(OCH(CH_3)_2)$ as readily as lanthanum isopropoxide does to $La(OOCCH_3)_x(OCH(CH_3)_2)_{3-x}$. Therefore, more acetic acid is available for exchange with the isopropoxide ligands in lanthanum diisopropoxide monoacetate when the lanthanum and strontium-containing solutions are mixed together, and gelation of the lanthanum acetate via the reaction described in equation 3.3b is produced. Gelation also occurs in a mixture of acetate-substituted lanthanum isopropoxide and cobalt methoxide. This reaction is far slower, taking place over a span of weeks or months. This indicates that the cobalt methoxide is far more strongly acetate-substituted than the strontium isopropoxide is, leaving a much smaller amount of acetic acid available for exchange reactions with the remaining isopropoxide ligands bonded with the lanthanum ion. These gels are cloudy and opaque from the lanthanum polymer, but are pink from the solvated cobalt compound's strong pigmentation.

In addition to the exchange reactions between the alkoxide ligands and acetic acid, an exchange reaction between the alkoxide ligands and the solvent

ethylene glycol may take place. Ethylene glycol is more electronegative in character than isopropanol or methanol, but much less electronegative than acetic acid or water. Alternatively, some ethylene glycol molecules may simply form a loose association around the metal acetate alkoxide in order to form a more highly coordinated complex. No direct evidence in the form of FTIR spectral changes or other data exists to support either theory. In view of the accumulated data on alkoxide-glycoxide reactions available in the book Metal Alkoxides[2], however, it seems likely that some such exchange reactions may take place over time, following the form

$$M(OOCCH_3)(OR)_{x-1} + HOCH_2CH_2OH \rightarrow (RO)_{x-2}(CH_3COO)M(OCH_2CH_2OH) + HOR \quad (3.4)$$

where the $M(OCH_2CH_2OH)$ group probably has the structure:

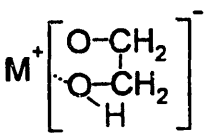

Such a glycoxide ligand is rather bulkier than the original alkoxide ligand, but helps fulfill the metal ion's coordination number better. Since ethylene glycol is being used as a solvent it is present in a large excess. It therefore seems unlikely that the following dimerization reaction would occur for a large number of molecules because of the mild solvation conditions, but it might be plausible at lower glycol concentrations and more active reaction conditions:

$$2(RO)_{x-2}(CH_3COO)M(OCH_2CH_2OH) \rightarrow \quad (3.5)$$

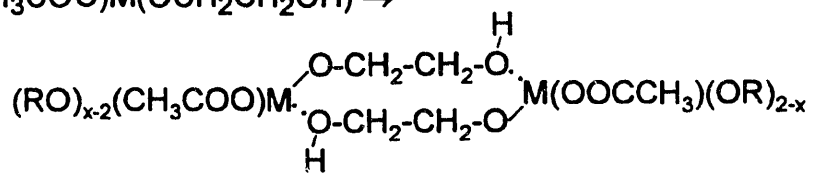

if the less sterically bulky and more electronegative acetate ligands do not begin constructing a polymer by linking in the form of equation 3.3b first. In any case, the glycoxide ligands are expected to be nearly as vulnerable to hydrolysis as the alkoxide ligands they replace, since they are not nearly so strongly electronegative in character as an acetate or hydroxide ligand.

A possible solution to the problem of premature gelation due to acetate bonding in this system would be to decrease the amount of acetic acid added to the strontium isopropoxide and the cobalt methoxide components, particularly the former. A 1:1 ratio of metal alkoxide to acetic acid causes rapid dissolution in both these systems but some acetic acid is not reacted with the metal alkoxide. A ratio of 1:0.5, for example, might result in less rapid dissolution, but less free acetic acid would be available for exchange reactions with the lanthanum diisopropoxide monoacetate solution when it is added in. An additional advantage to this possible solution is that more strontium and cobalt-oxygen chains can form when the solution is hydrolyzed.

Hydrolysis and Condensation Chemistry and Behavior

If no chemical modifications are made to the three metal alkoxides before adding water to the mixtures, the results can be quite different from the behavior of modified solutions. Solution behavior can also be changed by modifying the solvent used. For instance, a mixture of lanthanum isopropoxide, strontium isopropoxide and cobalt methoxide, originally 0.1 M metal in a mixture of half

ethylene glycol and half 2-methoxyethanol, condenses to form a soft, opaque, blue-gray gel after water is gradually added to obtain a final ratio of about 110 moles water to one mole metal alkoxide. A similar mixture using only ethylene glycol as a solvent produced an opaque blue-green liquid that did not gel either during or after the gradual addition of about 110 moles water to one mole metal alkoxide.

Unmodified lanthanum isopropoxide does not dissolve well in ethylene glycol and the cloudy white appearance of the mixture does not change even after considerable water is added. Strontium isopropoxide dissolves more readily, but a precipitate forms and falls out of solution as it hydrolyzes. Similar behavior has been observed in solutions with 2-methoxyethanol, methanol, and isopropanol. A slightly solvated cobalt methoxide in ethylene glycol mixture becomes a soft opaque greenish-blue gel as it hydrolyzes and condenses.

Adding DEA to any of these mixtures does not seem to improve the metal alkoxide solubilities to a significant degree until far more than a 2:1 molar ratio of DEA to metal alkoxide has been reached. At these high levels, the DEA effectively prevents enough hydrolysis and condensation from occurring to form a gel. The color of the mixed alkoxide solution may change from pink to green as water is added, probably from the cobalt ions' coordination numbers changing from four to six, but no other visible changes occur.

Modifying the mixed metal alkoxide solution with acetic acid slows the rate of hydrolysis and condensation of the solution considerably. As water is added, the character of the solution changes considerably. The color changes from pink or violet to a light brown, and the slight white cloud from the lanthanum isopropoxide seems to disappear, being replaced by an equally slight brown precipitate. This change takes place even after exposure to atmospheric

moisture, if the solution pH is above eight. This color change can be reasonably attributed to a hydrolytic change of coordination number by some of the cobalt (II) methoxide monoacetate. The octahedrally coordinated complexes tend to a green or blue color, while the tetrahedrally coordinated complexes tend to a red or pink color. A combination of red and green makes brown, the color of the hydrolyzed solution. The brown precipitation is therefore caused by the condensation of some of these hydrolyzed compounds.

The series of reactions that may be taking place to produce this visible change of the solution color and character are then

Hydrolysis:

$$Co(OOCCH_3)(OCH_3) + H_2O \rightarrow Co(OOCCH_3)(OH) + HOCH_3 \quad (3.6a)$$

$$Co(OOCCH_3)(OH) + H_2O \rightarrow Co(OOCCH_3)(OH)\cdot H_2O \quad (3.6b)$$

$$Co(OOCCH_3)(OH)\cdot H_2O + H_2O \rightarrow Co(OOCCH_3)(OH)\cdot 2H_2O \quad (3.6c)$$

$$Co(OOCCH_3)(OH)\cdot 2H_2O + H_2O \rightarrow Co(OOCCH_3)(OH)\cdot 3H_2O \quad (3.6d)$$

$$Co(OOCCH_3)(OH)\cdot 3H_2O + H_2O \rightarrow Co(OOCCH_3)(OH)_2\cdot 4H_2O \quad (3.6e)$$

Condensation:

$$2Co(OOCCH_3)(OH) \rightarrow (CH_3COO)Co\text{-}O\text{-}Co(OOCCH_3) + H_2O \quad (3.6f)$$

$$Co(OOCCH_3)(OH) + Co(OOCCH_3)(OCH_3) \rightarrow (CH_3COO)Co\text{-}O\text{-}Co(OOCCH_3) + HOCH_3 \quad (3.6g)$$

and similar reactions for the water-coordinated cobalt complexes. The condensed compounds are all dimers, so no gelation occurs in this system; only precipitation of some of the hydrated complexes.

An additional cause of this change in color is the presence of lanthanum diisopropoxide monoacetate in the solution. Adding water to a solution of cobalt monomethoxide monoacetate by itself or mixed with strontium monoisopropoxide monoacetate does not produce any color change or gelation, although too quick or massive an addition will produce some precipitation. The white lanthanum complex precipitates probably act as nucleation centers for the condensing cobalt-complex dimers to adhere to.

Strontium monoisopropoxide monoacetate begins to form precipitates as it hydrolyzes. This behavior is no worse than that of unmodified or 1:1 DEA-modified strontium isopropoxide, which also forms fine precipitates when reacted with water. Lanthanum diisopropoxide monoacetate forms a clear, rigid gel as it hydrolyzes (approx. 100 moles H_2O:1 mole lanthanum ion) and condenses, but the ever-present fine precipitates may form a surface layer, or be distributed throughout the gel. The reaction sequence taking place here is definitely

Hydrolysis:

$$La(OOCCH_3)(OCH(CH_3)_2)_2 + H_2O \rightarrow La(OOCCH_3)(OCH(CH_3)_2)(OH) + HOCH(CH_3)_2 \quad (3.7a)$$

$$La(OOCCH_3)(OCH(CH_3)_2)(OH) + H_2O \rightarrow La(OOCCH_3)(OH)_2 + HOCH(CH_3)_2 \quad (3.7b)$$

Condensation:

$$2La(OOCCH_3)(OCH(CH_3)_2)(OH) \rightarrow \quad (3.7c)$$

$$((CH_3)_2CHO)(CH_3COO)La\text{-}O\text{-}La(OOCCH_3)(OH) + HOCH(CH_3)_2$$

extends polymerically as condensation continues

$$2La(OOCCH_3)(OH)_2 \rightarrow (CH_3COO)(OH)La\text{-}O\text{-}La(OH)(OOCCH_3) + H_2O \quad (3.7d)$$

extends polymerically as condensation continues

$$O(La(OOCCH_3)(OH))_2 + La(OOCCH_3)(OH)_2 \rightarrow \quad (3.7e)$$

$$(CH_3COO)La\text{-}(O\text{-}La(OOCCH_3)(OH))_2 + H_2O$$

extends polymerically as condensation continues

and so on. All of the La-O- bonds are highly ionic in character.

A 0.2 M lanthanum-strontium-cobalt mixture forms a soft, cloudy light brown gel about 10 days after a gradual, massive (approximately 100 moles H_2O:1 mole metal ion) addition of water. The lanthanum complexes are expected to be the main source of network bonding to form this gel because they retain the largest number of sites active for polymerization since both acetate and hydroxide-type ligands are capable of bonding with another molecule. The compounds containing strontium and cobalt remain fairly well mixed into the gel on a molecular level without gelling much themselves, but some inhomogeneous precipitation of complexes of all three metals is probably present, and so this type of solution, while the best so far developed, is not entirely perfect. Decreasing the amount of acetic acid used to solvate the strontium isopropoxide and the cobalt methoxide may improve the solution characteristics for further experiments.

LSC Powder Preparations: Characteristics and Behavior

To evaluate the relative quality of the chosen alkoxide sol-gel ceramic preparation method, a series of alternative preparations were also made and their relative behaviors were compared. The first of these alternative preparations involved using lanthanum n-butoxide in place of lanthanum isopropoxide in a sol-gel preparation. The lanthanum isopropoxide solution was designated B, and the lanthanum n-butoxide preparation was labeled C. Two aqueous solutions of the metal nitrates, one with polyacrylic acid (PAA) and one with polyacrylamide (PAC) as gelling agents and an attritor-milled mixture of lanthanum hydroxide, strontium carbonate, and cobalt oxide were also synthesized. These three preparations were designated D, PAC, and E, respectively.

The five preparations were dried, hand-ground, and pressed into pellets. Batches of these pellets were then fired at different temperatures and examined for percent weight loss (shown in Figure 3.1), percent relative shrinkage (shown in Figure 3.2), and percent crystalline transformation, as deduced from their X-ray diffraction patterns and shown in Figures 3.3-3.6.

As can be seen from Figure 3.1, the nitrate preparations generally have the highest percent weight loss (up to 56%), while the standard preparation has the lowest (up to 12%). The B preparation loses no significant weight above 1000°C, while all the other preparations continue losing significant amounts between 1000 and 1100°C. Since the original organic content is removed below 400°C, this continued weight loss indicates that the transformation to LSC at 1000°C is more complete for preparation B than for the other preparations. This, in turn, implies that the component metals are more homogeneously distributed by the B synthesis than by any of the other syntheses.

In Figure 3.2, the percent volume shrinkage of the pellets as they are fired are compared. The two nitrate preparations are not included because cobalt nitrate and strontium nitrate melt before they decompose, producing significant distortion in the cylindrical pellet. Large blowholes and bloated "bubbles" also form even at low temperature ramp rates in these pellets. The amount of bloating the B and C pellets undergo make these shrinkage trends only approximate, but it is obvious that the ceramic obtained from preparation B shrinks and densifies far better than that obtained from preparation C. In all three cases, approximately one-third to one-half of the shrinkage obtained at 1100°C has occurred by 700°C. At 1100°C, the B pellet has obtained 48% of its theoretical density, while the C pellet has only 13% of its theoretical density, due to severe bloating. Pellet E, with a much higher green density, is actually equal to pellet B in its final density. From the standpoint of shrinkage and densification, therefore, the B-type preparation produces by far the best result in a pellet, and will probably produce equally good results in a film.

Quantitative examination of the X-ray diffraction patterns obtained for the different preparations at different temperatures in comparison with a standard mixture reveals the proportions of crystalline LSC, lanthanum hydroxide, strontium carbonate, and cobalt oxide (Co_3O_4) present for each set of conditions. These calculations were made using the mixed component method of Chung[3]. A graph showing the relative weight percents of crystalline LSC vs. temperature for the five different preparations is shown in Figure 3.3.

Several facts about these preparations become apparent upon examination of the trends in this graph. First, preparation B begins to transform significantly into LSC at 700°C, at least 100°C before any of the other preparations. The weight percent of crystalline LSC in B basically stops

increasing at 900°C, where it reaches a value of 92%. Also, it can be seen from Figures 3.4-3.6 (weight percent crystalline $La(OH)_3$ versus temperature, weight percent crystalline $SrCO_3$ versus temperature, and weight percent crystalline Co_3O_4 versus temperature, respectively) that the majority of the untransformed material above 900°C is strontium carbonate. There are two possible explanations for this observation.

First of all, the strontium carbonate not incorporated into the LSC may be due to an excess of strontium or lanthanum ions in the preparation, leading to a deficiency of cobalt ions and causing some of the strontium ions to not be preferentially absorbed into the LSC phase. This explanation is rather unlikely due to the fact that the B and C preparations were actually slightly strontium deficient and so some excess cobalt was available in the reaction mixture. The second, and more reasonable, explanation is that insoluble strontium carbonate precipitates form during firing and do not decompose easily into the LSC matrix. Similar behavior is seen in the fired C material, although complicated by other factors.

The C preparation shows characteristics similar to those of the B preparation, but with the undesirable properties magnified. A significant degree of transformation of the separate components to LSC occurs at 700°C, but only to a level of 70 wt%, compared to that of B, with 86%. Even at a firing temperature of 1100°C, only about 80% of the total weight of the C pellet is LSC. Significant quantities of Co_3O_4 and $SrCO_3$ remain present, and the overall pattern of the LSC peaks is more closely related to $LaCoO_3$ than $La_{0.6}Sr_{0.4}CoO_3$, indicating that little of the strontium is actually incorporated into the perovskite phase. These results indicate that a very inhomogeneous sol-gel is produced by preparation C, probably due to poor solvation of the lanthanum

methoxide in the original solution. In addition, the up-and down character of the C lines in Figures 3.3-3.6 indicates very poor mixing on the macro scale, with different proportions of the three components ending up in each of the analyzed pellets.

The transformation behavior of the D and E preparations is very similar, indicating that the PAA in D has very little effect in holding the component nitrates in solution together. Separated precipitates form, producing a beginning material no better than the standard powder preparation does. Major perovskite formation does not begin until 800°C, and complete transformation does not occur until a firing temperature of 1000 to 1100°C is used. However, 100% transformation is achieved, a distinct improvement over the results of the alkoxide preparations.

The PAC-nitrate preparation has converted to 77 wt% LSC by 700°C, better than any other preparation except B. The converted weight percent of LSC continues to rise gradually, reaching 93% at 900°C and full conversion at 1100°C. This behavior indicates that the PAC does a much better job than PAA of holding the mixture of nitrates in a microhomogeneous suspension, leading to a high degree of transformation at the lower temperatures.

Overall, the results of this analysis indicate that a high degree of transformation can be achieved by the sol-gel alkoxide or polymer-nitrate if the degree of solvation is good. However, complete or nearly complete transformation will not occur at any temperature below 900°C, and firing at 1100°C is probably best for complete certainty. Figures 3.7-3.11 compare the X-ray diffraction patterns for the five preparations at 700°C and 1100°C. The cobalt oxide peaks in the 1100°C E pattern can be ignored; excess cobalt oxide was present in this mixture due to an experimental error. This extra cobalt may

have improved the transformation behavior of this preparation; a 5-10 mol% excess of cobalt could also help transformation in the other preparations, but might also have a deleterious effect on the electrical properties of the material.

LSC Thin Film Characteristics and Appearance

The thin films of LSC deposited on various porous and nonporous substrates had a very different physical appearance than was initially expected. The yttria-stabilized zirconia films first prepared by Kueper[4] are nearly featureless in character, showing neither grain boundaries nor color variations. The LSC films laid down using an acetic acid-modified metal alkoxide solution showed both these characteristics as a rule, and experiments attempting to remove these features are described later in this section.

Alumina substrates, either 50 nm γ-alumina U.S. filters, 20 nm θ/δ-alumina Anotec filters, or nonporous α-alumina disks, were used for most of these coating experiments. Figure 3.12 shows SEM micrographs of the surfaces of the two filters.

Single Layer Films

The first attempts at achieving a thin film of crystalline LSC were made using spin-coating. A 20 nm pore size Anotec filter was coated using a speed of 1000 rpm and ramped at 0.5°C/min to the final firing temperature of 700°C. Two SEM micrographs of this film are displayed in Figure 3.13. The LSC film is granular in appearance, where the grains (vsible in Figure 3.13) have an average size of 0.25 microns. Threadlike microcracks, 0.1-0.3 microns long and less than 0.006 microns thick, are present between some of the grains. Surface inclusions on the filter are also coated, although at their edges the film has

peeled back and bare areas are visible. The film appears to be about 0.05 microns thick in this area, but occasional surface inclusions and large holes in the porous surface were not coated over. Shrinkage cracking was not found in the sample, and X-ray diffraction analysis of both surfaces showed nothing but the substrate pattern. Single-layer LSC films on Anotec filters were also fired at 800°C and 900°C, to see if the higher temperatures would increase the amount of sintering present in these films. No improvement was seen, and at 900°C the underlying substrate began to turn a bright blue color, indicating that enough cobalt was diffusing from the films into the substrate to form a visible cobalt aluminate spinel. This in turn indicates that firing these LSC films on alumina at 900°C or above will have the detrimental effect of pulling cobalt from the film via diffusion and (as shown later) causing it to break up instead of sinter. Again, X-ray diffraction analyses show only the aluminate filter pattern.

The edges of some of these films were very thick and showed a high degree of shrinkage cracking, exposing the substrate underneath (Figure 3.14a). At the same time, the central region of the filter could be very lightly covered and highly porous (Figure 3.14b). Decreasing the spin time and speed decreases this thickness variation, but the center of the filter often still suffers from poor coverage, indicating that spin-coating is not really the best way to obtain uniform, uncracked, and nonporous films.

In addition to the Anotec filter, a piece of single-crystal silicon was spin-coated with the LSC sol-gel mixture and fired at 800°C. A micrograph of this specimen is shown in Figure 3.15. Its appearance is somewhat different from that of the Anotec films. On silicon, the coating was considerably thicker, about 0.3 microns at one central area fracture surface, which indicates that much of the liquid coated on the Anotec filters was sucked into the pores. The surface of

the film on silicon is less homogeneous in character, with scattered lighter-colored precipitates in the matrix and deep surface micropores/cracks between 0.1 and 0.8 microns in length. Shrinkage cracks were not present, and the X-ray diffraction analysis of this film showed only the substrate pattern.

The success of coating these films with a layer of sol-gel derived YSZ was next examined. A piece of 0.02 micron Anotec filter with a single layer of LSC deposited on it was used as a substrate. The YSZ was then deposited on top via dip-coating, and fired at a slow rate to 700°C. In the darker areas, where the LSC film was thickest, the YSZ film was smooth and unbroken, as shown in Figure 3.16a. The film is about 70 nm thick in this region, and is broken by surface inclusions in some areas. As the underlying layer of LSC gets thinner, the YSZ layer begins to break up, resulting in the surface shown in Figure 3.16b.

A sintered pellet made of $La_{0.6}Sr_{0.4}CoO_3$ was spin-coated with a layer of the sol-gel solution and fired. The resultant surface, shown in Figure 3.17a, is a significant improvement over the uncoated surface of the pellet, seen in Figure 3.17b. If the larger pores in the substrate can be eliminated, a sol-gel coating of one or more layers of LSC on top should provide an excellent surface for depositing the YSZ on.

It therefore appears that single layer films on the porous substrates are generally too thin, and usually have areas that are inadequately covered. In addition, any surface dust or overly large pores in the surface will break the continuity of a single layer of film. The logical conclusion is that using multiple coatings of LSC may overcome these problems. As long as the total thickness of the films remains below one micron, shrinkage cracking is not expected to be a problem.

Multiple Layer Films

Initially, two sets of multiple-layer films were manufactured, one dip-coated with four layers of LSC sol-gel solution, and one with five layers. After each 0.02 micron pore size Anotec filter was dipped and the excess liquid was drained off, it was cured at 250°C after a slow ramp rate. This allowed for complete evaporation of the solvent, and for a portion of the organics in the sol-gel layer to burn out. This cycle was then repeated three or four more times, before the resulting film was given a final firing at 700°C.

The four layer films were 0.9 microns thick, and, as seen in Figure 3.18, were granular and porous both on and beneath the surface. Some areas, as seen in Figure 3.19a, were relatively dense with irregular, unconnected shrinkage cracking and small precipitates scattered at intervals. More typical areas, as shown in Figure 3.19b, were less dense, with pores and microcracks, but no shrinkage cracks and no distinct precipitates. Both areas contained the larger, angularly shaped inclusions seen in Figure 3.19b. An X-ray diffraction pattern (Figure 3.20a) of this film was analyzed, and showed a crystalline content of 43 wt% LSC, 35 wt% $SrCO_3$, and 22 wt% Co_3O_4. This is about half the expected degree of conversion to LSC taken from Figure 3.3, line B. The reason for this lower degree of conversion is probably that the B preparation powder had most of the solvent removed before being pressed into a pellet, resulting in a higher green density than is obtained in the thin film.

The five layer films were somewhat different in overall character than the four layer films. They were 1.1 microns thick and contained wide, unstable shrinkage cracks that broke the films into large, unconnected islands (Figure 3.21a), as expected for a film over the critical thickness of 1.0 micron. The surfaces of the films were similar in character to the less dense areas of the four

layer films (Figure 3.19b) but were much rougher vertically and bubbled in appearance, probably distorted from escaping vapors during the burnout stage of firing. Analysis of the X-ray diffraction pattern (Figure 3.20b) of one of these films produced a component proportion of 78 wt% LSC, 12 wt% $SrCO_3$, and 10 wt% Co_3O_4. An unknown amount of La_2O_3 was also present, probably lowering all these percentages by 3 or 4 points. Even so, the amount of material converted to LSC is significantly greater than for the four layer film, indicating that the alumina substrate may have an effect in suppressing transformation of the precursor sol-gel into crystalline LSC.

One of these five layer films was then re-fired at 1000°C, to determine how the thicker layer would behave under these conditions. As shown in Figure 3.22, this treatment causes the film to break up completely, probably due to the loss of cobalt from the film into the alumina substrate, turning it an intense, clear blue. The remaining film material, while badly separated, does appear to have sintered and lost its fine granular texture.

In general, these thicker coatings, particularly the four layer ones, give much better coverage of the porous surface than single coatings, and definitely contain some crystalline LSC. They are more porous and more likely to contain fine precipitates (discussed later) and high temperature sintering on alumina causes them to break up because of cobalt losses to the substrate. Using a finely porous LSC or LSMC substrate would remove this last problem entirely; sintering at 1000°C would then increase the amount of crystalline LSC, dissolve the precipitates, and densify the film.

High Ramp Rate Firing

The next variation which was investigated involved using a very high ramp rate from the 400°C burnout temperature to the firing temperature of 700°C. A regularly fired and a fast-ramped four layer film are compared in Figure 3.23. The regularly fired sample in Figure 3.23a is distinctly grainier than the fast-ramped sample in Figure 3.23b, indicating that this technique is successful in aiding low temperature densification in LSC. These coatings were laid down on 50 nm pore size U.S. Filter substrates, and were in general much more regular in nature than the films laid down on Anotec filters. Unfortunately, the curved surfaces of these filters made it impossible to perform X-ray diffraction analyses of the films.

Long-Term Behavior at Elevated Temperatures

Two fast-ramped films on U.S. Filter pieces, one made using two coatings and one made using four, was examined to determine their long-term behavior under a constant temperature of 650°C. Although the addition of an electrolyte layer and the other electrode will have a strong effect on this sort of behavior, these results are valuable in terms of isolated electrode testing, and for gas separation devices. The two layer film, as seen in Figure 3.24a, broke up completely after being held at 650°C for only twenty-four hours. It was about 0.3 microns thick. The four layer film, seen in Figure 3.24b, remained stable even after 96 hours at 650°C. It was not much thicker, being 0.4 microns in depth, but this seems to have been enough for continuing stability. Some of the surface material may have peeled off, from the unusually large amount of surface debris present, but the film is visibly intact. The film surface, seen in Figure 3.24b, is markedly more granular than the surface of the fast-ramped only sample in

Figure 3.23b, but contains no visible precipitates. The densification afforded by the fast-ramp firing is therefore probably temporary, but the homogeneity of the film may improve with time.

Some diffusion of cobalt into the surface of the γ-alumina filter does take place during these 650°C heat treatments. The more thinly coated filter, in particular, takes on a slight bluish tinge after 96 hours at 650°C, indicating the formation of cobalt aluminate spinel. The operational long-term stability of these films is therefore probably dependent on an LSMC substrate being used instead of the reactive alumina.

Precipitate Identification and Dissolution

The purpose of this experiment was to try and identify the fine precipitates present in many of the fired films. A thick coating of sol-gel solution was deposited on a flat α-alumina disk, which was then fast-ramp fired at 700°C as usual and heat treated at 650°C for 48, 96, and 144 hours. Micrographs of the film after each of these heat treatments are displayed in Figure 3.25. The accompanying X-ray diffraction patterns are shown in Figure 3.26. The precipitates definitely decrease in size (from an average of 0.10 μm at 48 hours to an average of 0.06 μm at 144 hours) as the heat treatment continues, indicating that the film quality does indeed improve as the treatment continues. X-ray diffraction pattern analysis indicates that the identity of the precipitate material is probably lanthanum oxide (La_2O_3); the relative intensity of the La_2O_3 2.97 d-spacing peak decreases from 1.4 at 48 hours to zero intensity at 144 hours. No cobalt oxide is detected in any of these tests; strontium carbonate may be present but its peaks, unfortunately, would be masked by the α-alumina peaks. Indirect evidence also suggests that these particles are lanthanum

oxide: the lanthanum isopropoxide solution is always slightly cloudy, indicating the presence of lanthanum-containing particulates in the sol-gel even at this early stage.

Cobalt Doping Anotec Filters

It was discovered that the Anotec filters could be doped with cobalt, forming a cobalt-aluminate spinel, without destroying the physical structure of the filter, although the 0.02 micron layer would peel away, leaving the 0.1 micron underlayer available as the deposition surface. It was thought that perhaps these doped filters would not absorb cobalt from the LSC layer, leaving it intact through a high temperature densification treatment. A three layer film fired at 700°C, shown in Figure 3.27, was continuous although with much larger grains than usual (an average size of 0.10 microns was observed), presumably because of the larger pores in the substrate. With the same film, fired at 1000°C, the specimen turned a more intense blue than before and the film broke up into fragments. Therefore, even though already heavily doped with cobalt, the filter continued to absorb cobalt from the film, causing it to destabilize.

Polymer-Nitrate Derived Films

In addition to the metal alkoxide sol-gel solutions, a polyacrylamide-metal nitrate solution was used to try and coat some substrates. Even when heavily diluted with water, however, films laid down using the solution tended to be patchy, and to contain bubbles of air. They also tended, as seen in Figure 3.28, to crack rather badly, although generally not into large separated islands.

3B: $SrCeO_3$ Sol-Gel Synthesis Results

Attempts to manufacture $SrCeO_3$ thin films from a sol-gel solution met with little success. The best solutions, with concentrations of up to 0.4 M metal alkoxide in 2-methoxyethanol, were clear, dark brown solutions with little or no visible precipitated material present before hydrolysis. If hydrolyzed in bulk, these solutions formed a firm orange-brown gel with a pale precipitate in suspension. This precipitate probably consists mainly of strontium complexes, while the gel is mostly cerium complexes, as concluded from observing the behavior of the separately hydrolyzed metal alkoxides.

The films made using these solutions were usually deposited on single crystal silicon wafer chips for easy X-ray diffraction analysis. If spun on, they were usually uncracked in appearance. However, none of these films, fired at temperatures ranging from 600°C to 1100°C, ever gave anything but high intensity cerium oxide, low intensity strontium carbonate, and occasional strontium silicate-related X-ray diffraction patterns. Figure 3.29 shows a typical X-ray diffraction pattern from one of these films, fired at 700°C.

The only time a true $SrCeO_3$ pattern was detected for a sol-gel prepared material was from a pellet fired at 800°C, seen in Figure 3.30. Films made using this solution did not transform into $SrCeO_3$. A high percentage of CeO_2 material was also present in this sample. Pellets made from mixed CeO_2 and $SrCO_3$ powders fired for 20 hours at 1400°C showed a clear $SrCeO_3$ pattern but again accompanied by a significantly intense CeO_2 pattern.

The lack of $SrCeO_3$ in the thin films is explained by a recent paper presented by Scholten et al.[5]. Strontium cerate is shown to be unstable in CO_2-containing atmospheres below a certain temperature range. The thin films in our experiments are fired, cooled, and stored in ordinary air. Their extreme thinness

and relatively high surface area make them very vulnerable to this sort of decomposition reaction, so that even if strontium cerate is formed during firing it decomposes as the film is cooled. A chart included with the paper reveals that in air strontium cerate is subject to decomposition below approximately 900°C. The presence of $SrCeO_3$ in the fired pellets is explained by the fact that material below the immediate surface of the pellet is not exposed to air and remains stable. With the thin films, however, this exposed surface layer is practically all that is present. Manufacturing thin films of $SrCeO_3$ and preventing them from decomposing is therefore a much more difficult problem than was originally expected.

References--Chapter 3

1 R. C. Mehrotra and R. Bohra, *Metal Carboxylates*, pp.12-15,48-60 (Academic Press, London 1983).

2 D. C. Bradley, R. C. Mehrotra, and D. P. Gaur, *Metal Alkoxides*, pp. 183-195 (Academic Press, London 1978).

3 F. H. Chung,"Quantitative Interpretation of X-ray Diffraction Patterns of Mixtures III: Simultaneous Determination of a Set of Reference Intensities," *J. Appl. Cryst.*, **8**, 17-19 (1975).

4 T. W. Kueper, "Sol-Gel Derived Ceramic Electrolyte Films on Porous Substrates," Ph.D. Thesis, University of California, Berkeley, 1992.

5 M. J. Scholten, J. Schoonman, J. C. van Miltenburg, and H. A. J. Oonk, "Synthesis of Strontium and Barium Cerate and Their Reaction with Carbon Dioxide," presented at SSPC 6, VIth European Conference on Solid State Protonic Conductors, Villard de Lans (France), Sept. 6-11, 1992.

Chapter 4: Conclusions

4A: $La_{0.6}Sr_{0.4}CoO_3$ Thin Film Synthesis Summary

An almost completely solvated LSC metal alkoxide solution can be synthesized by modifying the three alkoxides with acetic acid and using ethylene glycol as the solvent. Acetic acid reacts preferentially with cobalt methoxide or lanthanum isopropoxide over strontium isopropoxide. Too much acetic acid causes the lanthanum acetate-alkoxide compound to gel through acetate bonding, so as little acetic acid as possible should be used to prevent premature gelation. Some lanthanum-containing precipitates remain undissolved in any solution and are probably lanthanum hydroxides or oxides formed by decomposition of the lanthanum isopropoxide.

A comparison between the responses of five different powder preparations (two hydrolyzed metal alkoxide sol-gel, two polymer-metal nitrate gels, and one metal oxide-carbonate preparation) to heat treatment revealed that significant quantities of LSC formed from the metal alkoxide sol-gels and the PAC-metal nitrate preparations at 700°C, but full conversion cannot be expected at firing temperatures below 900°C. The lanthanum isopropoxide-strontium isopropoxide-cobalt methoxide preparation had the best densification and low-temperature LSC formation characteristics of the five materials.

The thin films of LSC manufactured using a metal alkoxide sol-gel precursor were uniformly unsintered and finely granular in appearance. Many of them also contain small inhomogeneous precipitates that are probably lanthanum oxide (La_2O_3). Thicknesses of up to 0.9 microns can be achieved by multiple coatings without inducing shrinkage cracking. If deposited on an alumina substrate, the film is not stable if heated over 900°C. This is due to the

formation of cobalt-aluminate spinel at the interface. Sintering may take place at 1000°C, but not at lower temperatures. Long heat treatments at 650°C will gradually dissolve the inhomogeneous precipitates into the surrounding film, but films less than 0.3 microns thick may break up under this treatment. A sintered porous LSC disc spin-coated with LSC sol-gel showed significant improvement in its surface characteristics.

In general, it can be concluded that finely porous LSC or LSMC is the best material to use as a supportive substrate for these LSC thin films. Firing the film at 1000°C is necessary to obtain a sintered film and to ensure complete transformation of the sol-gel precursor solution to LSC. Despite this requirement for high temperature treatment, the sol-gel technique remains valuable because of the homogeneity and smooth, even surface characteristics it imparts to the deposited films. Multiple coatings (total thickness 0.4 μm < x < 1.0 μm) are desirable to fill in larger pores, smooth surface roughnesses, and give the film enough strength to withstand high temperatures for long periods and remain intact.

4B: $SrCeO_3$ Thin Film Synthesis Summary

Synthesis of an $SrCeO_3$ thin film using the sol-gel method was not successful because of the instability of this material in carbon dioxide-containing atmospheres. The high surface area of the experimental films allowed any $SrCeO_3$ that formed during firing to decompose again upon cooling. A pellet pressed from sol-gel derived powder and fired at 800°C did contain $SrCeO_3$, mixed with CeO_2. Ordinarily, $SrCeO_3$ does not form until a temperature of 1000 to 1100°C is reached. Relatively low-temperature $SrCeO_3$ formation using a

metal alkoxide precursor is therefore a valid synthesis technique if the synthesis is performed and the film maintained in a CO_2-free atmosphere.

Tables and Figures

Table 1.1: Ionic and Electronic Conductivity Values for LSC and LSM

MATERIAL	TEST TEMPER-ATURE	CONDUCTIVITY (S cm-1)	TEST TYPE	REFERENCE NO.
$La_{0.7}Sr_{0.3}CoO_3$	600°C	σ_e = 150	4-pt DC	12
$La_{0.6}Sr_{0.4}CoO_3$	700°C	σ_i =0.15	4-pt ionic DC	15
$La_{0.6}Sr_{0.4}CoO_3$	800°C	σ_i = 0.40	4-pt DC	15
$La_{0.6}Sr_{0.4}CoO_3$	800°C	σ_e = 800	4-pt DC	15
$La_{0.7}Sr_{0.3}CoO_3$	800°C	σ_e = 400	4-pt DC	12
$La_{0.6}Sr_{0.4}CoO_3$	860°C	σ_i = 0.80	4-pt ionic DC	15
$La_{0.5}Sr_{0.5}CoO_3$	1000°C	σ_e = 5000	?	13
$La_{0.7}Sr_{0.3}MnO_3$	600°C	σ_e = 180	4-pt DC	12
$La_{.85}Sr_{.15}MnO_3$	600°C	σ_e = 90	4-pt DC	17
$La_{.79}Sr_{0.2}MnO_3$	700 C	$\sigma_i \cong 0.01$	ptntiostatic step	9, 16
$La_{0.7}Sr_{0.3}Mn$	800°C	σ_e = 260	4-pt DC	12
$La_{.85}Sr_{.15}MnO_3$	800°C	σ_e = 100	4-pt DC	17
$La_{.79}Sr_{0.2}MnO_3$	860°C	$\sigma_i \cong 0.10$	ptntiostatic step	9, 16
$La_{0.5}Sr_{0.5}MnO_3$	1000°C	σ_e = 300	?	13
$La_{.85}Sr_{.15}MnO_3$	1000°C	σ_e = 110	4-pt DC	17

Table 3.1 Solvation Characteristics of Unmodified La, Sr, and Co Alkoxides

Solvent (Dry)	Lanthanum Isopropoxide	Strontium Isopropoxide	Cobalt Methoxide
Methanol	Partial < 0.1 M	Soluble 0.1 M	No
Ethanol	<< 0.1 M	?	No
Isopropanol	Soluble 0.1 M	Partial 0.1 M	No
2-Methoxyethanol	Soluble 0.1 M	Soluble 0.1 M	No
Ethylene Glycol	< 0.1 M	Soluble 0.05 M	Partial <0.1 M
Toluene	Partial < 0.05 M	Partial < 0.05 M	No

Table 3.2 Solvation Characteristics of Acetic Acid Modified LSC Metal Alkoxides

Increased Solubility of:

Solvent (Dry)	Lanthanum Isopropoxide	Strontium Isopropoxide	Cobalt Methoxide
Methanol	No	No	Yes
Ethanol	No	?	Yes
Isopropanol	?	?	Slight
2-Methoxyethanol	Yes	?	Slight
Ethylene Glycol	Yes	Yes	Yes
Toluene	No	No	No

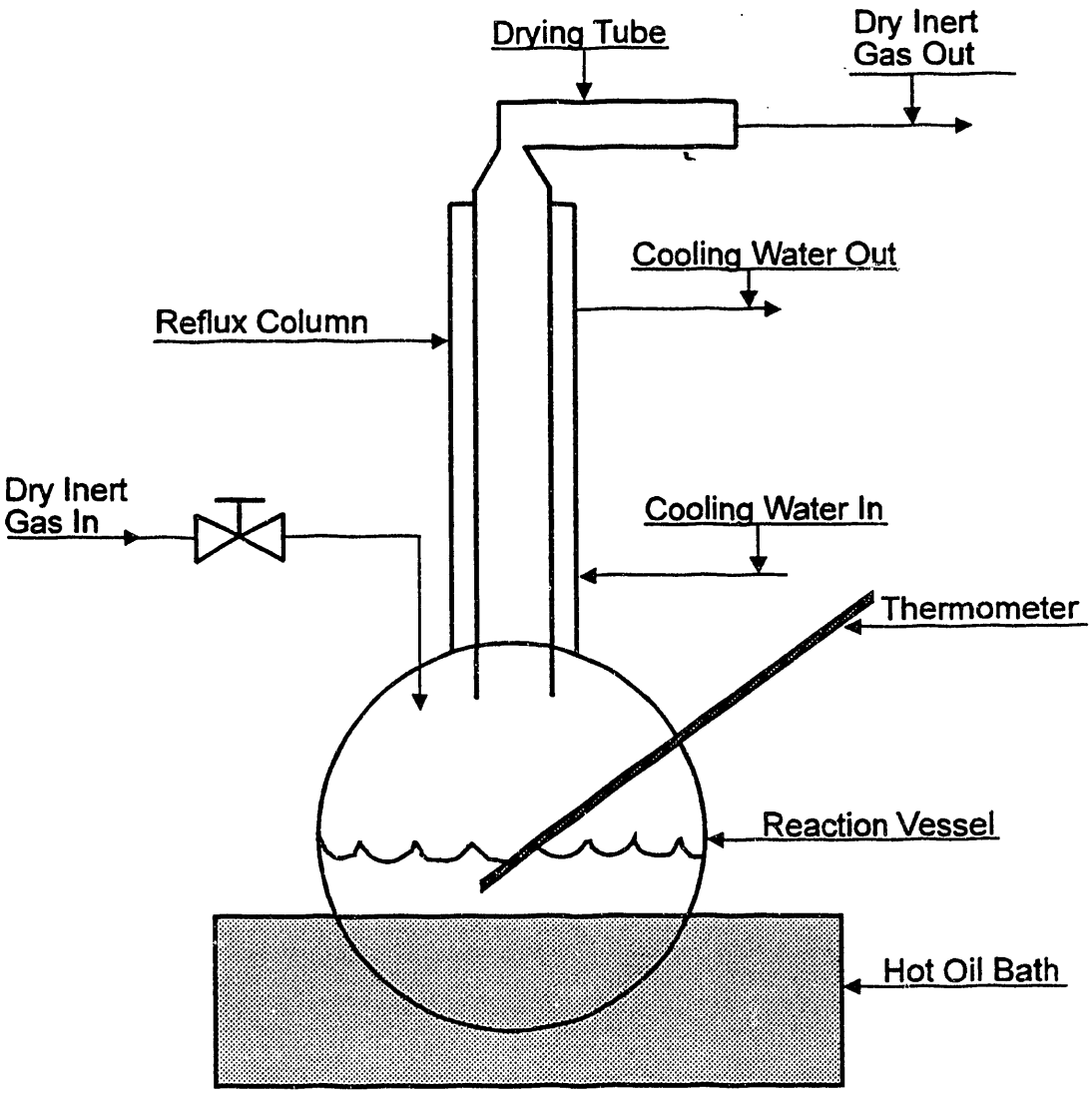

Figure 2.1 Reflux apparatus for $SrCe_{0.95}Y_{0.05}O_3$ sol-gel synthesis.

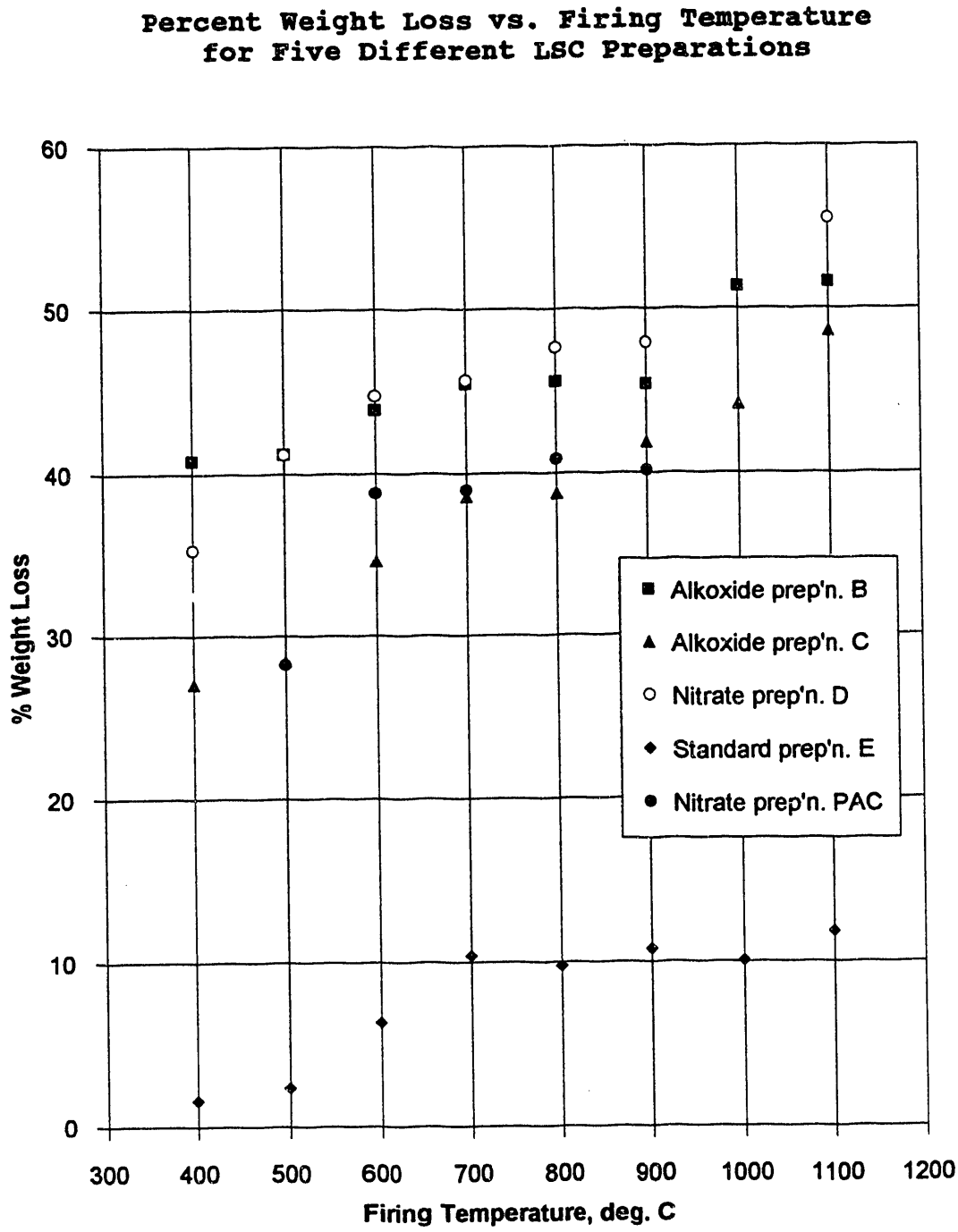

Figure 3.1 Percent weight loss versus temperature comparison for pellets synthesized from the five preparations.

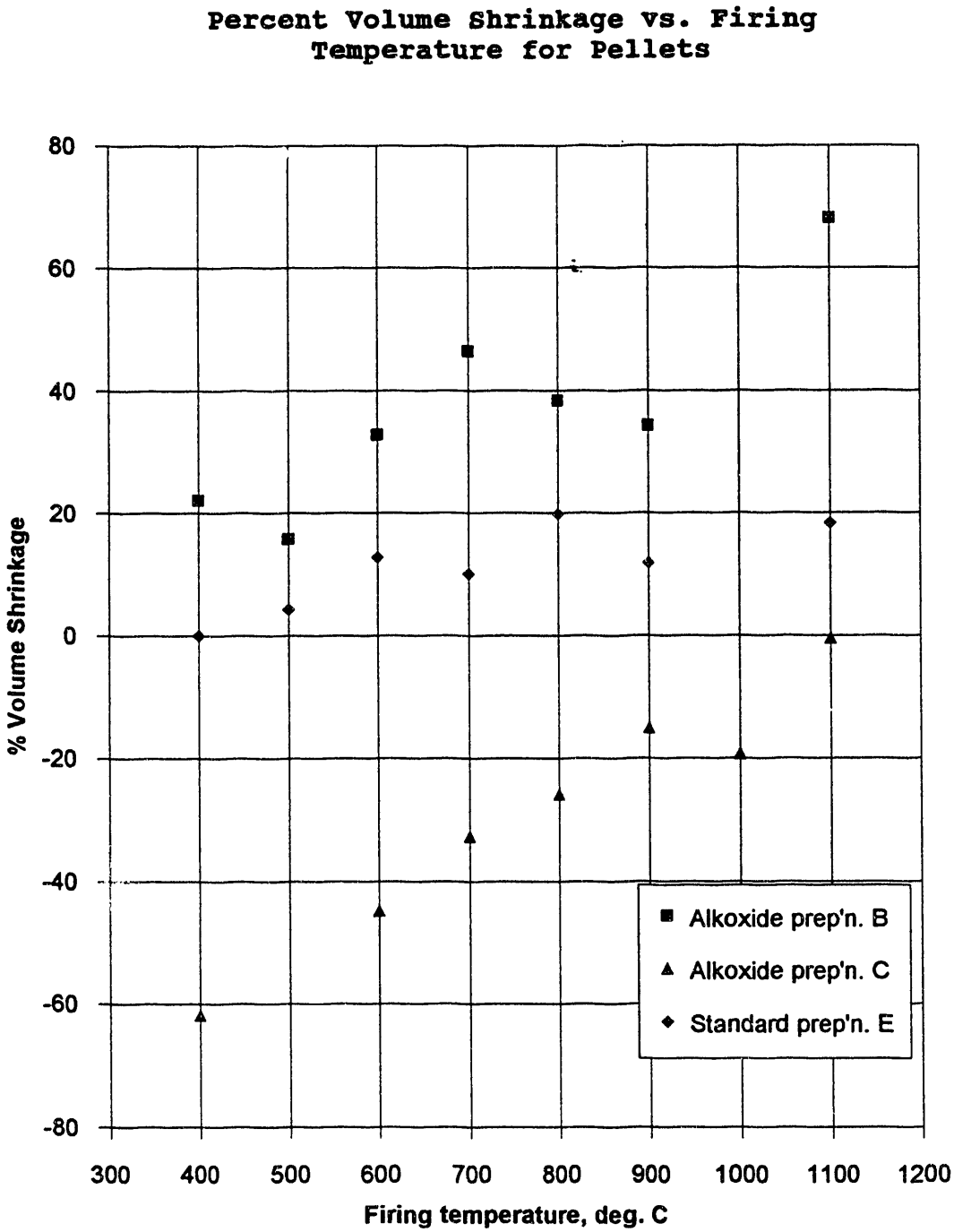

Figure 3.2 Percent volume shrinkage of the pellet versus temperature for the B and C sol-gel alkoxide preparations, and the standard powder preparation, E.

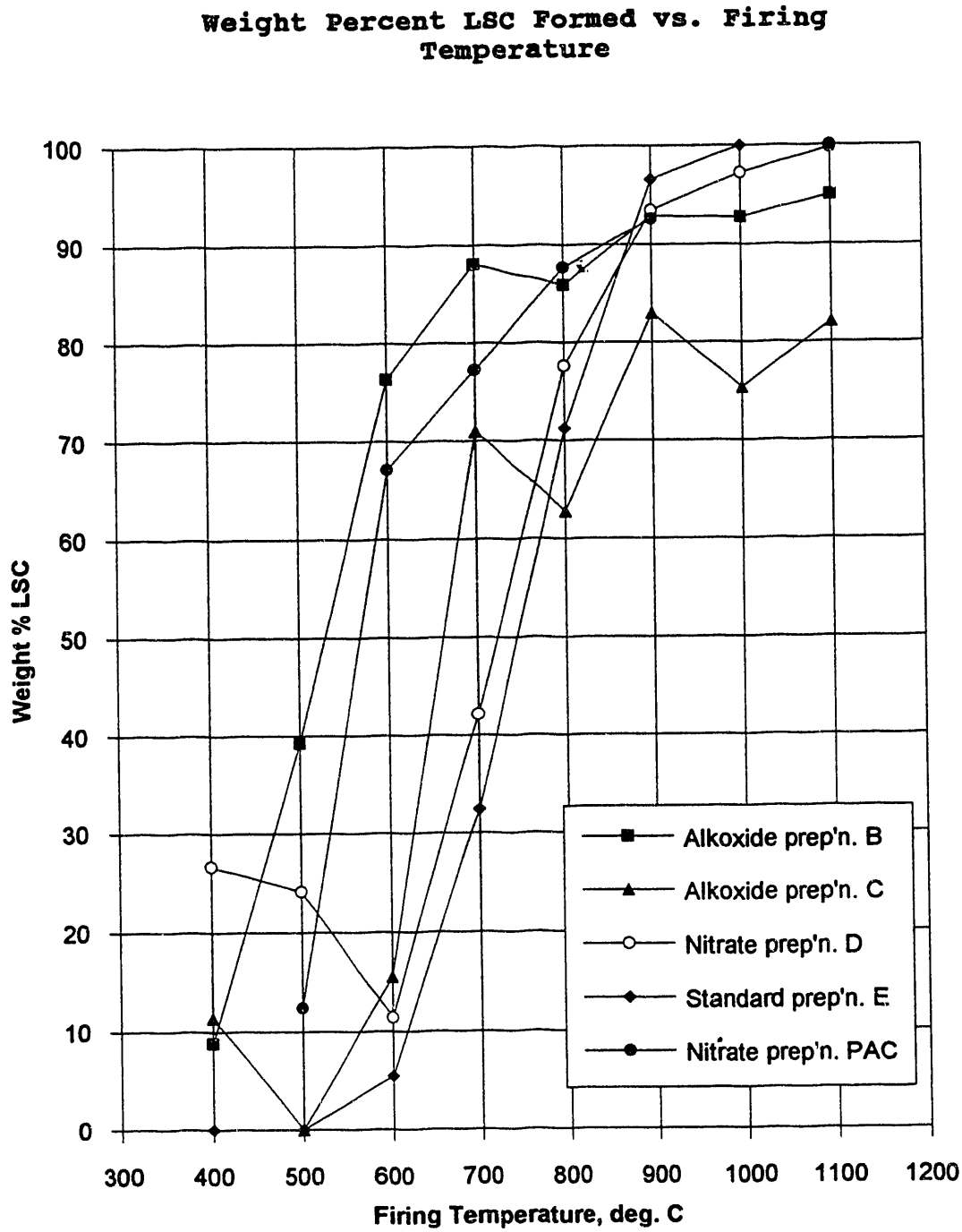

Figure 3.3 Graph of the percentage of crystalline $La_{0.6}Sr_{0.4}CoO_3$ versus firing temperature for pellets made from preparations B, C, D, E, and PAC. The quantitative analysis was performed using the method of Chung, and has an accuracy of $\pm$5 wt%.

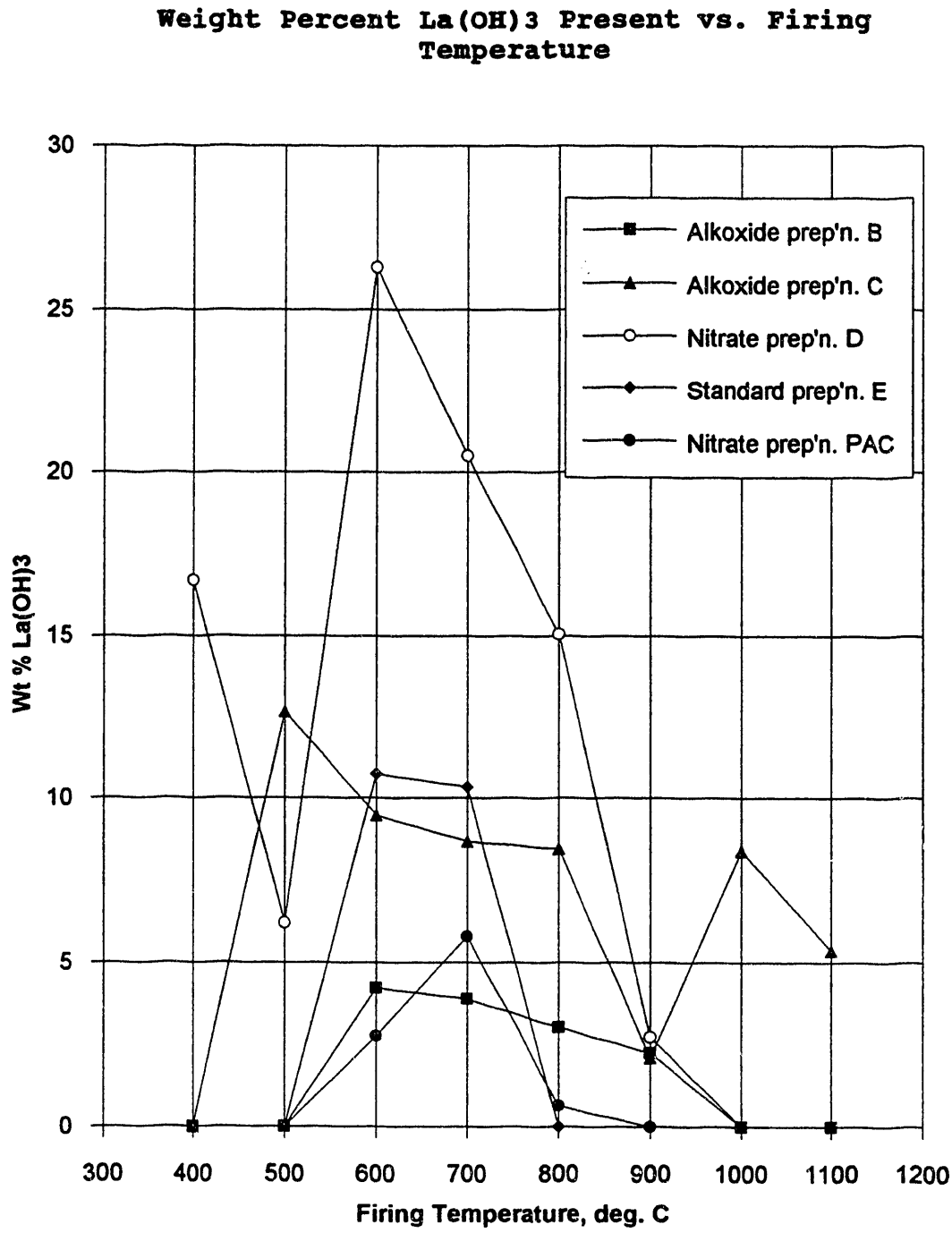

Figure 3.4 Graph of the percentage of crystalline $La(OH)_3$ present versus firing temperature for pellets made from preparations B, C, D, E, and PAC. The quantitative analysis was performed using the method of Chung, and has an accuracy of $\pm$5 wt%.

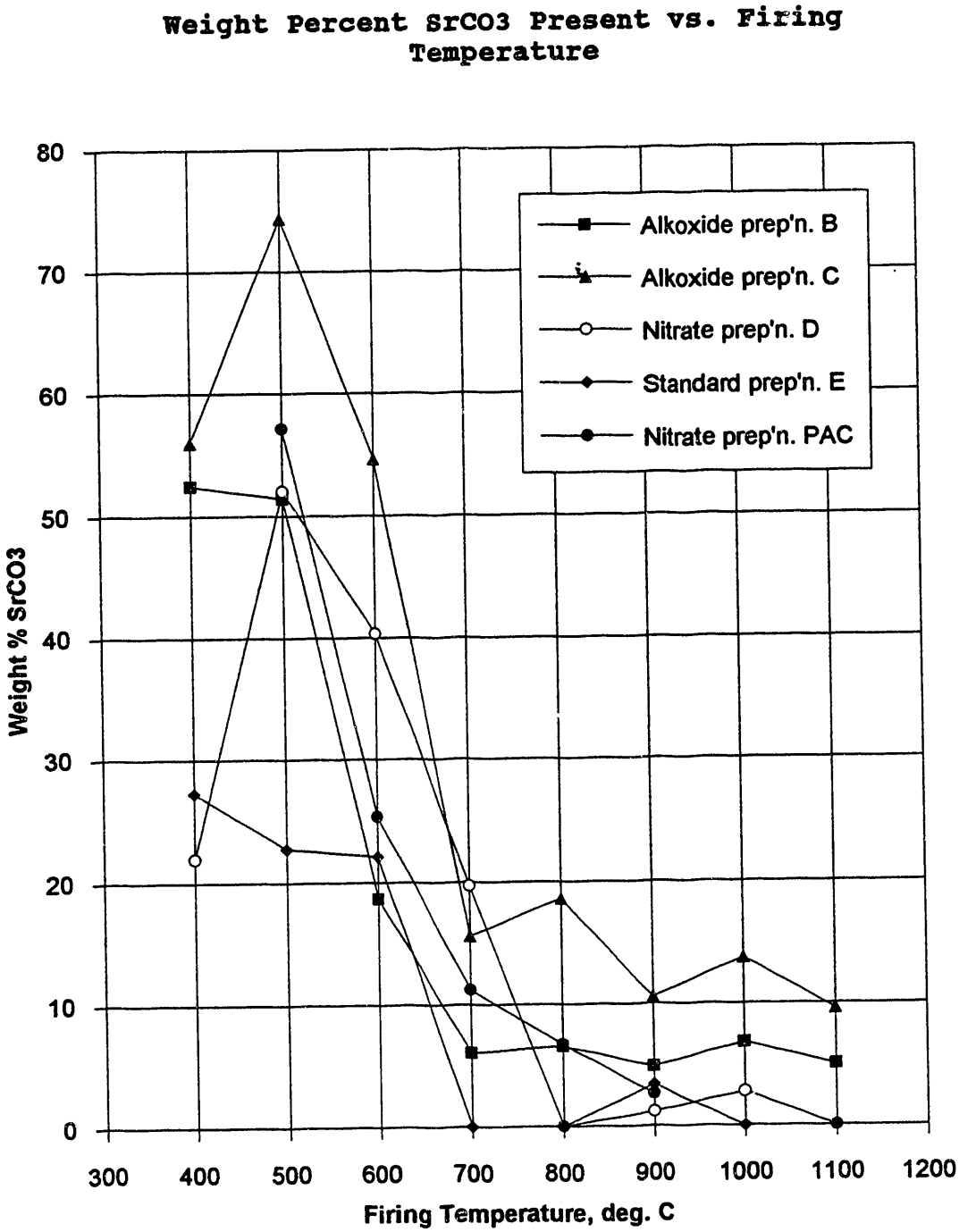

Figure 3.5 Graph of the percentage of crystalline $SrCO_3$ present versus firing temperature for pellets made from preparations B, C, D, E, and PAC. The quantitative analysis was performed using the method of Chung, and has an accuracy of $\pm$5 wt%.

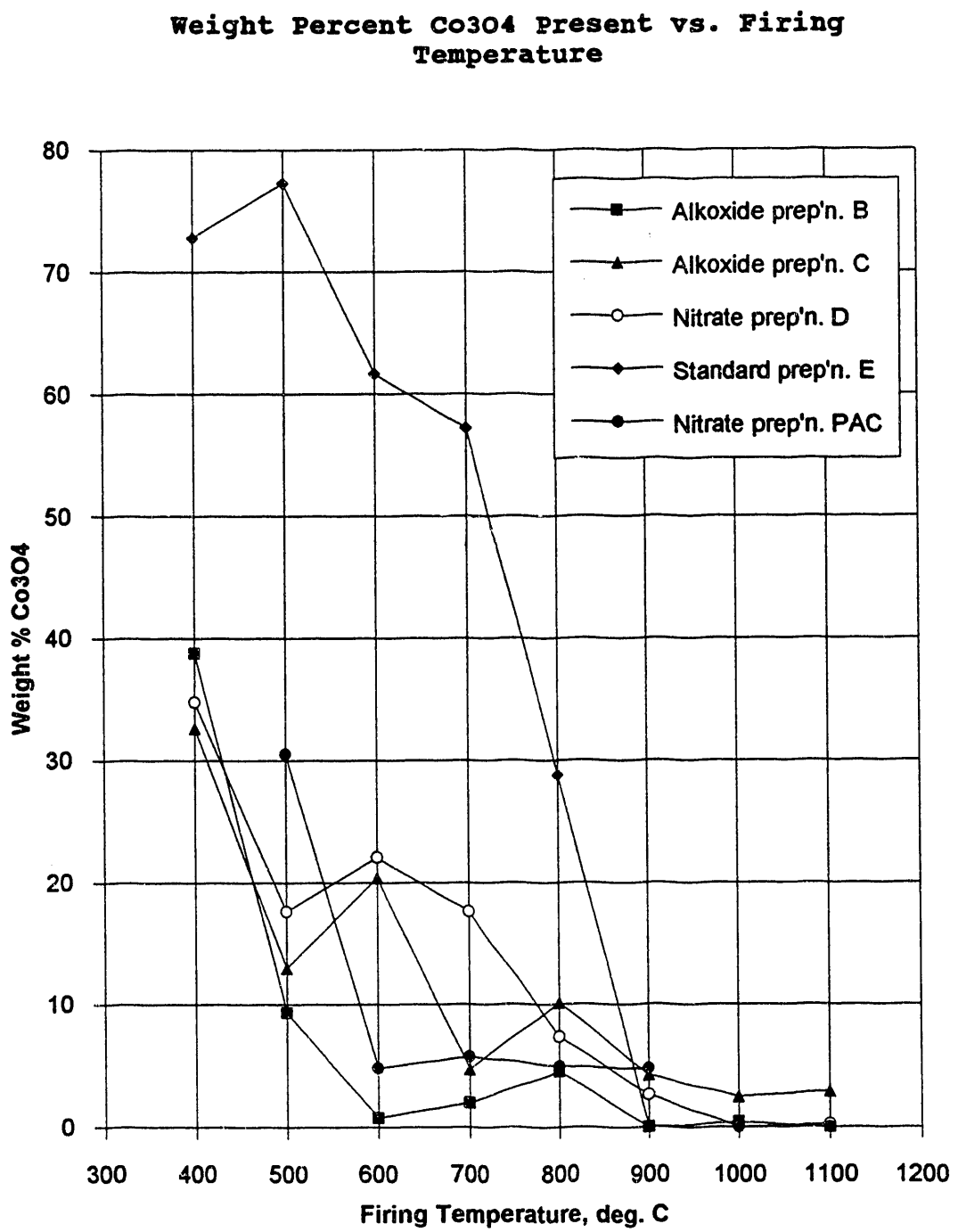

Figure 3.6 Graph of the percentage of crystalline Co_3O_4 present versus firing temperature for pellets made from preparations B, C, D, E, and PAC. The quantitative analysis was performed using the method of Chung, and has an accuracy of $\pm$5 wt%.

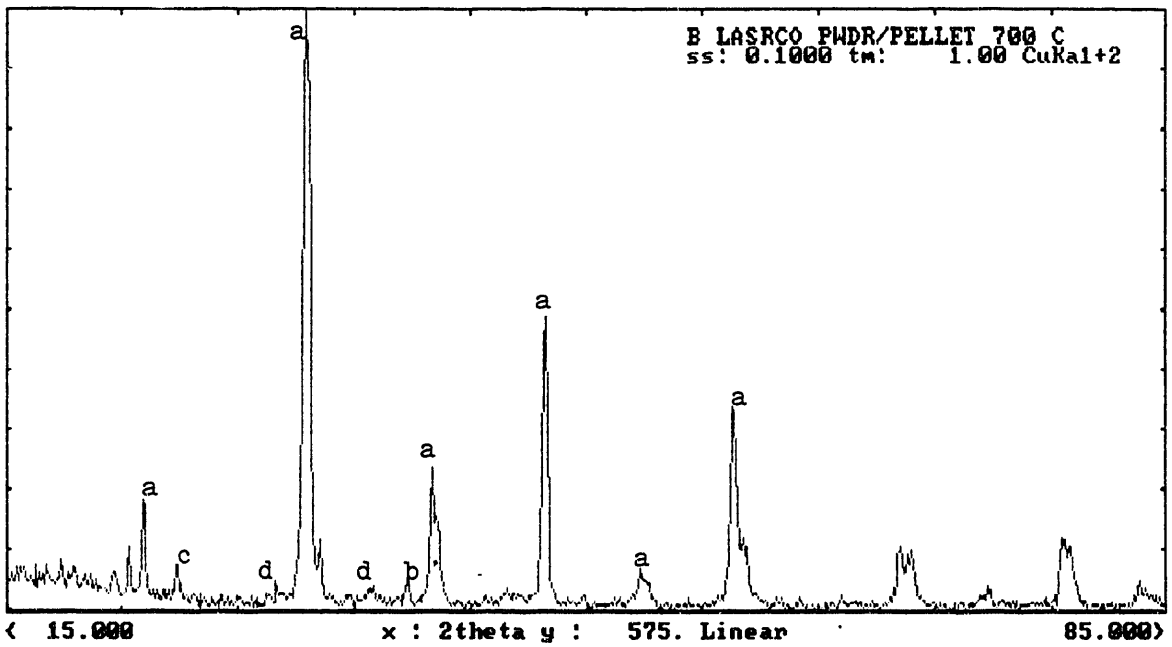

Figure 3.7a X-ray diffraction pattern recorded for the B sol-gel alkoxide preparation powder fired at 700°C. a=$La_{0.6}Sr_{0.4}CoO_3$, b=$La(OH)_3$, c=$SrCO_3$, d=Co_3O_4.

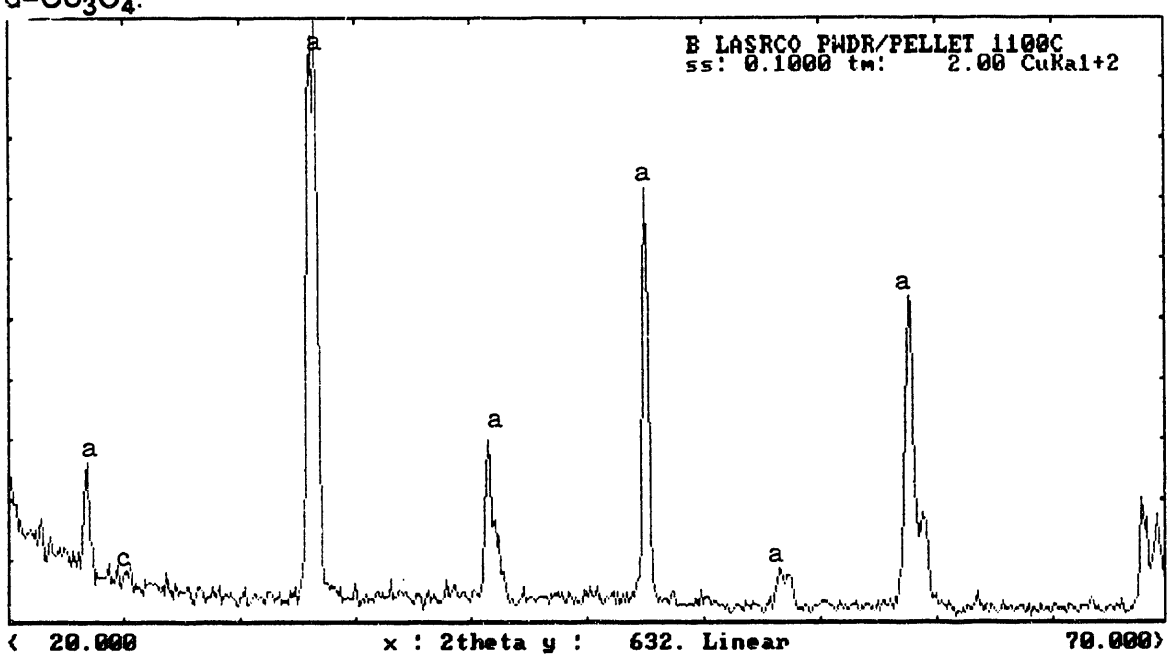

Figure 3.7b X-ray diffraction pattern recorded for the B sol-gel alkoxide preparation powder fired at 1100°C. a=$La_{0.6}Sr_{0.4}CoO_3$, c=$SrCO_3$.

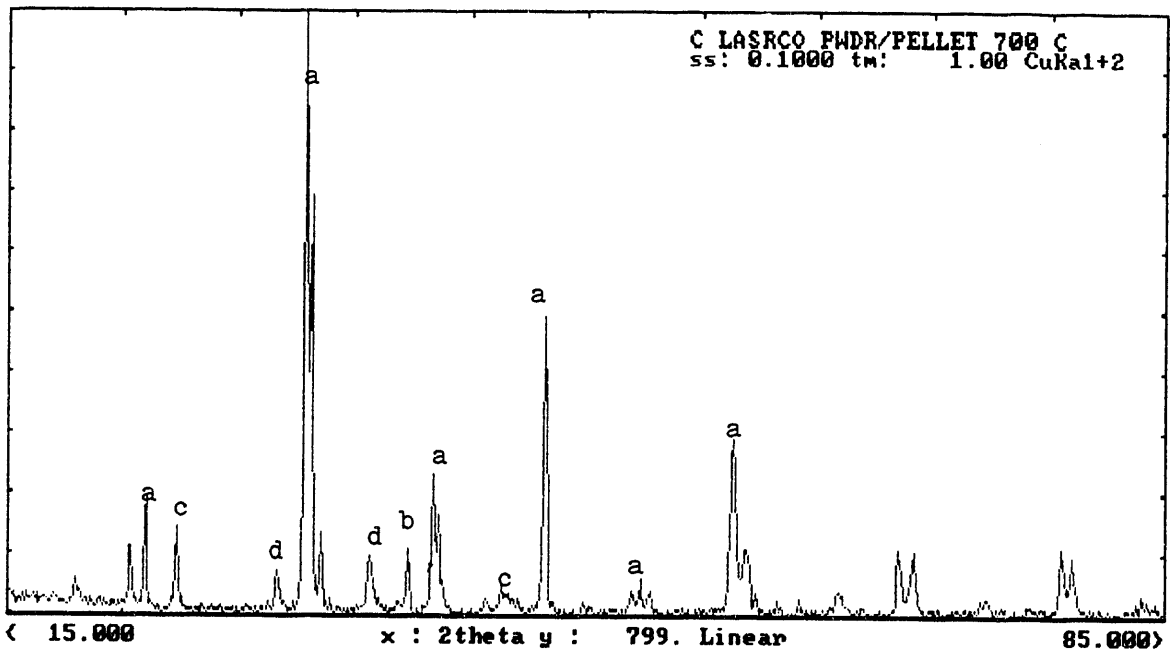

Figure 3.8a X-ray diffraction pattern recorded for the C sol-gel alkoxide preparation powder fired at 700°C. a=$La_{0.6}Sr_{0.4}CoO_3$, b=$La(OH)_3$, c=$SrCO_3$, d=Co_3O_4.

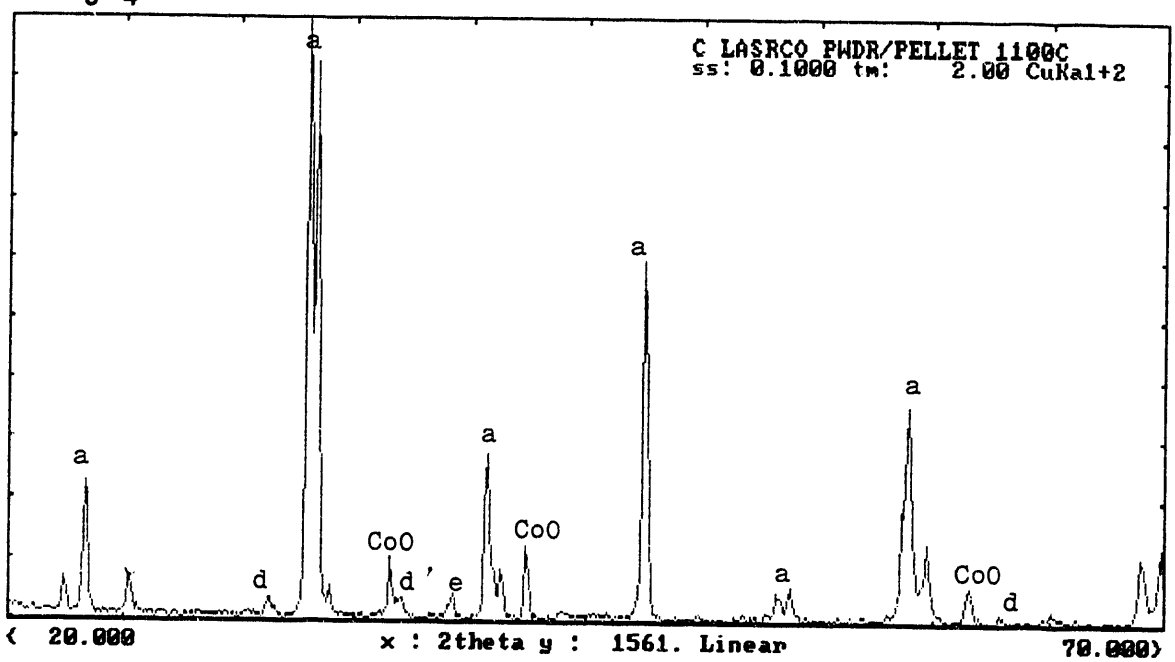

Figure 3.8b X-ray diffraction pattern recorded for the C sol-gel alkoxide preparation powder fired at 1100°C. a=$La_{0.6}Sr_{0.4}CoO_3$, c=$SrCO_3$, d=Co_3O_4, e=La_2O_3.

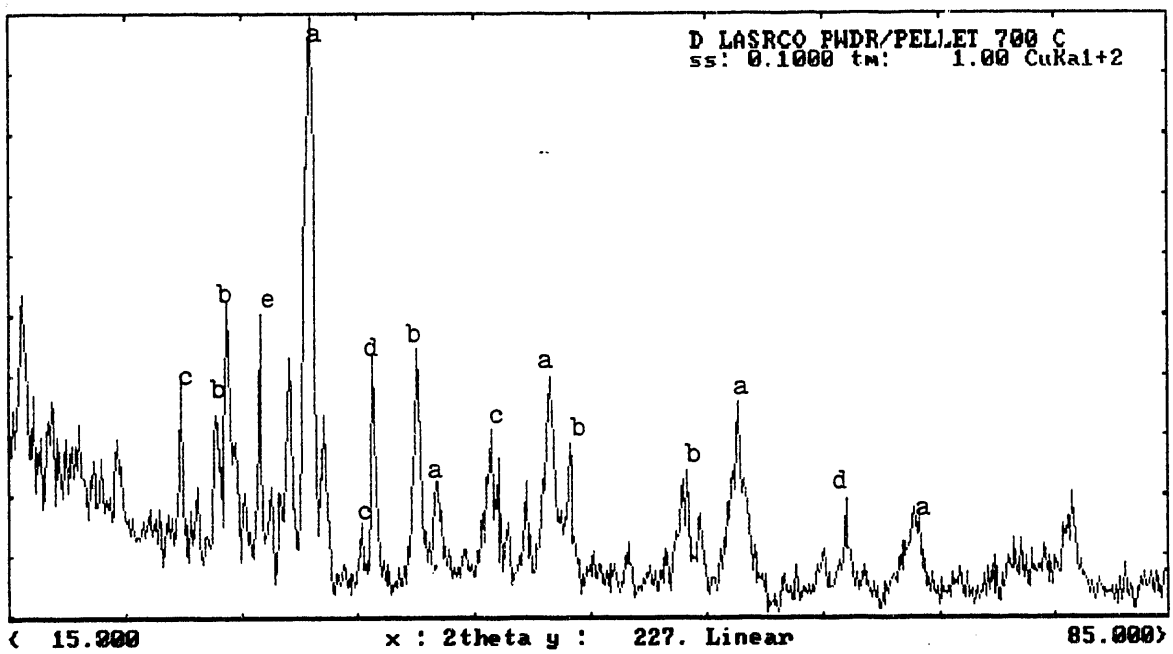

Figure 3.9a X-ray diffraction pattern recorded for the D polymer-nitrate preparation powder fired at 700°C. a=$La_{0.6}Sr_{0.4}CoO_3$, b=$La(OH)_3$, c=$SrCO_3$, d=Co_3O_4, e=La_2O_3.

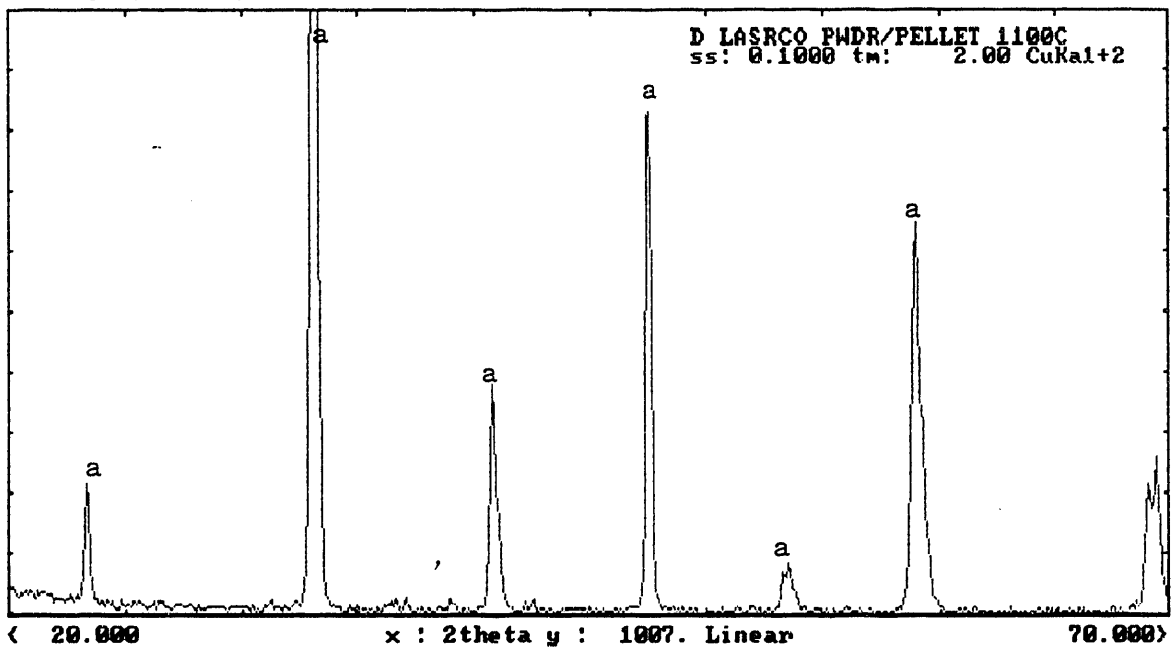

Figure 3.9b X-ray diffraction pattern recorded for the D polymer-nitrate preparation powder fired at 1100°C. a=$La_{0.6}Sr_{0.4}CoO_3$.

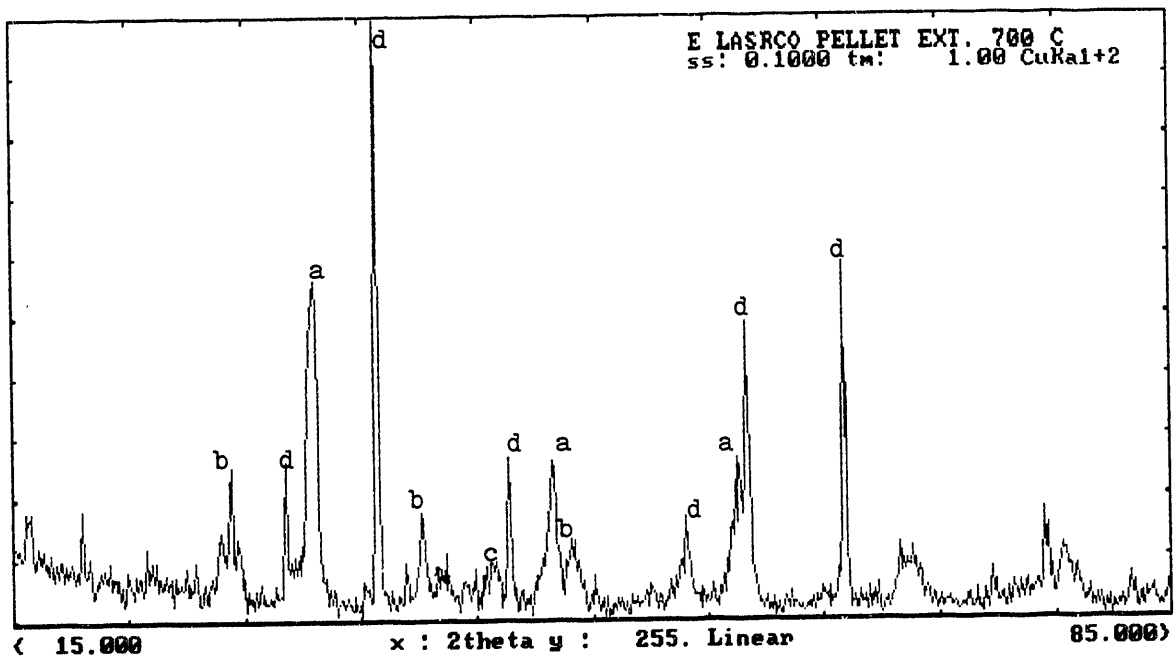

Figure 3.10a X-ray diffraction pattern recorded for the E oxides/carbonate preparation powder fired at 700°C. a=$La_{0.6}Sr_{0.4}CoO_3$, b=$La(OH)_3$, c=$SrCO_3$, d=Co_3O_4. Note: Co_3O_4 peaks in this pattern are due to surplus cobalt, not to cobalt that has not been assimilated into the $La_{0.6}Sr_{0.4}CoO_3$ matrix.

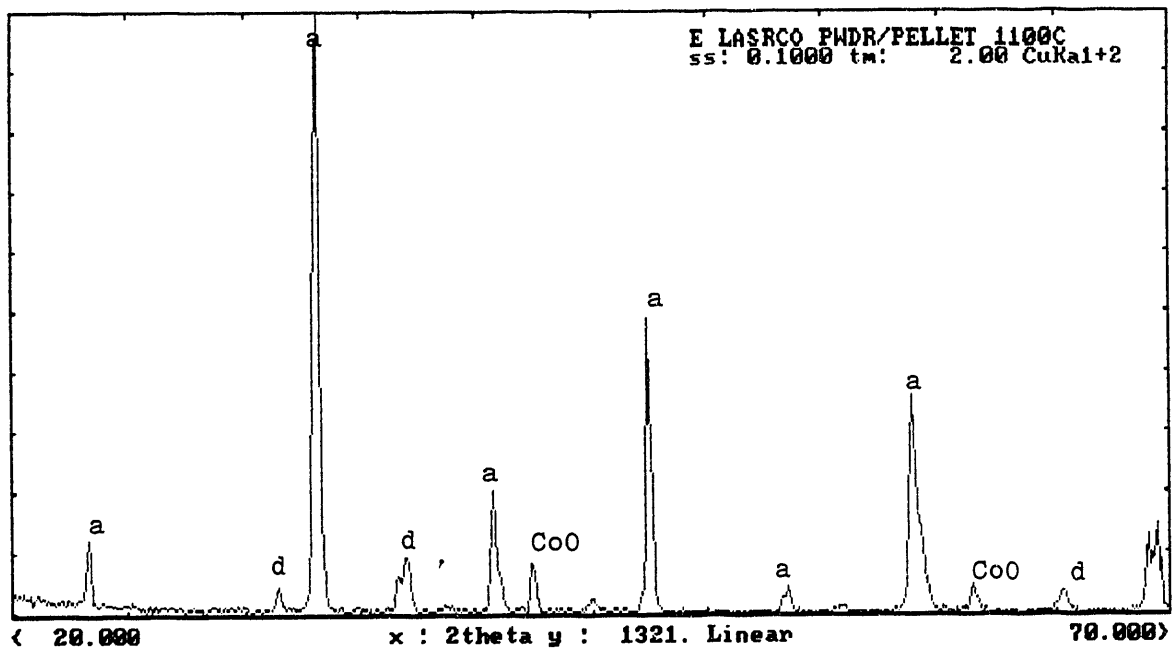

Figure 3.10b X-ray diffraction pattern recorded for the E oxides/carbonate preparation powder fired at 1100°C. a=$La_{0.6}Sr_{0.4}CoO_3$, d=Co_3O_4. Note: Co_3O_4 and CoO peaks in this pattern are due to surplus cobalt, not to cobalt that has not been assimilated into the $La_{0.6}Sr_{0.4}CoO_3$ matrix.

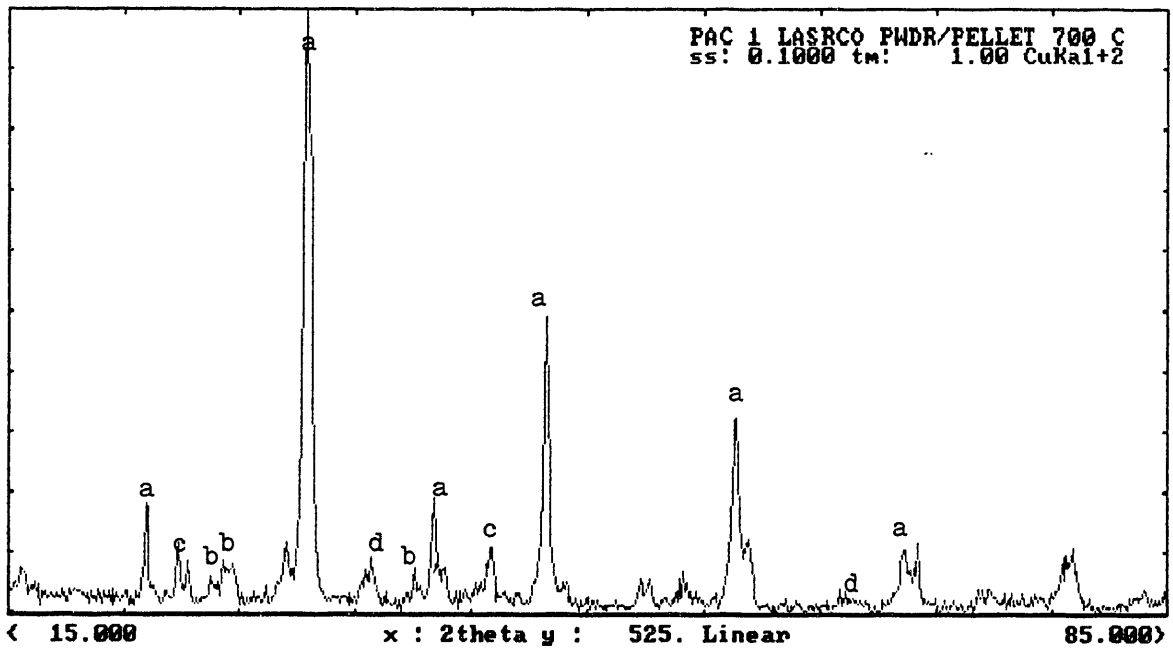

Figure 3.11a X-ray diffraction pattern recorded for the PAC polymer-nitrate preparation powder fired at 700°C. a=$La_{0.6}Sr_{0.4}CoO_3$, b=$La(OH)_3$, c=$SrCO_3$, d=Co_3O_4.

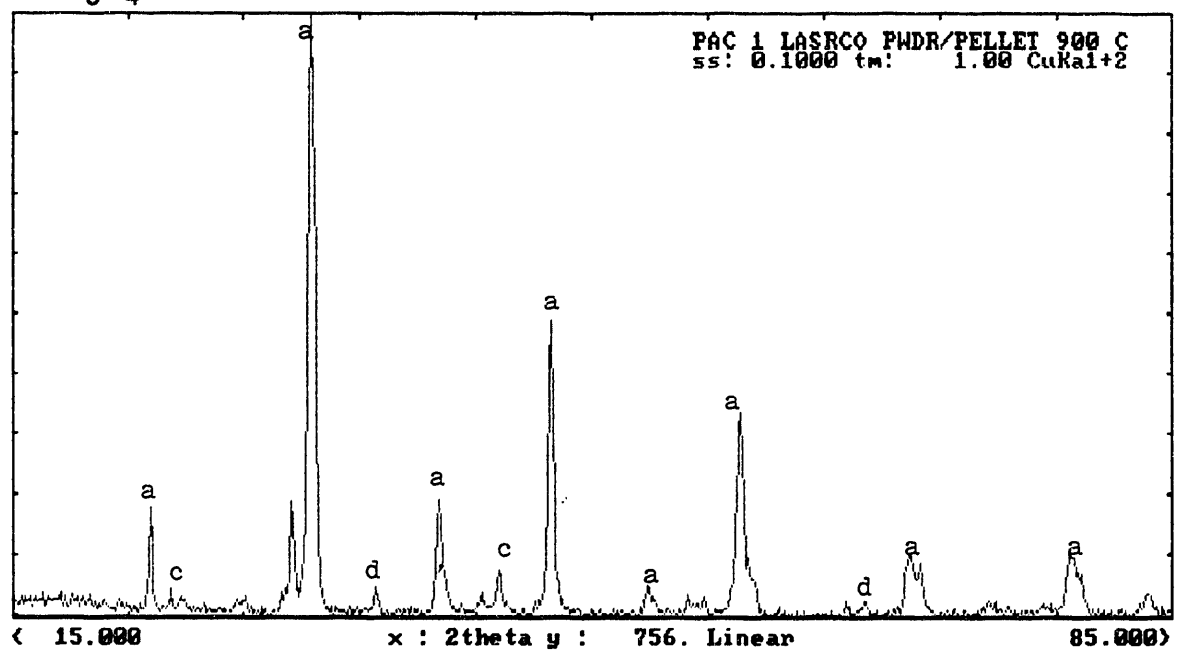

Figure 3.11b X-ray diffraction pattern recorded for the PAC polymer-nitrate preparation powder fired at 900°C. a=$La_{0.6}Sr_{0.4}CoO_3$, c=$SrCO_3$, d=Co_3O_4.

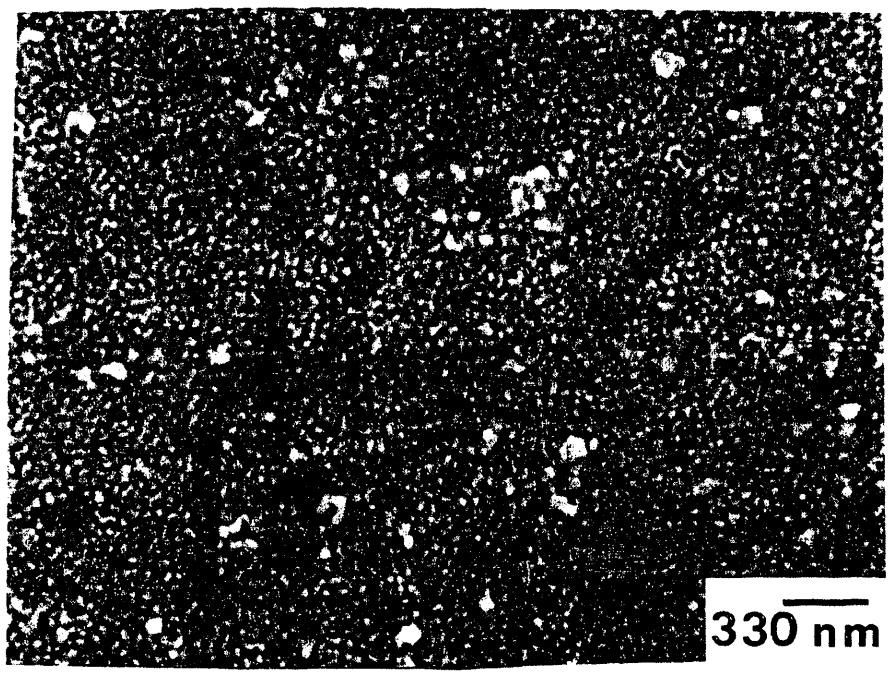

Figure 3.12a SEM micrograph of the surface of a 0.02 micron pore size Anotec filter.

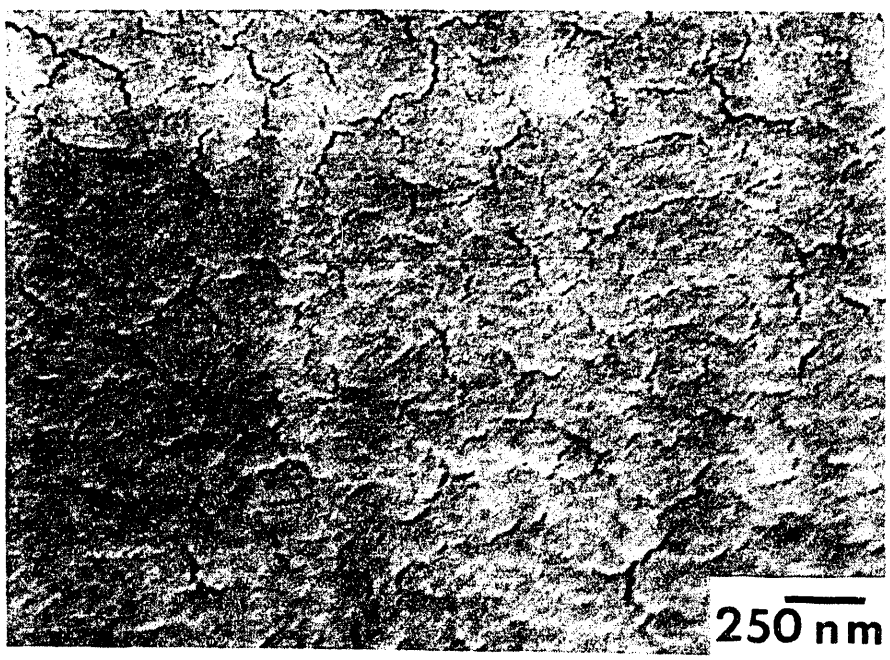

Figure 3.12b SEM micrograph of the surface of 0.05 micron pore size U.S. Filter tube.

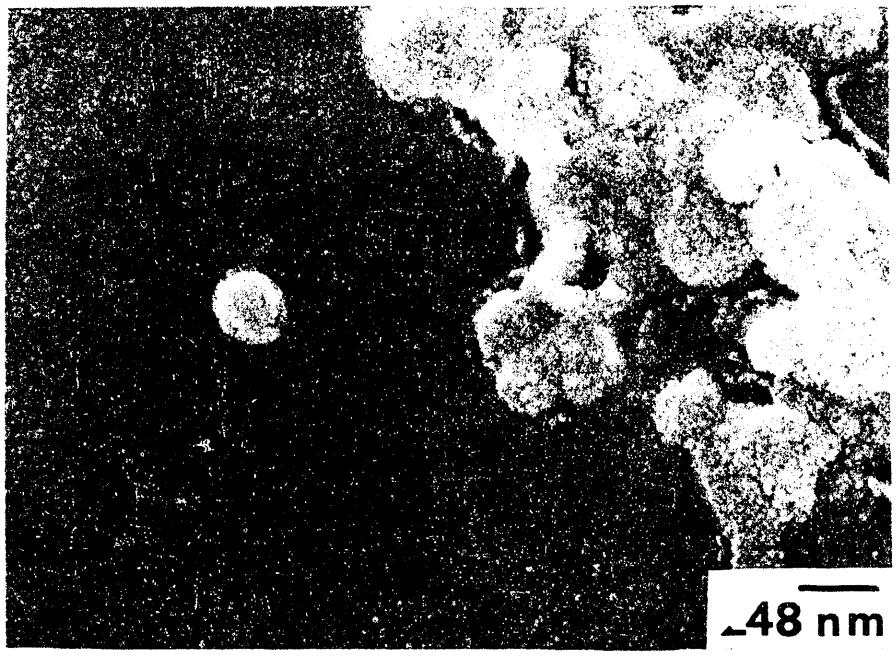

Figure 3.13a SEM micrograph of a single layer LSC film spin-coated onto a 0.02 micron pore size Anotec filter and fired at 700°C. The film has cracked away from the sides of the large surface inclusion.

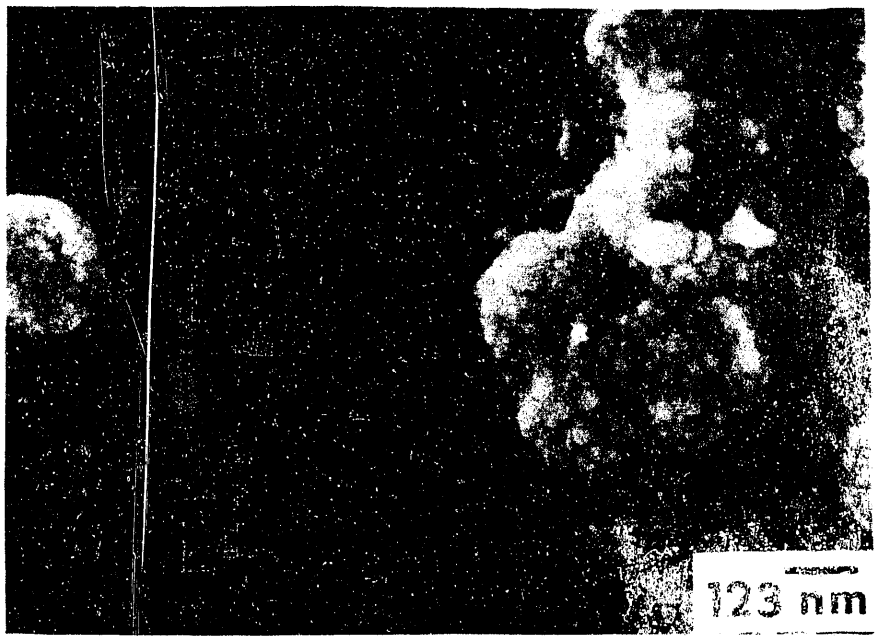

Figure 3.13b Higher magnification view of above film.

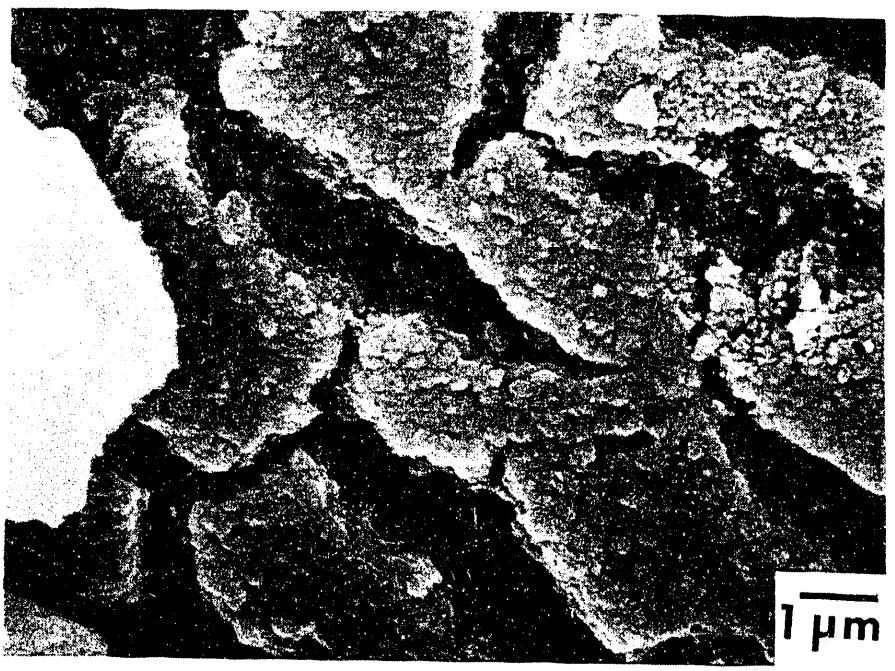

Figure 3.14a SEM micrograph of a thick area in a single layer LSC film spin-coated onto a 0.02 micron pore size Anotec filter and fired at 800°C. Shrinkage cracking and exposure of the underlying filter surface have occurred.

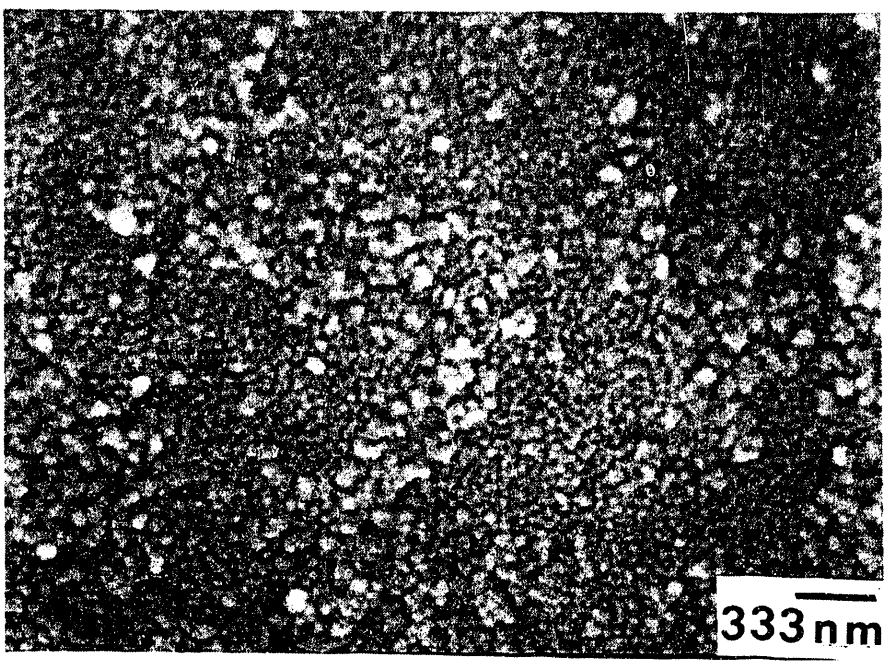

Figure 3.14b SEM micrograph of a thin area in the same film as above. Incomplete coverage of the filter is present.

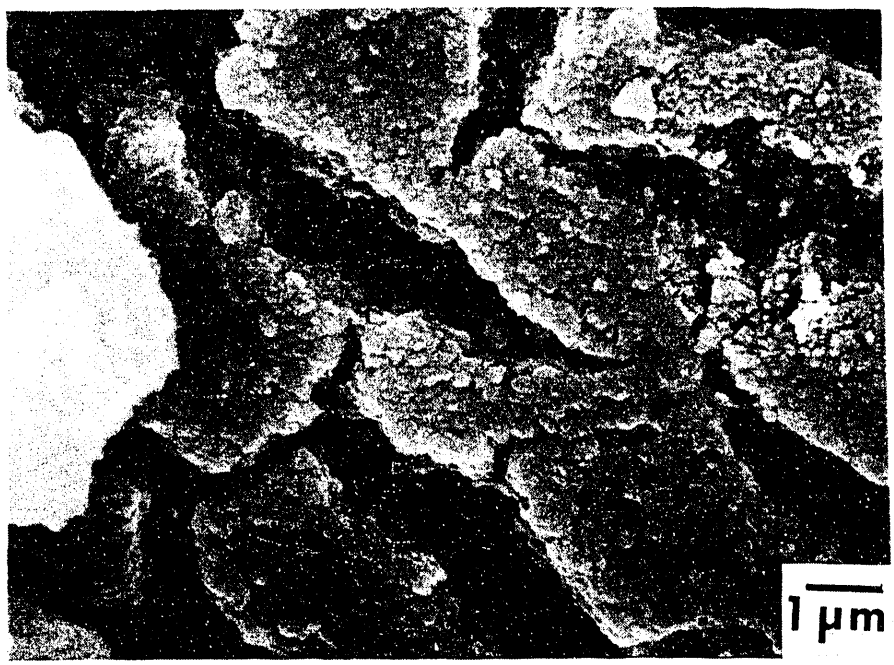

Figure 3.14a SEM micrograph of a thick area in a single layer LSC film spin-coated onto a 0.02 micron pore size Anotec filter and fired at 800°C. Shrinkage cracking and exposure of the underlying filter surface have occurred.

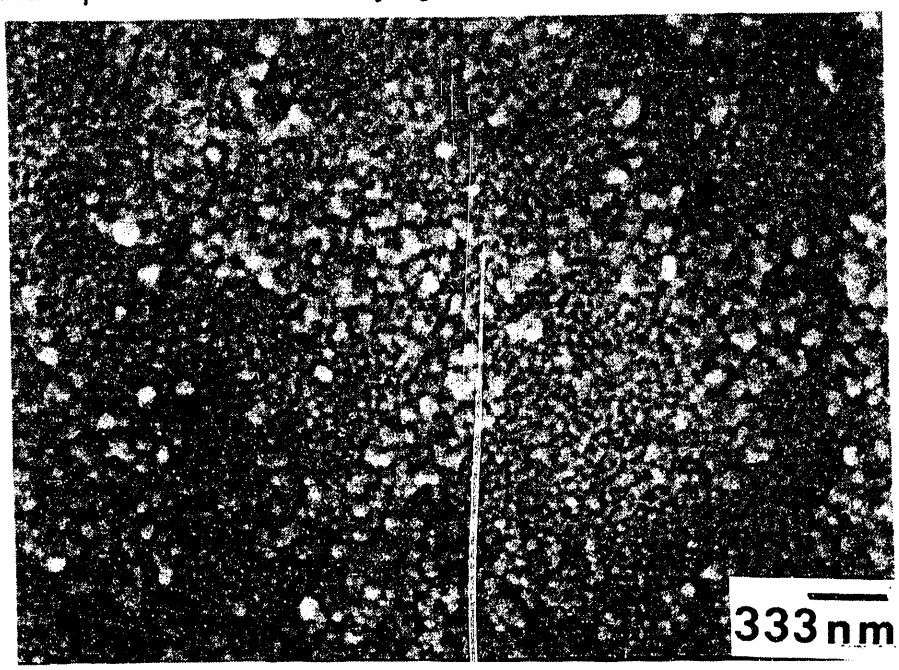

Figure 3.14b SEM micrograph of a thin area in the same film as above. Incomplete coverage of the filter is present.

Figure 3.15 SEM micrograph of a single layer LSC film spin-coated onto a single crystal silicon wafer chip and fired at 800°C. Surface pores and inhomogeneous precipitates are present.

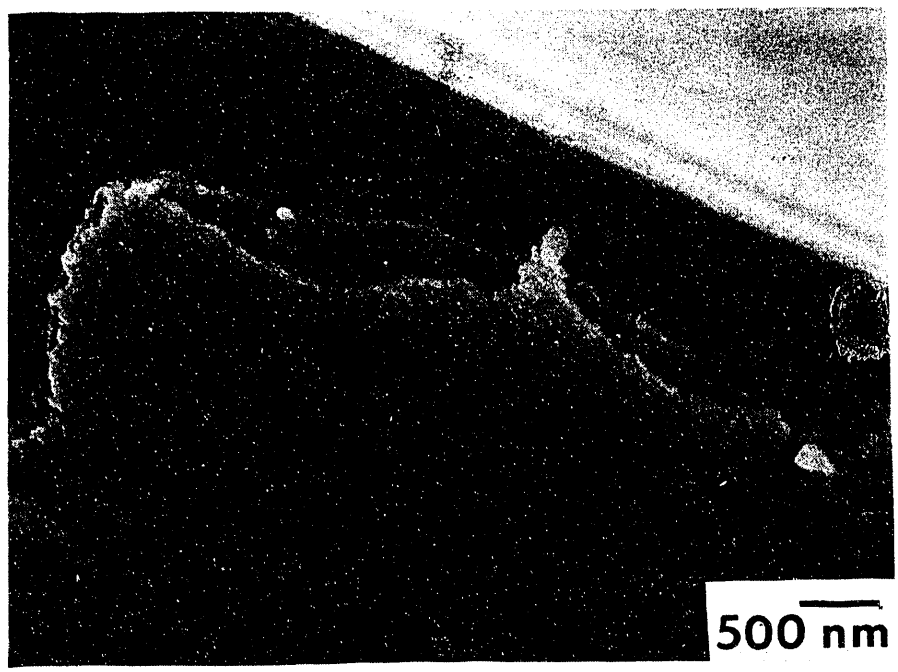

Figure 3.15 SEM micrograph of a single layer LSC film spin-coated onto a single crystal silicon wafer chip and fired at 800°C. Surface pores and inhomogeneous precipitates are present.

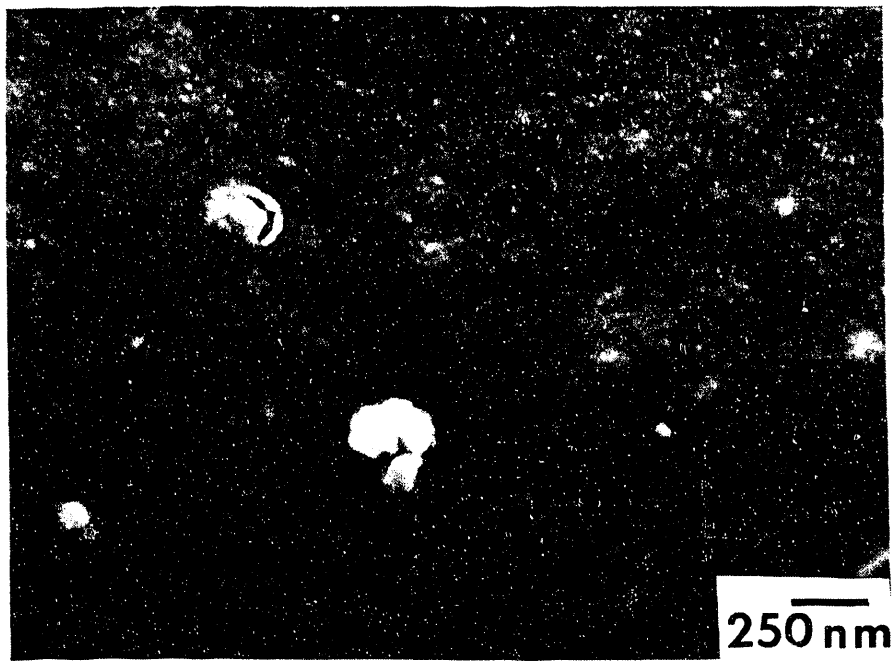

Figure 3.16a SEM micrograph of a single layer YSZ film dip-coated on top of a continuous LSC film spin-coated onto a 0.02 micron pore size Anotec filter and fired at 700°C (LSC film surface shown in Figure 3.13). Film is broken around the edges of the surface inclusions.

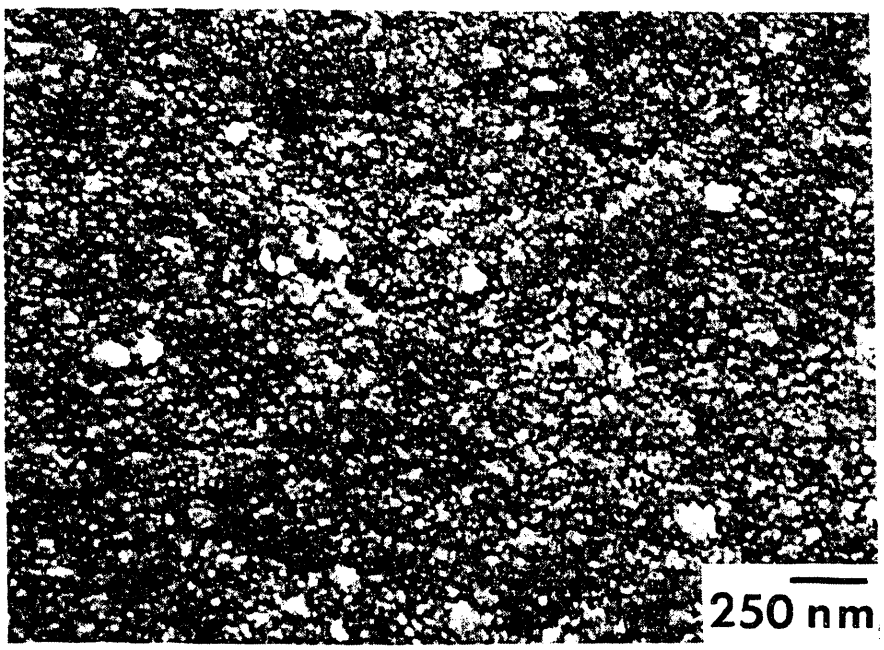

Figure 3.16b SEM micrograph of a single layer of YSZ film dip-coated onto a discontinuous LSC film spin-coated onto a 0.02 micron pore size Anotec filter and fired at 700°C. Discontinuous coverage by the YSZ is present.

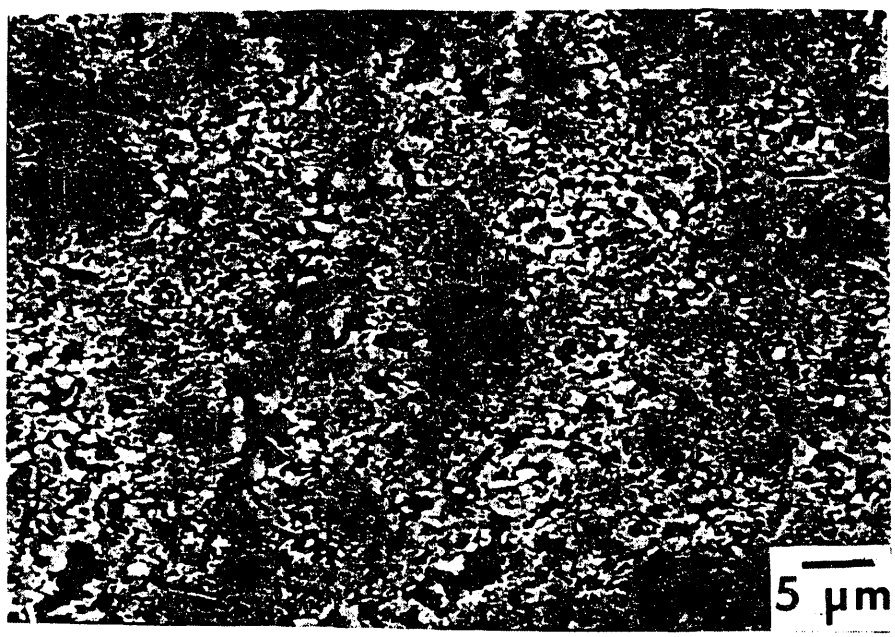

Figure 3.17a SEM micrograph of a single layer LSC film spin-coated onto a sintered porous LSC pellet. Film is discontinuous over large pores.

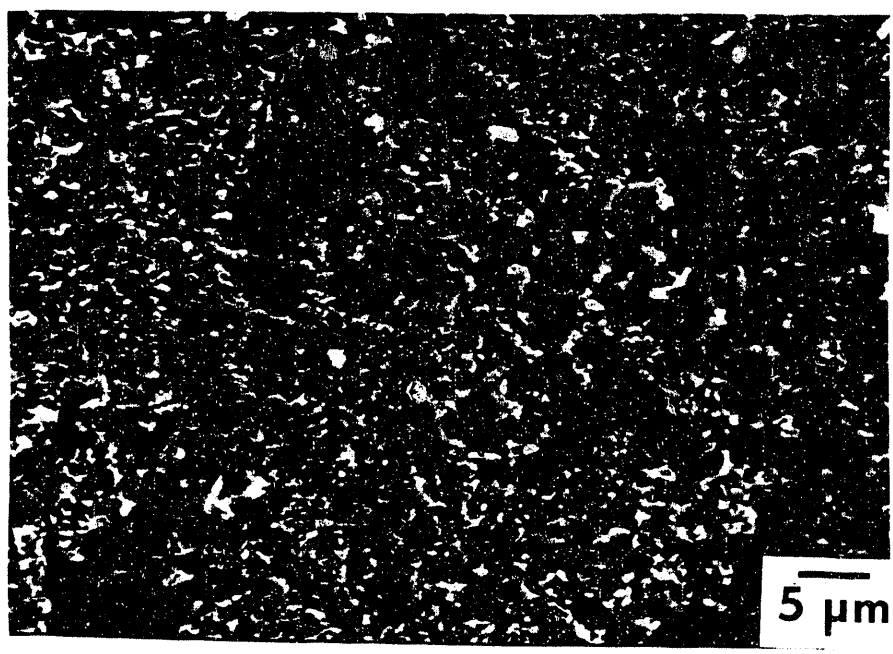

Figure 3.17b SEM micrograph of the surface of the uncoated, sintered, and porous LSC pellet used above.

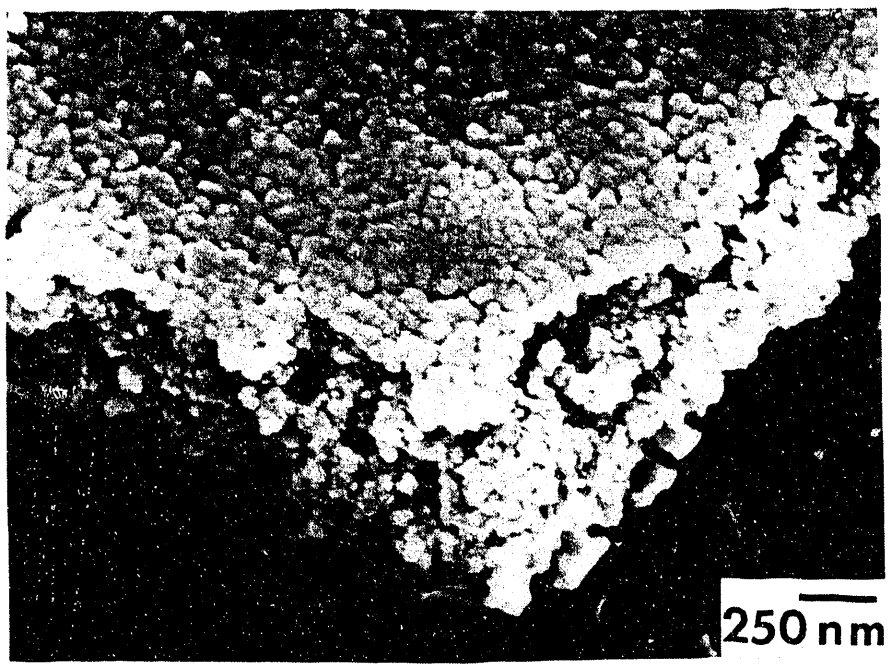

Figure 3.18 SEM micrograph of a fracture surface of a four layer LSC film dip-coated onto a 0.02 micron pore size Anotec filter and fired at 700°C. Film was photographed at a 15° tilt. Interior porosity of the film is clearly visible.

Figure 3.19a SEM micrograph of a four layer LSC film dip-coated onto a 0.02 micron pore size Anotec filter and fired at 700°C. Shrinkage cracking and inhomogeneous precipitation are present.

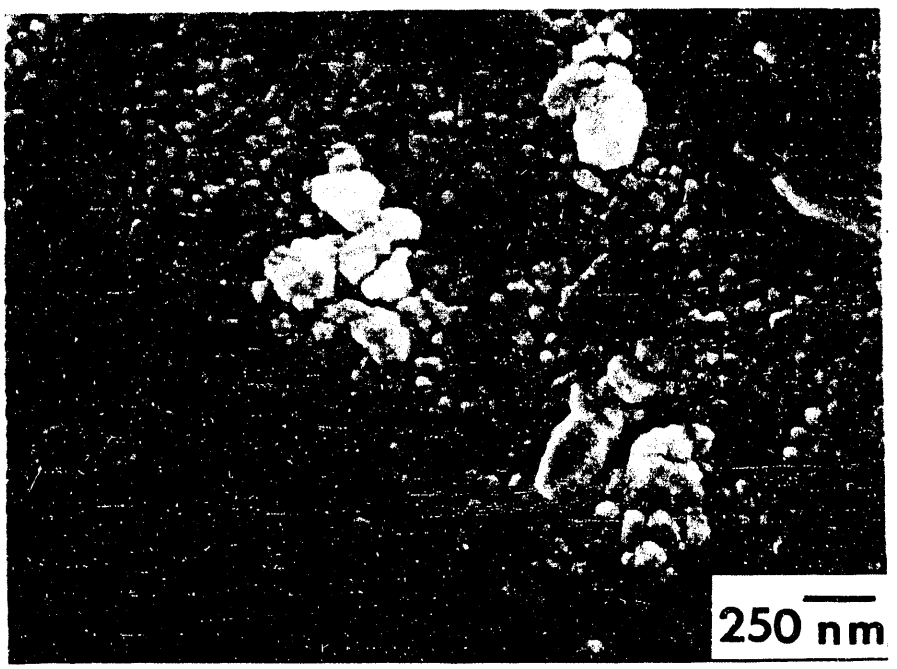

Figure 3.19b SEM micrograph of same film as above taken from a less dense area. High porosity and possible inhomogeneous precipitation are present.

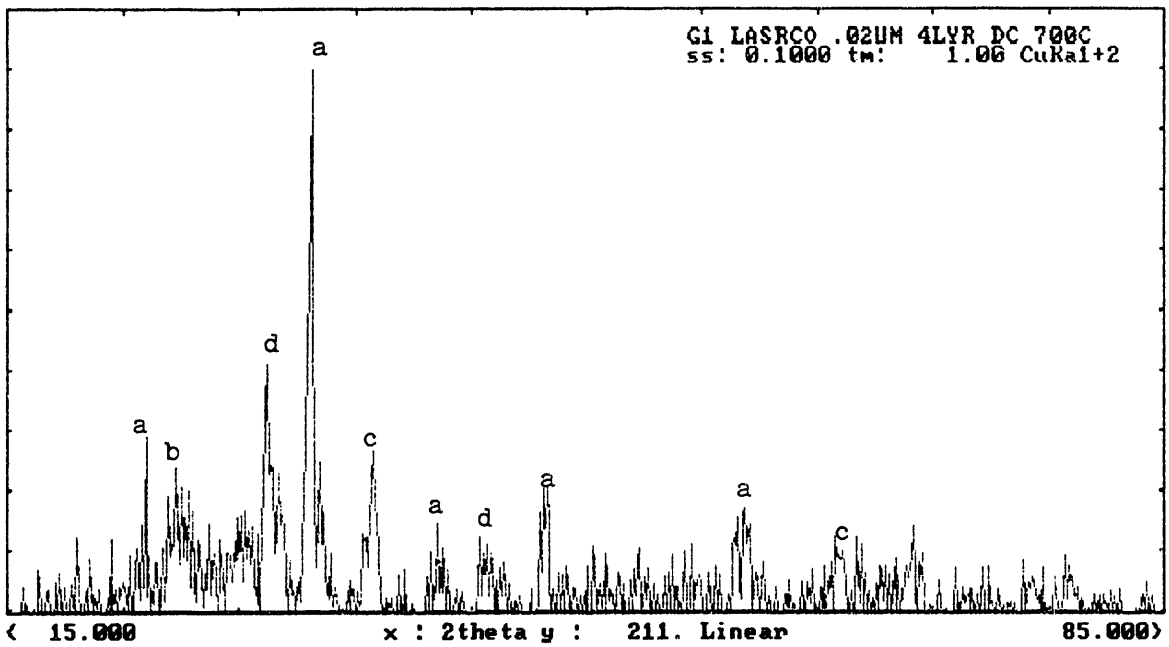

Figure 3.20a X-ray diffraction pattern recorded for a four layer LSC film dip-coated onto a 0.02 micron pore size Anotec filter and fired at 700°C. a=$La_{0.6}Sr_{0.4}CoO_3$, b=$SrCO_3$, c=Co_3O_4, d=La_2O_3.

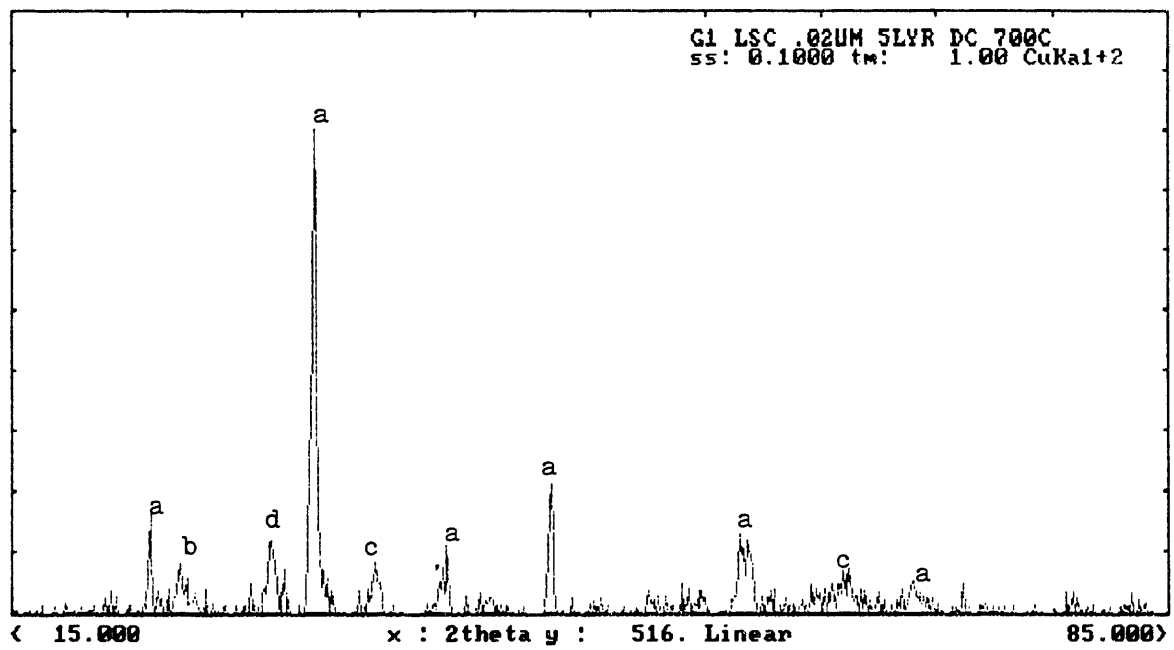

Figure 3.20b X-ray diffraction pattern recorded for a five layer LSC film dip-coated onto a 0.02 micron pore size Anotec filter and fired at 700°C. a=$La_{0.6}Sr_{0.4}CoO_3$, b=$SrCO_3$, c=Co_3O_4, d=La_2O_3.

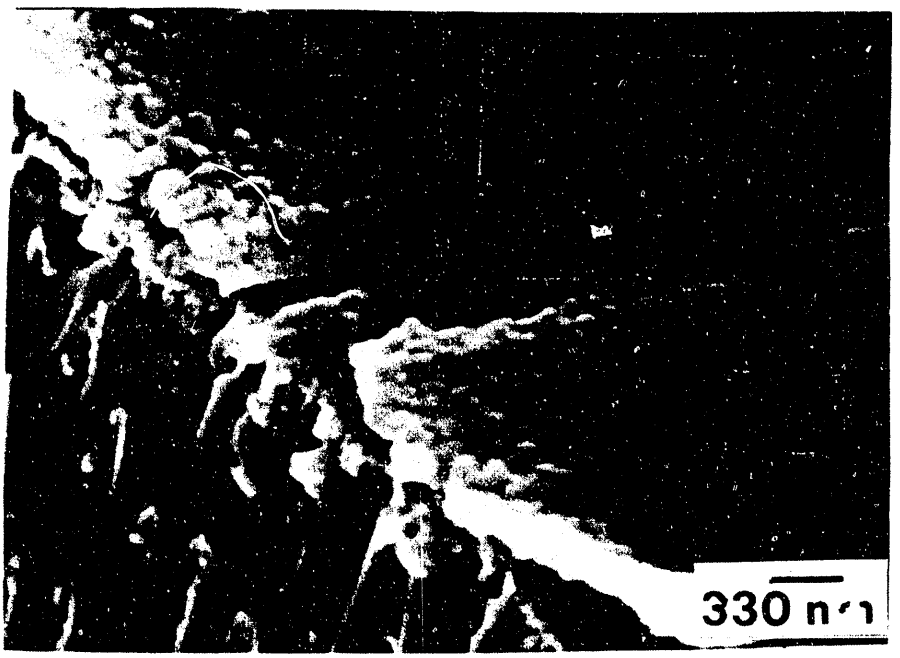

Figure 3.21a SEM micrograph of a five layer LSC film dip-coated onto a 0.02 micron pore size Anotec filter and fired at 700°C. Shrinkage cracking and surface roughness are visible.

Figure 3.21b Surface view of above film. High porosity and surface roughness are visible.

Figure 3.22 SEM micrograph of a five layer LSC film dip-coated onto a 0.02 micron pore size Anotec filter and fired at 1000°C. Filter has turned an intense blue color and the film has broken up into unconnected masses.

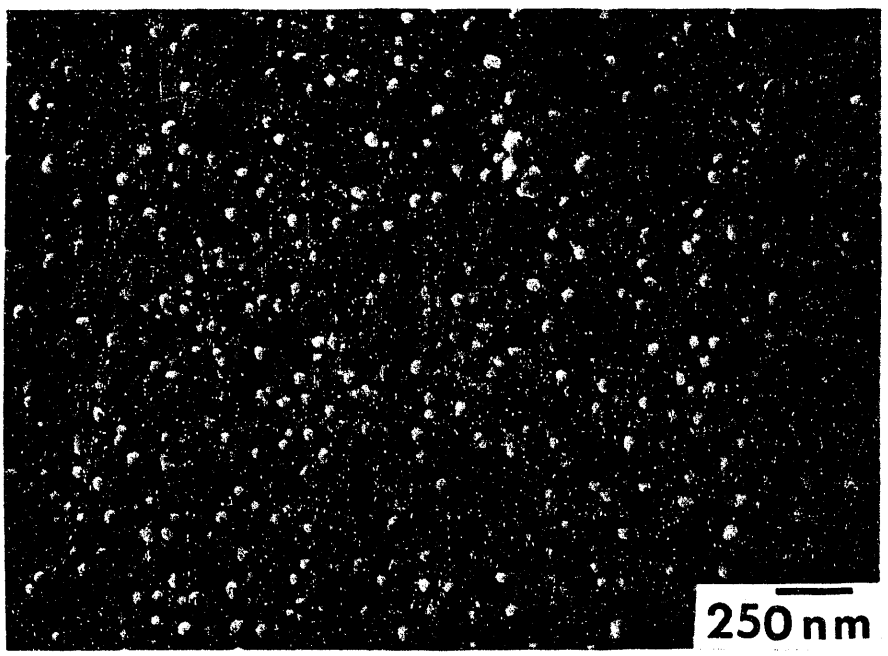

Figure 3.23a SEM micrograph of a four layer LSC film dip-coated onto a 0.05 micron pore size U.S. Filter tube piece and fired at 700°C. Micropores and inhomogeneous precipitates are present.

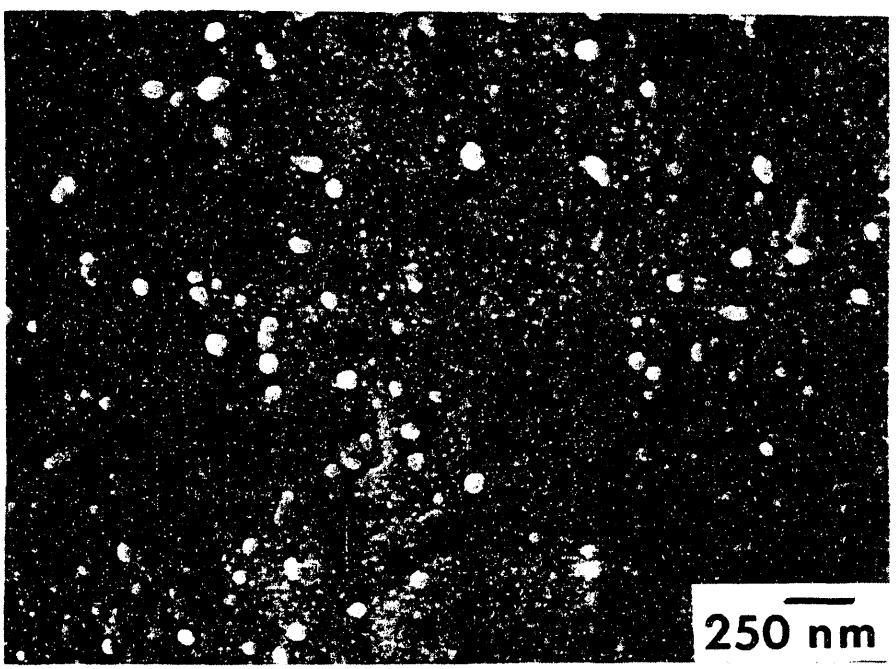

Figure 3.23b SEM micrograph of a four layer LSC film dip-coated onto a 0.05 micron pore size U.S. Filter tube piece and fast-ramped to the firing temperature of 700°C. Inhomogeneous precipitates are present, but pores are absent and matrix grain boundaries are less distinct than in above micrograph.

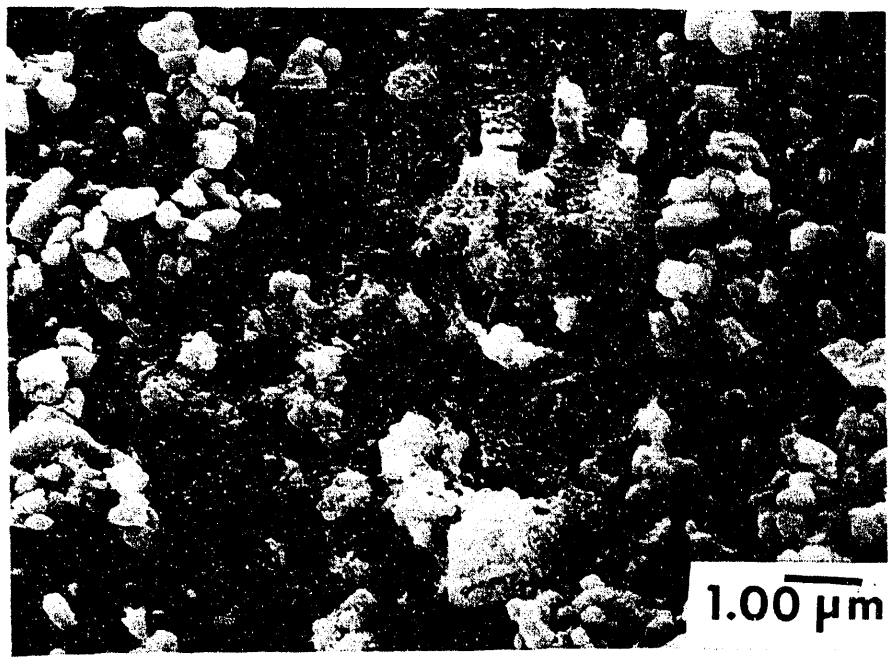

Figure 3.24a SEM micrograph of a two-layer LSC film dip-coated onto a 0.05 micron pore size U.S. Filter and heat-treated at 650°C for 24 hours. Film breakup is complete.

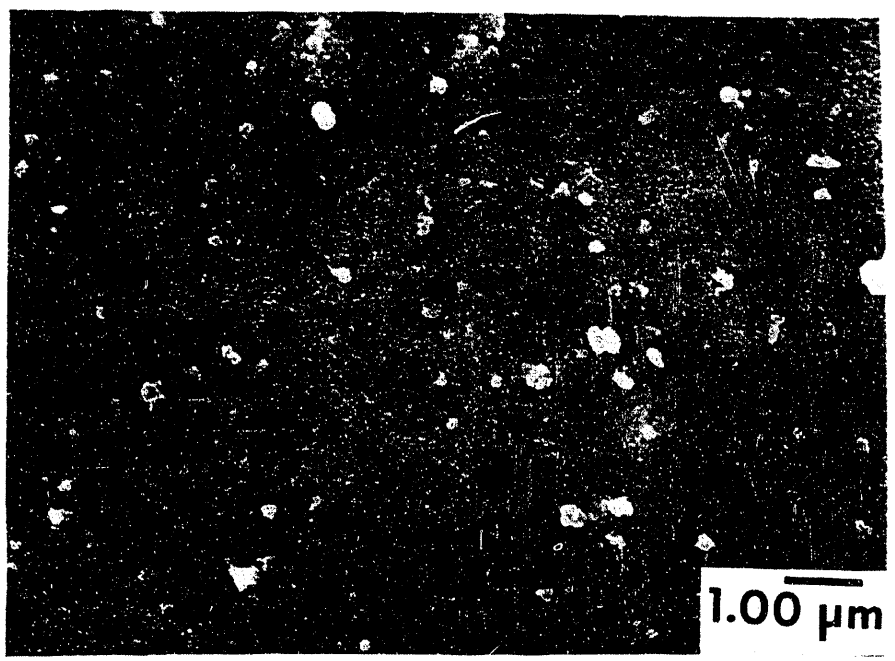

Figure 3.24b SEM micrograph of a four layer LSC film dip-coated onto a 0.05 micron pore size U.S. Filter tube piece and heat treated at 650°C for 96 hours. The film is intact.

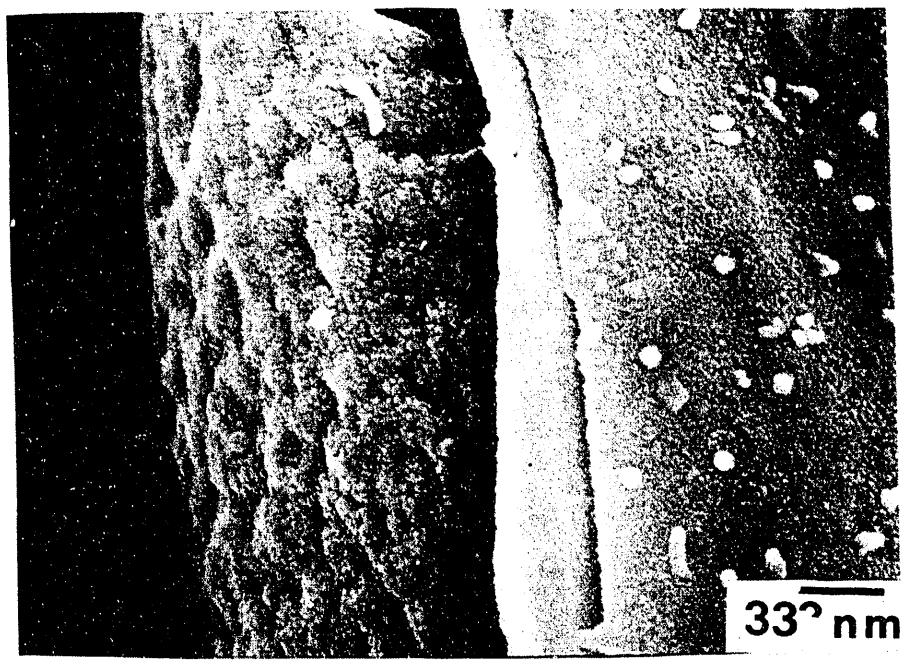

Figure 3.25a SEM micrograph of a thick LSC film dip-coated onto an α-alumina disc and heat treated at 650°C for 48 hours. Distinct inhomogeneous precipitates are present on the film surface visible to the right in the micrograph.

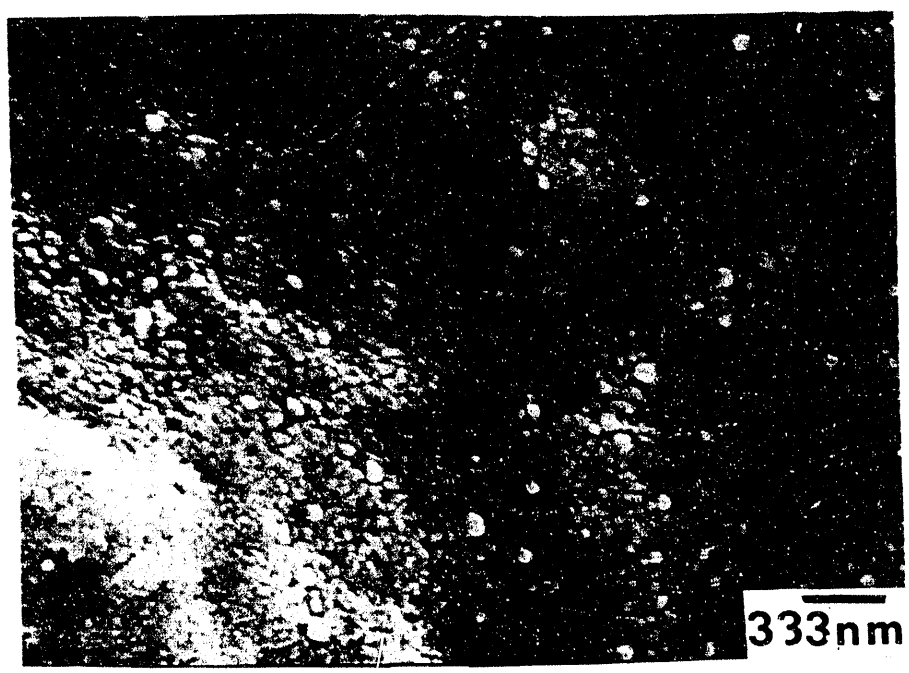

Figure 3.25b SEM micrograph of above film heat-treated at 650°C for 96 hours. Inhomogeneous precipitates are present but generally smaller.

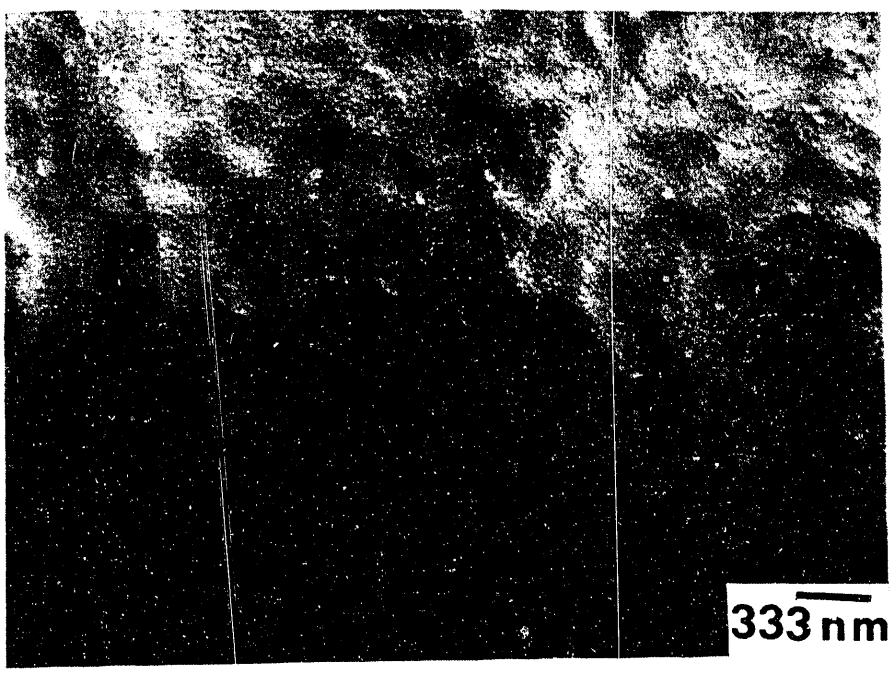

Figure 3.25c SEM micrograph of **3.25a** film heat treated at 650°C for 144 hours. Inhomogeneous precipitates are present but smaller and less distinct.

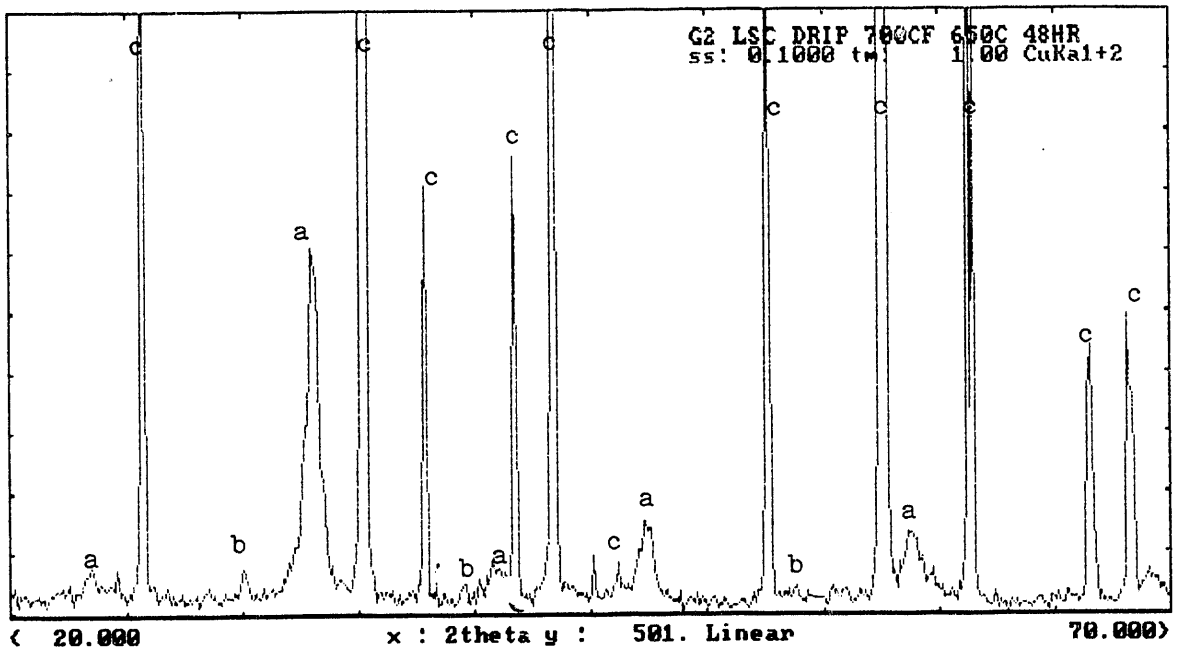

Figure 3.26a X-ray diffraction pattern recorded for a thick LSC film dip-coated onto an α-alumina disc and heat treated at 650°C for 48 hours. a=LSC, b=La_2O_3, c=α-Al_2O_3.

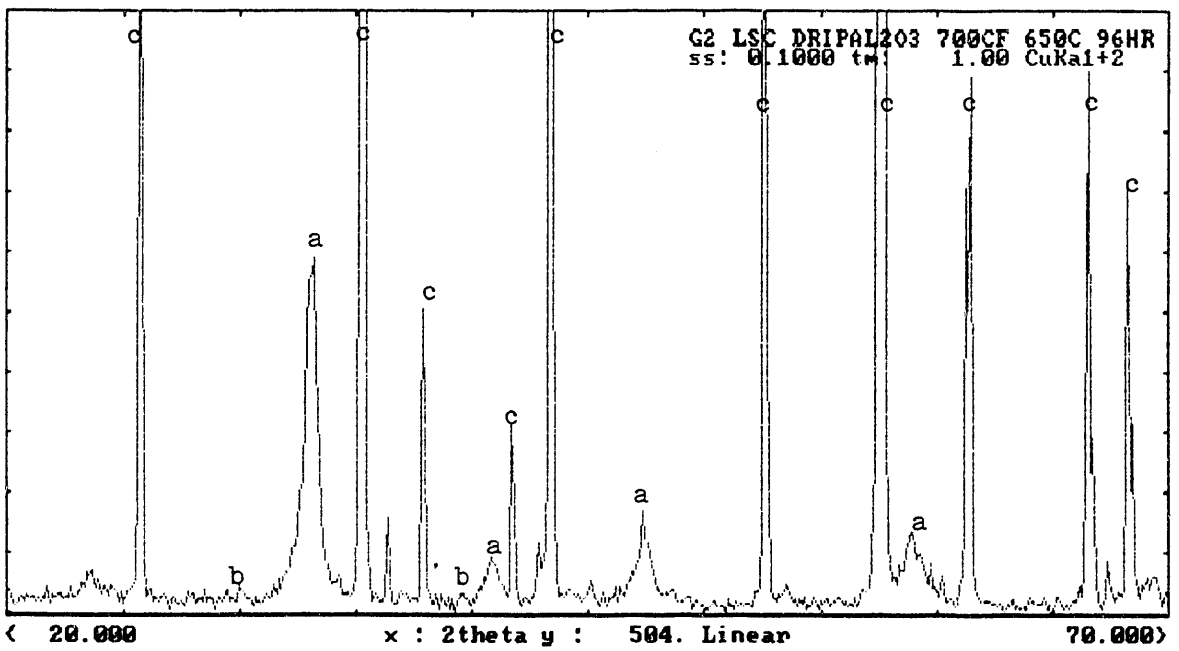

Figure 3.26b X-ray diffraction pattern recorded for a thick LSC film dip-coated onto an α-alumina disc and heat treated at 650°C for 96 hours. a LSC, b=La_2O_3, c=α-Al_2O_3.

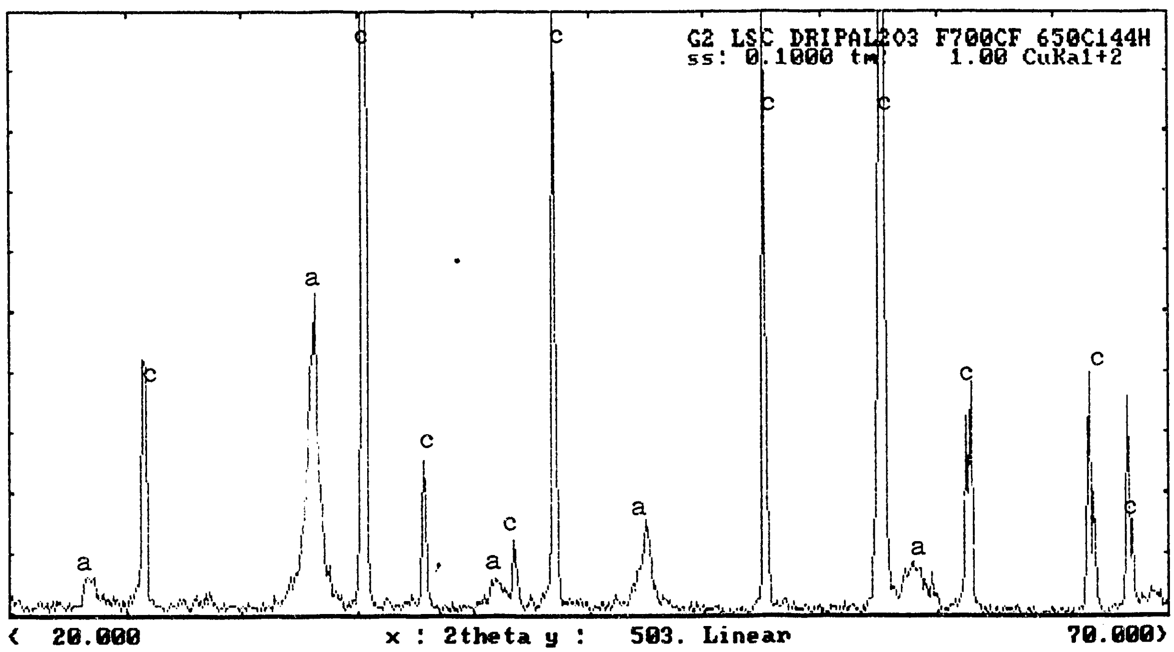

Figure 3.26c X-ray diffraction pattern recorded for a thick LSC film dip-coated onto an α-alumina disc and heat treated at 650°C for 144 hours. a=LSC, b=La_2O_3, c=α-Al_2O_3.

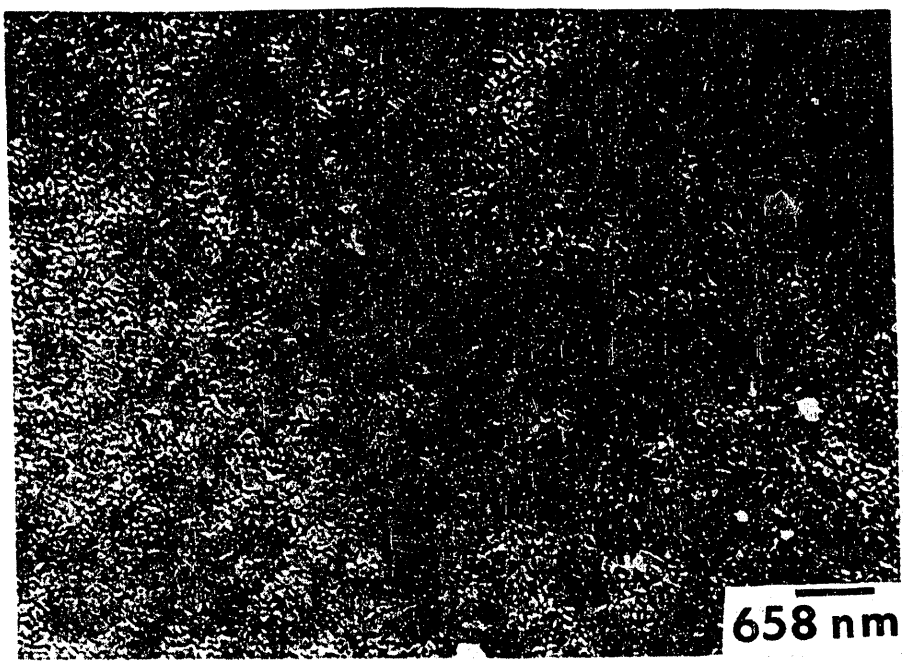

Figure 3.27 SEM micrograph of a three layer LSC film dip-coated onto a 0.1 micron pore size cobalt-doped Anotec filter and fired at 700°C. Grain size is much higher than usual, due to larger substrate pores.

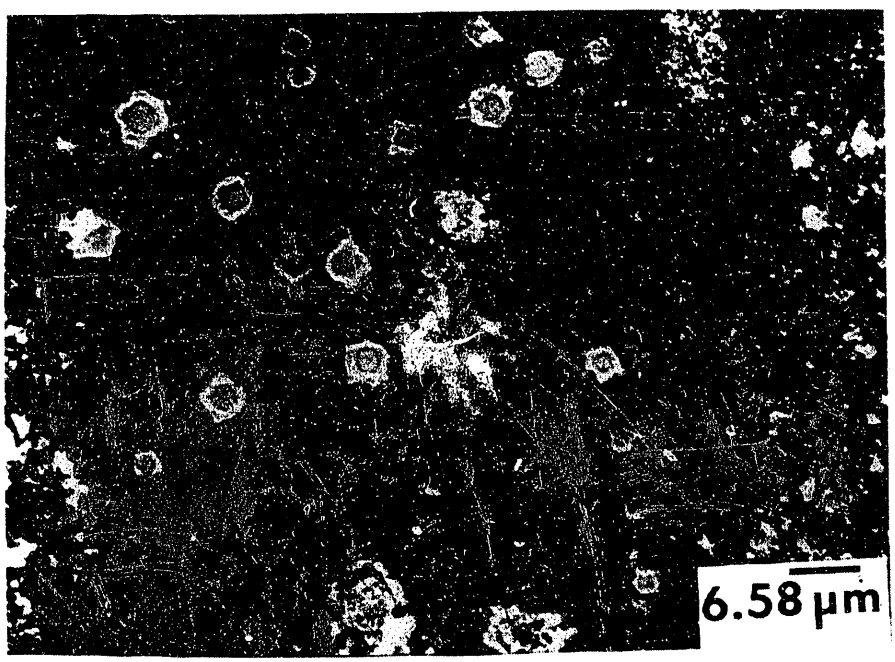

Figure 3.28 SEM micrograph of a thick LSC film from a PAC-nitrate solution spin-coated onto a piece of single crystal silicon wafer and fired at 700°C. Bubble pores and shrinkage cracks are present.

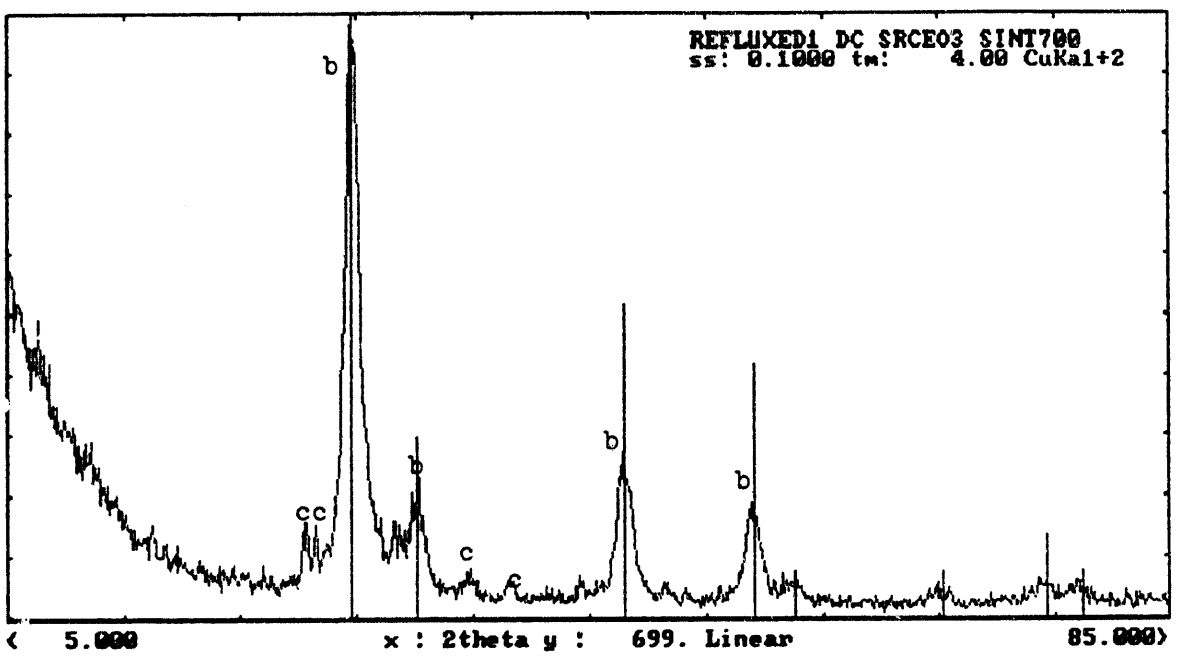

Figure 3.29 X-ray diffraction pattern recorded for a film spin-coated onto a piece of single crystal silicon wafer using a strontium-cerium alkoxide solution and fired at 700°C. a=$SrCeO_3$, b=CeO_2.

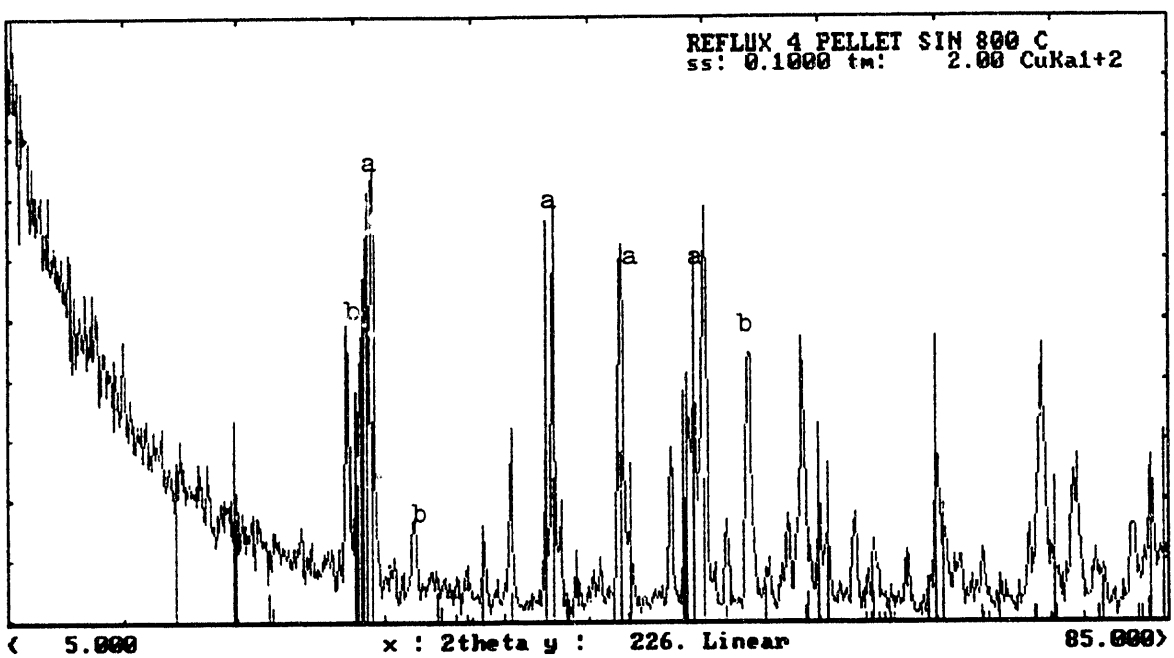

Figure 3.30 X-ray diffraction pattern recorded for pellet made using a hydrolyzed strontium-cerium alkoxide solution and fired at 800°C. a=$SrCeO_3$, b=CeO_2, c=$SrCO_3$.

END

DATE FILMED

4/20/93